Factors Governing Photodynamic Cross-linking of Ocular Coat

Thesis by

Joyce Huynh

In Partial Fulfillment of the Requirements

for the Degree of

Doctor of Philosophy

CALIFORNIA INSTITUTE OF TECHNOLOGY

Pasadena, California

2011

(Defended May 6, 2011)

Dedicated to Mom and Dad

ACKNOWLEDGMENTS

First, I would like to express my deepest gratitude to my thesis advisor, Prof. Julie Kornfield who is always understanding, supportive, and encouraging. I thank her for the guidance throughout my thesis project. She has provided me with advice when I needed it and at the same time granted me the freedom to explore my creativity. Julie's enthusiasm for science, passion for learning, and dedication to teaching have inspired me greatly throughout my graduate school experience.

I am grateful to have the opportunity to work with Matthew Mattson. He has been a wonderful mentor and friend since the first day I joined the Kornfield Lab. When I first joined the group, Matthew taught me everything I needed to know to get started with the research project. He continues to play an important role in my research project by providing valuable advice and contributions. I feel very fortunate to have had the opportunity to work closely with him over the last four years. He is always patient, kind, and encouraging when mentoring me. In addition to being an exceptional mentor, he is also a wonderful friend.

I thank our collaborators Dr. Daniel Schwartz and Dr. Keith Duncan at the University of California, San Francisco for providing resources and expertise on the clinical aspects of the project. I deeply appreciate everyone in the Kornfield group for their support and guidance. Group members were always very willing to share their expertise to help me accomplish what I needed to do. I would also like to thank the secretaries in the chemical engineering department, especially Ms. Anne Hormann, Ms. Marcy Fowler, and Ms. Kathy Bubash for handling all the logistics.

I am very glad to have the opportunity to work with undergraduate students: Viet Anh Nguyen Huu, Joyce Liu, and Alex Wang. Viet Anh is the first undergraduate student I worked with and it has been a remarkable experience mentoring him over the last three years. He is always very excited about the research and experiments which makes working with him an enjoyable and rewarding experience. Joyce and Alex are also very diligent students who have made valuable contributions to the research project as well.

I thank all my chemical engineering classmates who made going through first year manageable and fun. They continued to be an important source of support throughout the program. I also thank all my friends at Caltech for making my time here very memorable.

I would like to send very special thanks to my friends outside of Caltech as well. Diana, I am glad you were at UCLA making each weekend we hung out filled with fun activities and unforgettable memories. Gina, ever since you came back to LA, it has been an on-going party. Cindy, even though we have not lived in the same city since high school, it is wonderful to know you are always there for me. Eileen, I am grateful for all the laughter we share.

Finally, I am extremely grateful for my family. Most of all I would like to thank my mom and dad for their unconditional love and support. For as long as I can remember, they have always taught me to value education and knowledge. Growing up I listened to their teaching with faith and as I grew older I began to understand. Now more than ever before, I truly appreciate the value of education. I am very grateful for my sister, Candice, who is always interesting to talk to about anything and everything. She is filled

with intriguing ideas and theories that challenge me to think and provide me with profound insights. I thank my brother, sister-in-law, and nieces for their love and support.

ABSTRACT

This thesis addresses the challenge of minimizing toxicity of therapeutic protein-protein cross-linking of the cornea and sclera. Protein-protein cross-links include disulfide bonds, enzymatic cross-links and non-enzymatic cross-links. Disulfide bonds and enzymatic cross-links are closely regulated in the body. Non-enzymatic cross-links accumulate in an uncontrolled manner, often leading to deleterious effects. Clinically, non-enzymatic cross-links can be inserted in a controlled manner, both temporally and spatially, using photo-activation to achieve effects ranging from killing tumors to stabilizing ocular shape.

The shape of the eye is maintained by the ocular coat—the cornea and sclera. Diseases that result in progressive shape changes can lead to blindness (degenerative myopia) or necessitate a corneal transplant (keratoconus and post-LASIK ectasia). Photodynamic corneal cross-linking, pioneered by Wollensak *et al.* using riboflavin activated by near-ultraviolet light (riboflavin/UVA), halts the progression of keratoconus; if applied to the sclera, it might halt the progression of degenerative myopia, as well. However, this treatment suffers from severe cytotoxicity. The literature to date implicitly assumes that photodynamic cross-linking is inherently toxic. The present research demonstrates that protein-protein cross-linking can be achieved with minimal toxicity using eosin Y activated by visible light (eosin Y/visible).

At a molecular level, both eosin Y/visible and riboflavin/UVA are shown to act through a singlet oxygen mechanism; therefore, they are expected to produce similar covalent modifications of collagenous tissues. Real-time measurements of the increase in elastic

modulus during irradiation show that the eosin Y/visible and riboflavin/UVA produce similar rates of cross-linking. The transport coefficients of both eosin Y and riboflavin were measured for both sclera and de-epithelialized cornea. The diffusivity and partition coefficient values, together with the cross-linking kinetics, were used in a predictive model of the cross-linking profile as a function of treatment parameters. The predictive model also serves as an optimization tool for guiding the selection of treatment parameters in pre-clinical studies. In contrast to the dramatic toxicity of the riboflavin/UVA treatment (which kills all of the keratocytes and the endothelium in the rabbit model), the eosin Y/visible treatment achieves comparable cross-linking with negligible phototoxicity.

TABLE OF CONTENTS

Chapter 5: A Model for the Photodynamic Collagen Cross-linking Treatment

Chapter 6: Cross-linking the Cornea with Minimal Toxicity

LIST OF ILLUSTRATIONS AND TABLES

Chapter 1

Chapter 2

SYMBOLS AND ABBREVIATIONS

A	Absorbance
AA	Ascorbic Acid
AGE	Advanced Glycation End Products
BSS	Balanced Saline Solution
C	Concentration
CD	Corneal Diameter
CL	Corneal Length
CMC	Carboxymethylcellulose
CP	Corneal Perimeter
D	Diffusion Coefficient
D_{ab}	Diffusion Coefficient without Binding Effect
DPBS	Dulbecco's Phosphate Buffered Saline
ε	Extinction Coefficient
$erfc$	Complementary Error Function
EY	Eosin Y
g	Gravitational Acceleration Constant
G'	Storage modulus
$\Delta G'$	Change in Storage Modulus
$\Delta G'_{avg}$	Average of Change in Storage Modulus
$\dot{G}'$	Rate of Change in Storage Modulus
GAG	Glycosaminoglycan
h	Height

h_m	Mass Transfer Coefficient
HA	Hyaluronic Acid
I	Intensity
IOP	Intraocular Pressure
J	Flux
K	Partition Coefficient
$k_{^1O_2}$	Singlet Oxygen Chemical Reaction Rate Constant
K_{eq}	Ratio of Free-to-bound Molecules in the Tissue at Equilibrium
L	Sample Thickness
LASIK	Laser-assisted In Situ Keratomileusis
LED	Light Emitting Diode
Λ	Ratio of the Optical Penetration Depth to Sample Thickness
MC	Methylcellulose
μ	Sample Absorptivity
N	Number of Samples
OD	Oculus Dexter (Right Eye)
OS	Oculus Sinister (Left Eye)
P	Permeability
ρ	Density
S	Mean-square Deviation
SA	Sodium Alginate or Sodium Azide
t	Time
t_c	Drug Contact Time or Creep Time

t_e	Extraction Time
t_f	Time at the End of Irradiation Period
t_i	Time at the Beginning of Irradiation Period
t_{irr}	Irradiation Time
τ	Time Since Drug Solution Was Removed From the Cornea
USP	United States Pharmacopeia
UV	Ultraviolet
UVA	Ultraviolet A
z	Position Inside Sample

Chapter 1

Introduction

1.1 Protein-Protein Cross-links

Protein-protein cross-links are ubiquitous in biological systems. The most familiar are disulfide bonds, which form both intramolecularly and/or intermolecularly to yield proper protein folding and function. Similarly, enzymatic cross-links are inserted to confer proper function (e.g., maturation of collagen during development). Enzymatic cross-linking is regulated to confer precise spatial and temporal control, yielding a cross-linking density that is appropriate for the tissue function. A third, familiar class of protein-protein cross-links are the non-enzymatic cross-links that occur throughout our lifetime in a manner that is sensitive to diet and lifestyle (e.g., they are inhibited by consuming anti-oxidants and vitamins and are exacerbated by exposure to sunlight). In contrast to enzymatic cross-links, non-enzymatic cross-links accumulate in an uncontrolled manner. Non-enzymatic cross-links are formed without spatial or temporal regulation. Proteins with low turn-over rates accumulate these cross-links, which can have deleterious effects (e.g., wrinkles in skin[1, 2], hardening of arteries[3, 4], formation of amyloid plaques[5, 6]). Perhaps the least familiar type is "therapeutic cross-linking" in which a disease is treated by triggering protein-protein cross-links. Therapeutic cross-

links are inserted in a controlled manner, both spatially and temporally, to serve purposes that range from killing tumors to stabilizing the shape of the eye.

1.2 PHOTODYNAMIC THERAPY

Clinically, spatial and temporal control is achieved with photo-activated cross-linkers that remain inactive until they are irradiated. Using photo-activated molecules decouples the reaction and diffusion processes, allowing diffusion to penetrate the desired tissue while the drug is inactive. By irradiating only at desired locations, cross-linking can be achieved selectively in the intended tissues; inactive molecules present in other tissues simply diffuse away with time.

In contrast to treatments that rely on phototoxicity, such as photodynamic therapy for cancer or macular degeneration, other applications of photodynamic cross-linking aim to strengthen diseased tissue with minimal toxicity. Two important examples are strengthening the sclera to halt the progression of degenerative myopia, and strengthening the cornea to halt the progression of keratoconus and other corneal ectasias. The present thesis focuses on photodynamic cross-linking therapy for stabilizing the shape of the eye, with particular attention to designing treatments that minimize toxicity.

1.3 DISEASES THAT DESTABILIZE OCULAR SHAPE

The shape of the eye is maintained by the ocular coat, which consists of the cornea and sclera. The sclera is the white part of the eye making up 5/6 of the total surface area of the eye. Its function is to provide support and protect the eye. The cornea is the clear tissue in front of the eye, which provides ~2/3 of the total focusing power. Diseases

associated with changes in the shape of the sclera (e.g. degenerative myopia, Figure 1.1) or cornea (e.g. keratoconus and post-LASIK ectasia, Figure 1.1c) lead to loss of visual acuity due to distortion of the retina or of the refractive surface that is responsible for most of the lens power of the eye, respectively.

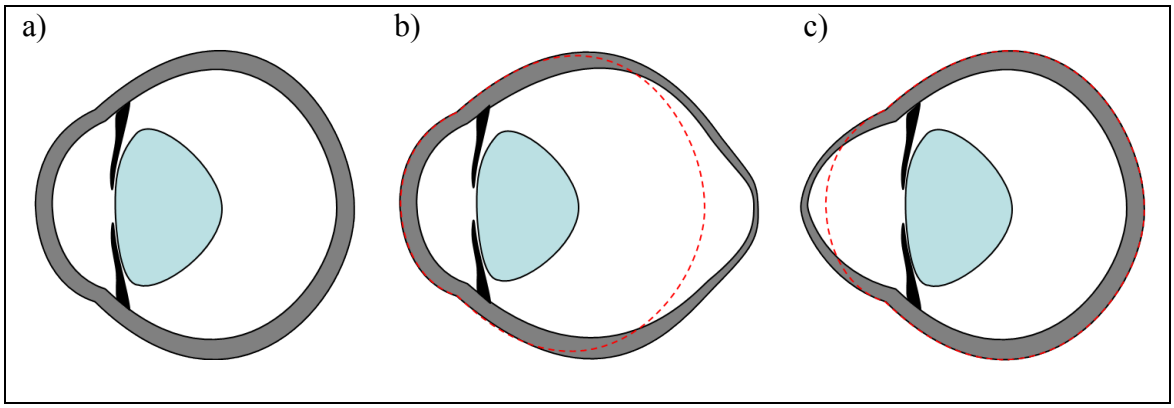

Figure 1.1. a) A normal eye. Thinning and stretching in the **b)** posterior sclera in degenerative myopia and **c)** cornea in keratoconus. (Images adapted from Mattson[7])

Degenerative myopia is the leading cause of blindness in Asian countries and is ranked 7th in the United States[8-12]. While there are treatments that can reduce the symptoms associated with the disease, there is no treatment that halts the progressive stretching and thinning of scleral tissues (Figure 1.1b). Axial elongation due to stretching of the sclera causes objects far away to be focused in front of the retinal photoreceptor plane, resulting in blurry vision. As the disease progresses, stretching of retinal and choroidal tissues damages these tissues resulting in loss of vision. In degenerative myopia, the sclera is found to be up to 5% thinner than normal at the posterior pole[13]. The altered structure of the sclera is considered to be a significant factor in contributing to the chorio-retinal damage.

Various efforts have been made to enhance the weakened sclera such as polymerization of foam at the posterior pole and scleroplasty but none showed the ability to arrest the disease[14, 15]. Scleroplasty is a scleral reinforcement surgery which places a graft at the posterior pole to support the weakened structure. Different surgical methods and a variety of materials have been tried for scleroplasty but none were successful.

Keratoconus is a bilateral corneal thinning disorder. This disease has a prevalence of 1/2000 with no racial or gender bias[16, 17]. This disease is characterized by progressive corneal thinning, protrusion, and scarring, resulting in irregular astigmatism and myopia (Figure 1.1c). Corneal steepening due to protrusion of the cornea causes the cornea's focusing power to increase; images come to a focus in front of the retina, resulting in blurry vision.

Corneal thinning due to keratoconus results in visual impairment that can initially be corrected by spectacles. When eyeglasses are no longer sufficient to provide clear vision, contact lenses are used. Surgical procedures, such as thermokeratoplasty[18], epikeratophakia[19], and intracornea ring segments[20] have been performed on those who are intolerant of contact lenses. These treatments do not halt the progression of keratoconus; they only correct refractive errors induced by irregular corneal thinning associated with the disease. When the disease progresses to the stage that refractive correction is no longer effective, a corneal transplant (keratoplasty) is required. About 20% of patients with keratoconus ultimately require keratoplasty[16].

Similarities between degenerative myopia and keratoconus – Similar to the sclera in degenerative myopia, change in the structure of the cornea is a significant factor in

contributing to protrusion. Collagen type I is the major structural component of the sclera, accounting for 23% of its total mass and 75% of its dry mass[21]. The cornea's chemical composition is very similar to the sclera, with collagen type I being the major structural component, contributing 15% of its total mass and 68% of its dry mass[21]. On a molecular level, collagen type I consists of three alpha chains spiraling around one another to form a triple helix. Individual triple-helical molecules are enzymatically cross-linked to one another during development to create long parallel collagen fibrils (Figure 1.2a). In both the sclera and the cornea, collagen fibrils are embedded in a gel-like matrix of proteoglycans and water (Figure 1.2b-c). Proteoglycans consist of protein cores with glycosaminoglycans attached along their lengths.

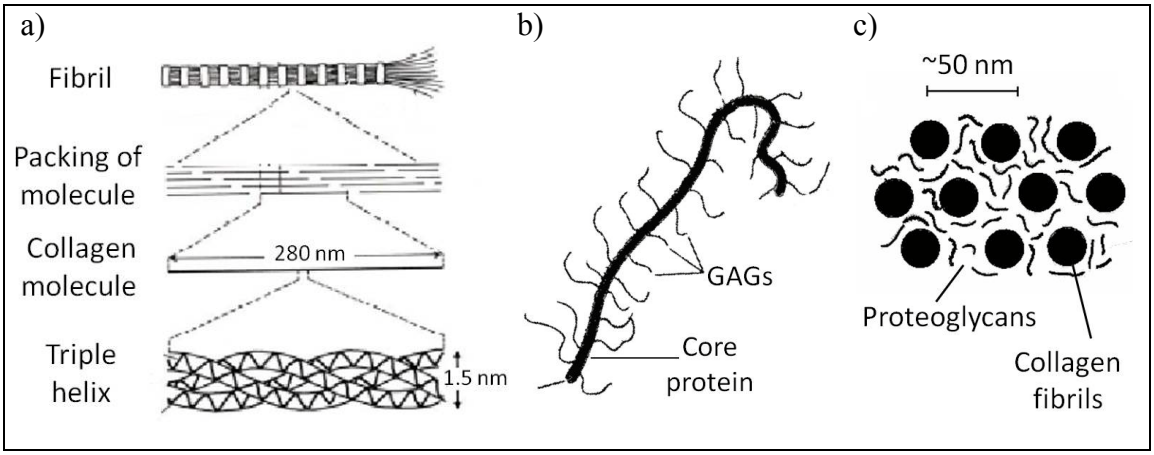

Figure 1.2. Structure of **a)** a collagen fibril (image adapted from www.nanobiomed.de). **b)** a proteoglycan **c)** collagen fibrils immersed in a gel-like matrix of water and proteoglycans. (Images b and c are adapted from Oyster[22])

The difference in optical properties between the sclera and cornea is due to the differences in the size, spacing and orientation of the collagen fibrils. Scleral collagen fibrils vary in both diameter (30 to 300 nm) and spacing (250 to 280nm)[23]. They form an interweaving morphology conferring great strength to the sclera to protect the eye

(Figure 1.3a). The white appearance of the sclera (and the opacity that is vital to its function) is due to light scattering from heterogeneities in fibril diameter, fibril spacing and fibril orientation on length scales from 150 to 600 nm. In contrast, corneal collagen fibrils are very regular in their diameters (20 to 33 nm) and spacing (~60 nm)[23]. The highly regular fibril/proteoglycan structures form sheets ("lamellae") that are stacked such that the collagen fibrils lie in the plane of the tissue, giving the cornea its unique combination of transparency and strength (Figure 1.3b).

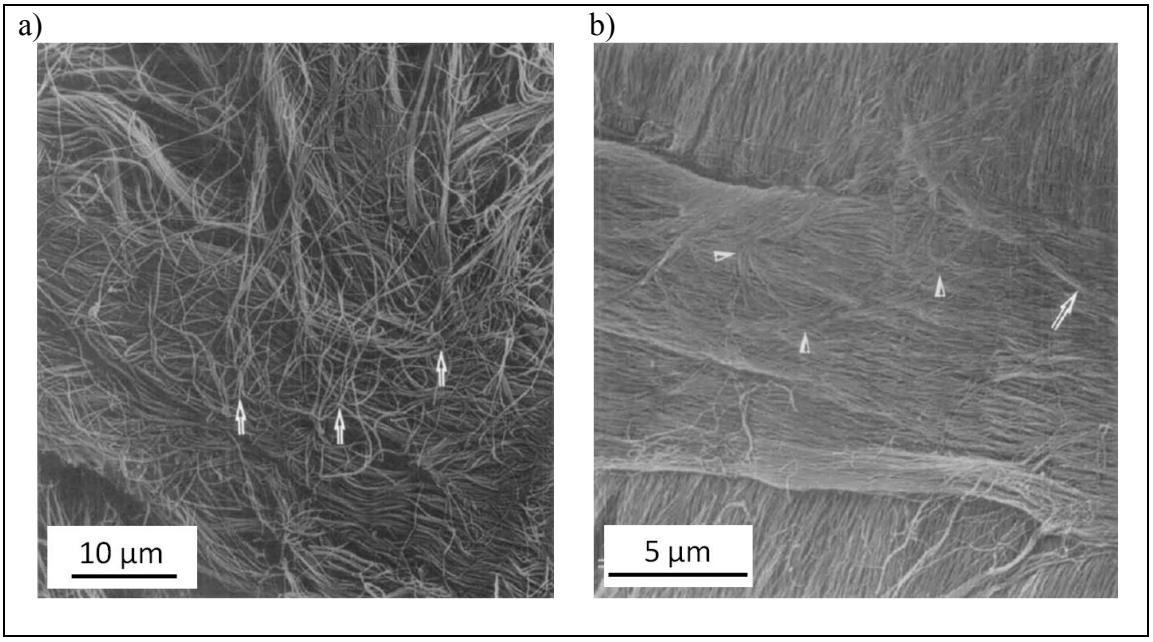

Figure 1.3. Fibrils form **a)** parallel lamellae in the cornea and **b)** interweaving morphology in the sclera. (Images adapted from Komai[24])

Abnormalities in these structures either in their building block materials or in their morphology can result in malfunctioning of the eye. Studies of degenerative myopia and keratoconus reveal that similar factors contribute to the thinning process. In degenerative myopia, the sclera has a lower content of collagen due to a decrease in production rate of

collagen and an increase in degradation rate of collagen[25-29]. There is also a shift in the distribution of fibril diameter resulting in smaller fibrils with the greatest reduction occurring in the outer layer of the sclera[30]. Similarly, in keratoconus, cornea thinning results from loss of material due to an increase in degradation rate of collagen[16, 31-33]. This leads to cornea of keratoconus eyes to have fewer collagen lamellae and fewer collagen fibrils per lamella[16, 34]. Thus, in both degenerative myopia and keratoconus, inadequate tissue strength and over-active collagen turnover result in mechanically weakened tissue.

Based on the similarities in composition of the sclera and cornea, and the similarities in the molecular basis of both degenerative myopia and keratoconus, Wollensak and Spoerl[35] suggested that it might be possible to develop similar treatments for the two diseases. Specifically, they examined the possibility that photodynamic cross-linking might be effective in strengthening the sclera and the cornea.

1.4 CROSS-LINKING TREATMENT

Based on the hypothesis that additional cross-links in the cornea protect against development of keratoconus, Wollensak, Seiler, Spoerl, *et al.* searched for ways to cross-link the cornea. Common cross-linkers such as glyceraldehyde and glutaraldehyde do not allow for control over when and where the cross-linking occurs. The diffusion process and reaction are coupled in these molecules; they diffuse until they are consumed by the reaction. Even though the use of glyceraldehyde lacks spatial and temporal control, efforts have been invested to develop clinical cross-linking treatments[36, 37]. Using photo-activated molecules allows for spatial and temporal control over the cross-linking

process. Riboflavin, also known as vitamin B2, was selected as the photosensitizer to cross-link the cornea since it was recently demonstrated to cross-link vitreous collagen[36].

In their earliest study in 1997, Wollensak, Seiler, Spoerl, *et al.* increased the mechanical strength of porcine corneas cross-linked with riboflavin and UVA irradiation 365 nm[36]. Their subsequent studies examined changes in the thermomechanical[38], hydration[39], ultrastructural[40], and biochemical[41, 42] behaviors in treated tissue. The results showed that cross-links formed between collagen molecules and are stable with respect to reducing agents (mercaptoethanol) chemical, heat, and peptidase (collagenase, pepsin and trypsin). They found that the extent of cross-linking induced by riboflavin/UVA varies with stromal depth, essentially confined to the anterior 300 μm.

Promising results with riboflavin/UVA in pre-clinical studies led Wollensak *et al.* to begin treating progressive keratoconus patients in 1998[43] (Figure 1.4). The pilot study in Dresden included a total of 22 patients. The treatment protocol involved removing the epithelium in the central 7-mm diameter. Next a riboflavin solution (0.1% riboflavin, 20% dextran) was applied to the cornea 5 minutes before, and then every 5 minutes during a 30-minute UVA irradiation (3 mW/cm^2 at 370 nm). Patient follow-up ranged from 3 months to 4 years. The treatment halted the progression of the disease in all eyes and in 70% of the eyes, regression occurred. After re-epithelialization and repopulation of keratocytes, there were no adverse effects on corneal transparency and endothelial cell density. This treatment is currently being used in Europe and going through FDA clinical trials in the United States.

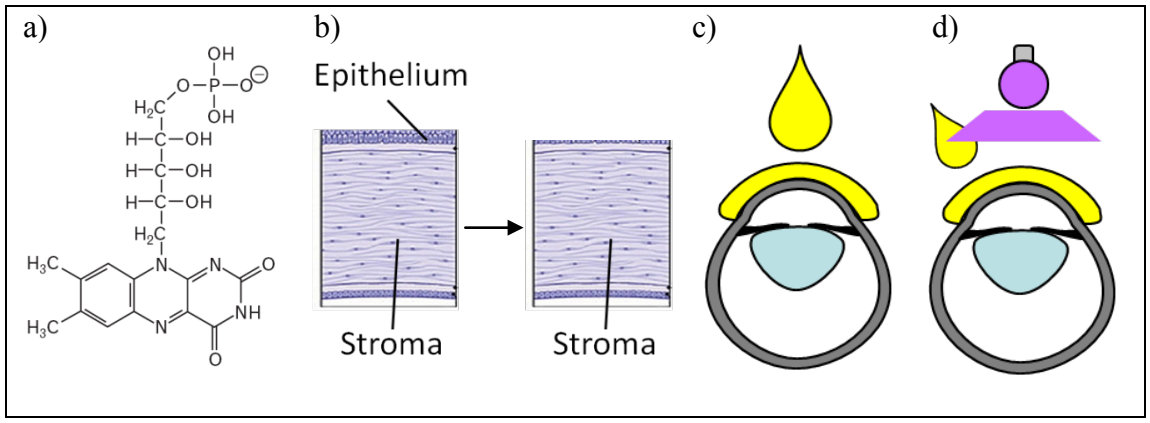

Figure 1.4. a) Riboflavin as a photosensitizer for inducing cross-links. b) Treatment involves removing the epithelial cell layer, **b)** applying drops of riboflavin solution onto the cornea, **c)** irradiating the cornea. (Images c & d adapted from Mattson[7])

Since the cornea and sclera consist of the same building blocks, it is hypothesized that treatments that can strengthen the cornea might also strengthen the sclera. Therefore, investigators have also tested riboflavin/UVA cross-linking treatment in rabbit sclera in order to treat degenerative myopia[44]. Cross-linking treatment increased scleral strength as hypothesized.

Riboflavin/UVA cross-linking treatment halts the progression of keratoconus and can potentially be used treat degenerative myopia. This treatment is novel and is the first clinical procedure to address keratoconus directly, instead of only correcting refractive errors resulting from the disease.

1.5 Corneal Cross-linking with Minimal Toxicity

Even though riboflavin/UVA corneal cross-linking has demonstrated the ability to halt the progression of keratoconus, the treatment is cytotoxic to the cornea. The combination

of riboflavin and UVA light is toxic to both keratocytes and endothelial cells in the cornea[45, 46]. Keratocytes are present throughout the entire corneal stroma to heal wounds, to maintain corneal transparency and to maintain protein content[22, 47]. Keratocytes can regenerate in human. The endothelium regulates the amount of water entering the corneal stroma from the anterior chamber. Damage to this layer leads to swelling of the cornea resulting in corneal haze, and it causes the cornea to lose its refractive function. A corneal transplant is required to restore vision. Unlike keratocytes, endothelial cells do not regenerate in human. Therefore, the treatment was carefully designed to restrict toxicity to the anterior 340 μm to protect the endothelial cell layer[48-50]. Damage to keratocytes leads to corneal haze for weeks to months after the surgery[43, 51]. Repopulation of keratocytes begins 2-3 months after the procedure and completes after 6 months[50, 52, 53]. The haze persists in 8.6% of patients[54] resulting in impaired vision.

Building on the success of Wollensak, Seiler, Spoerl *et al.*, we explore photo-activated treatments of keratoconus, post-LASIK ectasia, and degenerative myopia that add therapeutic cross-links to the tissues. We diverge from Wollensak *et al.* in selecting a sensitizer that minimizes cytotoxic effects. Mattson[7] has demonstrated that photosensitizer eosin Y is effective in strengthening of the cornea and the sclera. Eosin Y has a maximum absorption at 514 nm (green) (Figure 1.5). In addition, eosin Y has been approved by the FDA for use in the body as part of a lung and dural sealant (FocalSeal)[55, 56]. Eosin Y has also demonstrated biocompatibility in a range of applications (Table 1.1). In order to assess if eosin Y can produce a treatment that is both

effective and safe, it is necessary to determine the stability of the cross-links formed, the extent of cross-linking activated, and treatment biocompatibility.

Table 1.1. Eosin Y biocompatibility

Authors	Application
Alleyne *et al.*[55]	Dural Sealant in Canine Craniotomy
Nakayama *et al.*[57]	Hemostatis of Liver Tissue
Orban *et al.*[58]	Cardiovascular Applications
Cruise et al., Pathak *et al.* Desmangles *et al.*[59-61]	Islet Cell Encapsulation/ Microencapsulation
Elisseeff *et al.*[62]	Transdermal Polymerization
Luman *et al.,* Carnahan *et al.*[63, 64]	Close linear corneal incision, Secure Lasik flaps
West *et al.*[65, 66]	Thrombosis Inhibition

(Reproduced from Mattson[7])

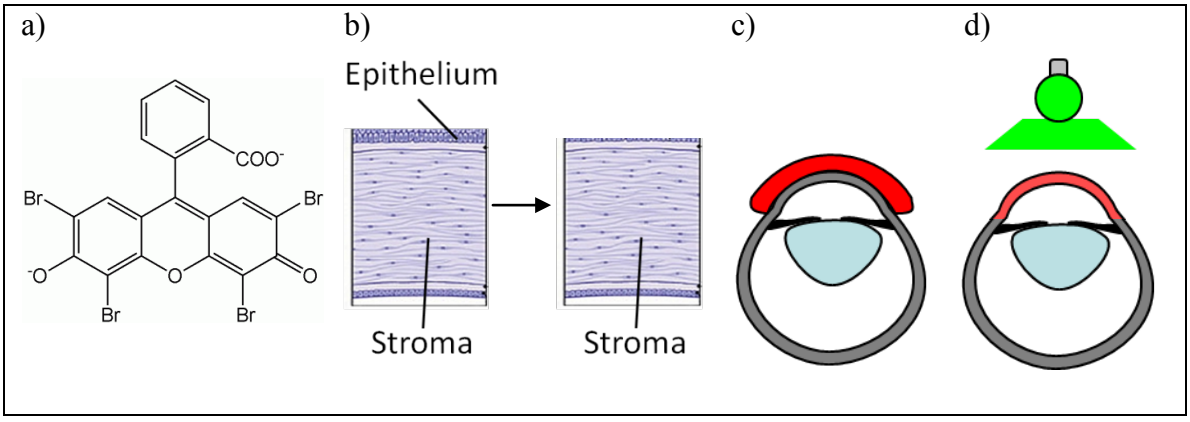

Figure 1.5. a) Eosin Y is a visible light activated cross-linker. b) Treatment involves removing the epithelial cell layer, **b)** applying a viscous gel containing eosin Y onto the cornea, **c)** irradiating the cornea. (Images c & d adapted from Mattson[7])

1.6 THESIS OUTLINE

Treatment efficacy relies on stability of the cross-links formed, the extent and the distribution of cross-linking induced in the tissue. Stability of the cross-links depends on the reaction pathways leading to their formations. Chapter 2 investigates the reaction pathways of photodynamic cross-linking in collagen gel. Both riboflavin/UVA and eosin Y/visible light cross-link collagen via the singlet oxygen reaction pathway producing cross-links that are stable. The extent of cross-linking in the tissue depends on the reaction rate, which is a function of the local drug concentration and local light intensity at each depth in the tissue. Chapter 3 examines how different cross-linking conditions affect collagen cross-linking efficacy in collagen gels with a uniform drug concentration. There is an optimal photosensitizer concentration for cross-linking. In the tissue, the drug concentration profile resulting from topical delivery depends on the transport properties of the tissues. Chapter 4 studies the transport properties of the cornea and sclera. Quantification of the amount of drug delivered as a function of time and together with a diffusion model, the partition coefficient and diffusion coefficient were determined. Different drug delivery techniques to the cornea were assessed to establish a protocol for clinical use. A viscous gel formulation consisting of carboxymethylcellulose is the most suitable method for topically delivering drug to the cornea. Chapter 5 combines kinetics data and transport calculations to predict the cross-linking profile as a function of tissue depth for a given set of treatment parameter (drug concentration, drug contact time, delay time between the end of drug contact time to the beginning of irradiation period, irradiation intensity and duration). The model provides a tool for optimizing treatment parameters. Insights from the model were used to design treatments to assess efficacy and

safety in a rabbit model. Chapter 6 establishes efficacy by treating rabbit eyes *in vitro* and *in vivo*, and then tissue stability was determined *ex vivo* by an intact globe expansion method. Eosin Y/visible light treatment produces equivalent stabilization in the cornea and induces much less cytotoxicity compared to riboflavin/UVA.

1.7 BIBLIOGRAPHY

1. Wulf, H.C., Sandby-Møller, J., Kobayasi, T., Gniadecki, R., *Skin Aging and Natural Photoprotection.* Micron, 2004. **35**(3): p. 185.
2. Dyer, D.G., Dunn, J.A., Thorpe, S.R., K.E., Bailie, T.J., Lyons, McCance, D.R.*, et al.*, *Accumulation of Maillard Reaction Products in Skin Collagen in Diabetes and Aging.* The Journal of Clinical Investigation, 1993. **91**(6): p. 2463.
3. MacDonald, E., Lee, W.K., Hepburn, S., Bell, J., Scott, P.J. Dominiczak, M.H., *Advanced Glycosylation End Products in the Mesenteric Artery.* Clinical Chemistry, 1992. **38**(4): p. 530.
4. Sims, T.J., Rasmussen, L.M., Oxlund, H., Bailey, A.J., *The Role of Glycation Cross-links in Diabetic Vascular Stiffening.* Diabetologia, 1996. **39**(8): p. 946.
5. Vitek, M.P., K, Bhattacharya, J.M., Glendening, Stopa, E., Vlassara, H., Bucala, R.*, et al.*, *Advanced Glycation End Products Contribute to Amyloidosis in Alzheimer Disease.* Proceedings of the National Academy of Sciences 1994. **91**(11): p. 4766.
6. Niwa, T., Sato, M., Katsuzaki, T., Tomoo, T., Miyazaki, T., Tatemichi, N.*, et al.*, *Amyloid Bold Beta$_2$-microglobulin is Modified with N epsilon-(carboxymethyl) Lysine in Dialysis-related Amyloidosis.* Kidney international, 1996. **50**(4): p. 1303.
7. Mattson, M., *Understanding and Treating Eye Diseases: Mechanical Characterization and Photochemical Modification of the Cornea and Sclera.* Dissertation (Ph.D), California Institute of Technology, 2008.

8. Tano, Y., *Pathologic Myopia: Where Are We Now?* American Journal of Ophthalmology, 2002. **134**(5): p. 645-60.

9. Curtin, B.J., *The Myopias: Basic Science and Clinical Management*. 1985: Harpercollins College Div.

10. Hsu, W.M., Cheng, C.Y., Liu, J.H., Tsai, S.Y., Chou, P., *Prevalence and Causes of Visual Impairment in an Elderly Chinese Population in Taiwan: The Shihpai Eye Study*, in *International Congress of Ophthalmology*. 2004. p. 62.

11. Iwase, A., Araie, M., Tomidokoro, A., Yamamoto, T., Shimizu, H. Kitazawa, Y., *Prevalence and Causes of Low Vision and Blindness in a Japanese Adult Population: The Tajimi Study.* American Academy of Ophthalmology Annual Meeting, 2006. **113**(8): p. 1354.

12. Xu, L., Wang, Y., Li, Y., Wang, Y., Cui, T., Li, J.*, et al.*, *Causes of Blindness and Visual Impairment in Urban and Rural Areas in Beijing: The Beijing Eye Study.* Ophthalmology, 2006. **113**(7).

13. McBrien, N.A., Gentle, A., *Role of the Sclera in the Development and Pathological Complications of Myopia.* Progress in Retinal and Eye Research, 2003. **22**(3): p. 307.

14. Avetisov, E.S., Tarutta, E.P., Iomdina, E.N., Vinetskaya, M.I., Andreyeva, L.D., *Nonsurgical and Surgical Methods of Sclera Reinforcement in Progressive Myopia.* Acta Ophthalmologica Scandinavica, 1997. **75**(6): p. 618-623.

15. Belyaev, V.S., Ilyina, T.S., *Late Results Of Scleroplasty In Surgical Treatment Of Progressive Myopia.* Eye Ear Nose And Throat Monthly, 1975. **54**(3): p. 109-113.

16. Rabinowitz, Y.S., *Keratoconus.* Survey of Ophthalmology, 1998. **42**(4): p. 297-319.

17. Bron, A.J., *Keratoconus.* Cornea, 1988. **7**(3): p. 163-9.

18. Gasset, A.R., Kaufman, H.E., *Thermokeratoplasty in Treatment of Keratoconus.* American Journal of Ophthalmology, 1975. **79**(2): p. 226-232.

19. McDonald, M.B., Kaufman, H.E., Durrie, D.S., Keates, R.H., Sanders, D.R., *Epikeratophakia for Keratoconus. The Nationwide Study.* Archives of Ophthalmology, 1986. **104**(9): p. 1294-1300.

20. Colin, J., Cochener, B., Savary, G., Malet, F., *Correcting Keratoconus with Intracorneal Rings.* Journal of Cataract & Refractive Surgery, 2000. **26**(8): p. 1117-1122.

21. Edwards, A., Prausnitz, M.R., *Fiber Matrix Model of Sclera and Corneal Stroma for Drug Delivery to the Eye.* AIChE journal, 2006. **44**(1): p. 214.

22. Oyster, C.W., *The Human Eye: Structure and Function*. 1999.

23. Fatt, I., *Physiology of the Eye: An Introduction to the Vegetative Functions*. 1992.

24. Komai, Y., Ushiki, T., *The Three-dimensional Organization of Collagen Fibrils in the Human Cornea and Sclera.* Investigative Ophthalmology & Visual Science, 1991. **32**(8): p. 2244-58.

25. Zorn, M., Hernandez, M.R., Norton, T.T., Yang, J., Ye, H.O., *Collagen Gene-expression in the Developing Tree Shrew Sclera.* Investigative Ophthalmology & Visual Science, 1992. **33**(4): p. 1053-1053.

26. McBrien, N. A., Cornell, L. M., Gentle, A., *Structural and Ultrastructural Changes to the Sclera in a Mammalian Model of High Myopia.* Investigative Ophthalmology & Visual Science, 2001. **42**(10): p. 2179-87.

27. Guggenheim, J.A., McBrien, N.A., *Form-deprivation Myopia Induces Activation of Scleral Matrix Metalloproteinase-2 in Tree Shrew.* Investigative Ophthalmology & Visual Science, 1996. **37**(7): p. 1380-95.

28. Aimes, R.T., Quigley, J.P., *Matrix Metalloproteinase-2 is an Interstitial Collagenase. Inhibitor-free Enzyme Catalyzes the Cleavage of Collagen Fibrils and Soluble Native Type I Collagen Generating the Specific 3/4- and 1/4-length Fragments.* The Journal of Biological Chemistry, 1995. **270**(11): p. 5872-6.

29. Rada, J.A., Nickla, D.L., Troilo, D., *Decreased Proteoglycan Synthesis Associated with Form Deprivation Myopia in Mature Primate Eyes.* Investigative Ophthalmology & Visual Science, 2000. **41**(8): p. 2050-8.

30. Curtin, B.J., Iwamoto, T., Renaldo, D.P., *Normal and Staphylomatous Sclera of High Myopia. An Electron Microscopic Study.* Archives of ophthalmology, 1979. **97**(5): p. 912-5.

31. Kao, W.W.Y., Vergnes, J.P. , Ebert, J. , Sundar-Raj, C.V. , Brown, S.I., *Increased Collagenase and Gelatinase Activities in Keratoconus.* Biochemical and Biophysical Research Communications, 1982. **107**(3): p. 929.

32. Sawaguchi, S., Yue, B.Y., Sugar, J., Gilboy, J.E., *Lysosomal Enzyme Abnormalities in Keratoconus.* Archives of Ophthalmology, 1989. **107**(10): p. 1507-1510.

33. Smith, V.A., Hoh, H.B., Littleton, M., Easty, D.L., *Over-expression of a Gelatinase A Activity in Keratoconus.* Eye, 1995. **9**(4): p. 429-433.

34. Bron, Aj A. J., *Keratoconus.* Cornea, 1988. **7**(3): p. 163-9.

35. Wollensak, G., Spoerl, E., *Collagen Crosslinking of Human and Porcine Sclera.* Journal of Cataract & Refractive Surgery, 2004. **30**(3): p. 689-695.

36. Spoerl, E., Huhle, M., Seiler, T., *Induction of Cross-links in Corneal Tissue.* Experimental Eye Research, 1998. **66**(1): p. 97.

37. Wollensak, G., Iomdina, E., *Long-term Biomechanical Properties After Collagen Crosslinking of Sclera Using Glyceraldehyde.* Acta Ophthalmologica, 2008. **86**(8): p. 887-893.

38. Spoerl, E., Wollensak, G., Dittert, .D.D., T., Seiler, *Thermomechanical Behavior of Collagen-cross-linked Porcine Cornea.* Ophthalmologica, 2004. **218**(2): p. 136.

39. Wollensak, G., Aurich, H., Pham, D.T., Wirbelauer, C., *Hydration Behavior of Porcine Cornea Crosslinked with Riboflavin and Ultraviolet A.* Journal of Cataract & Refractive Surgery, 2007. **33**(3): p. 516-521.

40. Wollensak, G., Wilsch, M., Spoerl, E., Seiler, T., *Collagen Fiber Diameter in the Rabbit Cornea After Collagen Crosslinking by Riboflavin/UVA.* Cornea, 2004. **23**(5): p. 503-507.

41. Spoerl, E., Wollensak, G., Seiler, T., *Increased Resistance of Crosslinked Cornea Against Enzymatic Digestion.* Current Eye Research, 2004. **29**(1): p. 35.

42. Wollensak, G., Redl, B., *Gel Electrophoretic Analysis of Corneal Collagen After Photodynamic Cross-linking Treatment.* Cornea, 2008. **27**(3): p. 353.

43. Wollensak, G., Spoerl, E., Seiler, T., *Riboflavin/ultraviolet-a-induced Collagen Crosslinking for the Treatment of Keratoconus.* American Journal of Ophthalmology, 2003. **135**(5): p. 620-627.

44. Wollensak, G., Iomdina, E., Dittert, D., Salamatina, O., Stoltenburg G, *Crosslinking of Scleral Collagen in the Rabbit Using Riboflavin and UVA.* Acta Ophthalmologica Scandinavica, 2005. **83**(4): p. 477.

45. Wollensak, G., Spoerl, E., Wilsch, M., Seiler, T., *Keratocyte Apoptosis After Corneal Collagen Cross-linking Using Riboflavin/UVA Treatment.* Cornea, 2004. **23**(1): p. 43-49.

46. Wollensak, G., Spoerl, E., Wilsch, M., Seiler, T., *Endothelial Cell Damage After Riboflavin-ultraviolet-A Treatment in the Rabbit.* Journal of Cataract & Refractive Surgery, 2003. **29**(9): p. 1786-90.

47. Müller, L.J., Pels, L., Vrensen, G.F., *Novel Aspects of the Ultrastructural Organization of Human Corneal Keratocytes.* Investigative Ophthalmology & Visual Science, 1995. **36**(13): p. 2557.

48. Wollensak, G., Spöerl, E., Reber, F., Pillunat, L., Funk, R., *Corneal Endothelial Cytotoxicity of Riboflavin/UVA Treatment In Vitro.* Ophthalmic Research, 2003. **35**(6): p. 324.

49. Wollensak, G., Spoerl, E., Reber, F., Seiler, T., *Keratocyte Cytotoxicity of Riboflavin/UVA-treatment In Vitro.* Eye, 2004. **18**(7): p. 718.

50. Spoerl, E., Mrochen, M., Sliney, D., Trokel, S., Seiler, T., *Safety of UVA-riboflavin Cross-linking of the Cornea.* Cornea, 2007. **26**(4): p. 385.

51. Mazzotta, C., Balestrazzi, A., Baiocchi, S., Traversi, C., Caporossi, A., *Stromal Haze After Combined Riboflavin/UVA Corneal Collagen Cross-linking in Keratoconus: In Vivo Confocal Microscopic Evaluation.* Clinical & Experimental Ophthalmology, 2007. **35**(6): p. 580.

52. Mazzotta, C., Balestrazzi, A., Traversi, C., Baiocchi, S., Caporossi, T., Tommasi, C.*, et al.*, *Treatment of Progressive Keratoconus by Riboflavin-UVA-induced Cross-linking of Corneal Collagen: Ultrastructural Analysis by Heidelberg Retinal Tomograph II In Vivo Confocal Microscopy in Humans.* Cornea, 2007. **26**(4): p. 390.

53. Seiler, T., Hafezi, F., *Corneal Cross-linking-induced Stromal Demarcation Line.* Cornea, 2006. **25**(9): p. 1057.

54. Raiskup, F., Hoyer, A., Spoerl, E., *Permanent Corneal Haze After Riboflavin-UVA-induced Cross-linking in Keratoconus.* Journal of Refractive Surgery, 2009. **25**(9): p. S824-8.

55. Alleyene, C.H., Cawley, C.M., Barrow, D.L., Poff, B.C., Powell, M.D., Sawhney, A.S.*, et al.*, *Efficacy and Biocompatibility of a Photopolymerized, Synthetic, Absorbable Hydrogel as a Dural Sealant in a Canine Craniotomy Model.* Journal of Neurosurgery, 1998. **88**(2): p. 308-13.

56. Torchiana, D.F. , F., David, *Polyethylene Glycol Based Synthetic Sealants: Potential Uses in Cardiac Surgery.* Journal of Cardiac Surgery, 2003. **18**(6): p. 504-6.

57. Nakayama, Y., Kameoa, T., Ohtakaa, A., Hiranob, Y., *Enhancement of Visible Light-induced Gelation of Photocurable Gelatin by Addition of Polymeric Amine.*

Journal of Photochemistry and Photobiology A - Chemistry, 2006. **177**(2-3): p. 205.

58. Orban, J.M., Faucher, K.M., Dluhy, R.A., Chaikof, E.L., *Cytomimetic Biomaterials. 4. In-Situ Photopolymerization of Phospholipids on an Alkylated Surface.* Macromolecules, 2000. **33**: p. 4205-4212.

59. Cruise, G.M., Hegre, O.D., Scharp, D.S., Hubbell, J.A., *A Sensitivity Study of the Key Parameters in the Interfacial Photopolymerization of Poly(ethylene glycol) Diacrylate upon Porcine Islets.* Biotechnology and Bioengineering, 1997. **57**(6): p. 655-665.

60. Pathak, C.P., Sawhney, A.S., Hubbell, J.A., *Rapid Photopolymerization of Immunoprotective Gels in Contact with Cells and Tissue.* Journal of American Chemical Society, 1992. **114**: p. 8311-8312.

61. Desmangles, A.I., Jordan, O., Marquis-Weible, F., *Interfacial Photopolymerization of B-Cell Clusters: Approaches to Reduce Coating Thickness Using Ionic and Lipophilic Dyes.* Biotechnology and Bioengineering, 2000. **72**(6): p. 634-641.

62. Elisseeff, J., Anseth, K., Sims, D., McIntosh, W., Randolph, M. Langer, R., *Transdermal Photopolymerization for Minimally Invasive Implantation.* Proceedings of National Academy of Sciences, 1999. **96**: p. 3104-3107.

63. Luman, N.R., Kim, T., Grinstaff, M.W., *Dendritic Polymers Composed of Glycerol and Succinic Acid: Synthetic Methodologies and Medical Applications.* Pure Applied Chemistry, 2004. **76**: p. 1375-1385.

64. Carnahan, M. A., Middleton, C., Kim, J., Kim, T., Grinstaff, M.W., *Hybrid Dendritic-Linear Polyester-Ethers for in Situ Photopolymerization.* Journal of American Chemical Society, 2002. **124**: p. 5291-5293.

65. West, J.L., Hubbell, J.A., *Separation of the Arterial Wall from Blood Contact Using Hydrogel Barriers Reduces Intimal Thickening After Balloon Injury in the Rat: The Roles of Medial and Luminal Factors in Arterial Healing.* Proceedings of the National Academy of Sciences, 1996. **93**: p. 13188-13193.

66. Hill-West, J.L., Chowdhury, S.M., Slepianu, M.J., Hubbell, J.A., *Inhibition of Thrombosis and Intimal Thickening by In Situ Photopolymerization of Thin Hydrogel Barriers.* Proceedings of the National Academy of Sciences, 1994. **91**: p. 5967-5971.

Chapter 2

Reaction Pathways for Photodynamic Collagen Cross-linking

2.1 INTRODUCTION

There has been great interest in photodynamic protein cross-linking due to the wide range of photodynamic applications. In some photodynamic applications, the aims are not to cross-link proteins but to rely on such mechanisms to achieve the desired outcome. Examples of such applications include photodynamic therapies for cancer (aim to kill cancer cells)[1, 2] and the photodynamic therapy for macular degeneration (aims to create vessel occlusions by damaging the neovascular endothelial cells)[3]. In other photodynamic applications, the cross-links themselves contribute to the desired effects. Examples of such applications include tissue engineering applications[4, 5] and modification of tissue strength[6, 7], which aim to increase material strength by inserting protein cross-links. Various proteins undergo covalent cross-linking when irradiated with light in the presence of a photosensitizer[8-10]. There are two major photosensitization pathways: type I or direct reaction pathway and type II or indirect reaction pathway.

These photodynamic reactions begin with the photosensitizer absorbing light which transitions the molecule from its ground state to an excited state. In type I, the photosensitizer in this excited state reacts with the protein molecule by hydrogen or electron transfer[11]. In type II, the photosensitizer in its excited state transfers its energy to ground state molecular oxygen to produce singlet oxygen. This highly reactive singlet oxygen species then oxidizes the protein[11]. Photosensitization reactions can occur via both type I and type II pathways at the same time. The relative contribution of the two pathways depends on the sensitizer, protein, solvent composition, and other experimental conditions[12, 13]. Here, we are interested in the photodynamic cross-linking therapy for enhancing weakened ocular tissues, particularly for diseases including keratoconus [14, 15], post-LASIK ectasia[16, 17], and degenerative myopia[18, 19]. Therefore, we give particular attention to collagen cross-linking and examine the role of type I and type II reaction pathways in the case of two drug/irradiation systems of interest for therapeutic cross-linking: riboflavin/UVA and eosin Y/visible.

Pioneering work of Wollensak, Seiler, Spoerl, *et al.* has led to the development of a corneal cross-linking treatment for keratoconus[20, 21]. Cross-linking the corneal stroma strengthens the tissue and halts progression of the disease. Cross-linking is achieved by activating riboflavin with UVA light (370 nm irradiation). Collagen cross-links formed by riboflavin/UVA are stable to chemical, heat, and enzymatic treatment[22]. Because the addition of cross-links both enhances tissue strength and provides protection from enzymatic degradation, the treatment stabilizes the cornea both by reinforcing the protein present at the time of treatment and by reducing the rate of protein turnover that is the underlying cause of diseases such as keratoconus and degenerative myopia[19, 23, 24].

Clinical trials for riboflavin/UVA cross-linking therapy lasting up to 5 years have demonstrated long-term efficacy. The strengthening effect due to cross-linking observed in the cornea is also seen in the sclera[7, 25]. So cross-linking may be able to halt the progression of degenerative myopia, which is a disease associated with weakening and thinning of the sclera that is a major, untreatable cause of blindness[26].

The drawbacks of the riboflavin/UVA treatment are due to the toxicity of the combination of riboflavin with UVA[27-29]. The treatment induces apoptosis of more than 90% of the keratocytes in the anterior 400 μm of the corneal stroma[30, 31] and full recovery requires up to 12 months in some patients[32]. Of greater concern is the potential for endothelial toxicity due to the limited recovery of the human endothelium after injury. Consequently, keratoconus patients with corneas thinner than 400 μm are excluded from receiving this therapy[30, 31]. To establish a safer cross-linking treatment, we are investigating a visible light activated photosensitizer, eosin Y, that produces cross-linking in the cornea and sclera at comparable rates to riboflavin/UVA (Chapter 3). Biocompatibility studies in the cornea show that eosin Y activated by green light results in much lower cytotoxicity than riboflavin/UVA (some keratocytes in the anterior 100 μm undergo apoptosis, Chapter 6).

Here we examine the relationship between the reaction pathway that produces cross-linking in the eosin Y/visible treatment and the reaction pathway of the riboflavin/UVA treatment. The extensive literature on photodynamic protein cross-linking reaction mechanisms guides the selection of a small set of experiment can lead to a broad set of

deductions regarding the chemical reactions that occur in both riboflavin/UVA and eosin Y/visible light therapeutic cross-linking treatments.

Photorheology is used to monitor the rate of cross-linking by measuring the sample's modulus during irradiation. Rates of photo-activated cross-linking of collagen gels are compared as a function of the presence of molecular oxygen in the environment and the concentration of singlet oxygen quenchers. This provides a simple method of establishing the relative importance of type I and type II reaction pathways.

2.2 METHODS

Collagen Gel Preparation – A mixture of 2.5 g gelatin from bovine skin (Sigma Aldrich G6650 Lot #047K0005) and 6.0 mL Dulbecco's phosphate buffered saline (DPBS, Sigma D8662) was heated at 75°C for 30 ± 1 minutes to dissolve all the gelatin. After the gelatin solution was removed from the heat bath, 1 mL of 0.5% riboflavin-5′-monophosphate (riboflavin, Sigma Aldrich R7774) or 1 mL of 0.2% eosin Y (Sigma Aldrich E6003 Lot# 022K3692) solution, and 0.5 mL of a quenching reagent (sodium azide or ascorbic acid) stock solution having 20 times the final desired concentration were added to the gelatin solution. The solution was swirled for a few seconds to yield a uniform final mixture containing 25% w/w gelatin, 0.05% riboflavin or 0.02% eosin Y, and the desired quencher concentration. Two quenching conditions were examined: 100 mM sodium azide and 20 mM ascorbic.

To produce a uniform layer of gel, a mold was prepared using a Teflon spacer between two Plexi-glass plates, which were held together with clamps (Figure 2.1a). The Teflon

spacer provided a controlled gap to form 500 μm thick gels. Prior to dispensing the solution into a mold, both the glass Pasteur pipette and the gel mold were warmed using a heat gun (for ~15 seconds). The warm solution was then dispensed into the warm mold; then the filled mold was wrapped in aluminum foil to prevent dehydration and interaction with light. The gel mold was stored at ~4°C for at least 8 hours to form a solid gel. This procedure was used to create eosin Y and riboflavin gels with varying quencher concentrations. All samples were measured within 48 hours of the beginning of gel preparation.

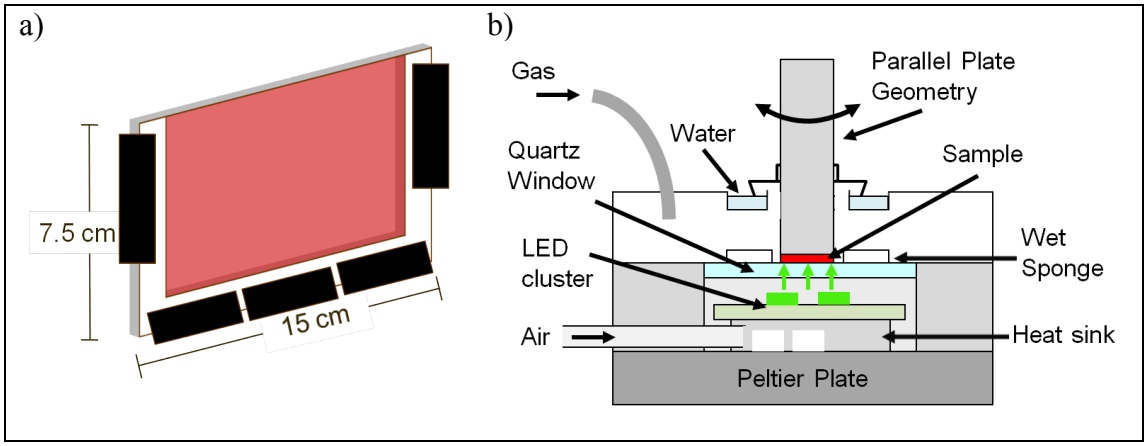

Figure 2.1. a) Forming a gel in a mold made of two Plexi-glass plates and a Teflon spacer all held together by clamps. **b)** A schematic of the photorheology set up for measuring real-time changes in sample modulus. The chamber with the sponge and water at the top sealed off by a cap prevented sample dehydration. LEDs below the quartz window provided light for sample irradiation. The gas inlet provides the option to create an oxygen free environment inside the chamber.

Photorheology Apparatus – Collagen gel photorheology was performed on a stress-controlled shear rheometer (TA Instrument AR1000). The lower, stationary tool was modified to deliver light to the sample. A custom-built light delivery device was mounted

onto the Peltier plate of the rheometer (Figure 2.1b) similar to those described by Khan, Plitz, *et al.*[33] (TA Instrument has similar UV LED accessories for the rheometer). The lower plate was replaced with an aluminum plate with a 50-mm diameter quartz window positioned at the center allowing the transmission of both visible and ultraviolet (UV) light. Irradiation was achieved by placing a cluster of four light emitting diodes directly below the quartz window; two different LED clusters were constructed, one using Luxeon Star LXML-PM01-0080 at 530 ± 15 nm for irradiating gels containing eosin Y and the other using Roithner Lasertechnik UVLED-365-250-SMD at 370 ± 12 nm to irradiate gels containing riboflavin. To maintain the LED cluster at a steady operating temperature, it was mounted on an aluminum heat sink attached to a tube that provided a steady flow room temperature air over the heat sink. During irradiation, the light intensity 3 mW/cm^2 with 370 nm light for riboflavin samples and 6 mW/cm^2 with 525 nm light for eosin Y samples controlled by adjusting the input voltage provided by a power supply (Hewlett Packard E3620A). The intensity profile as a function of position at the top of the quartz window was characterized using a fiber optic with "cosine corrector" (Ocean Optics Jaz) and was found to vary less than 5% from the value at the center of the 8-mm diameter sample area.

Oscillatory Shear Storage Modulus Measurement – A circular sample 8-mm in diameter was cut from the gel sheet. The sample was placed onto the upper tool (8-mm aluminum parallel plate) to ensure proper alignment. Then the upper tool was lowered to bring the sample in contact with the lower plate. The normal force reading began to register at a gap thickness that was consistent with the spacer's thickness (within 2%). To ensure good contact between the specimen and the tools, the gap was reduced to 90% of the

nominal sample thickness with typical initial normal force registering ~2 N. To prevent gel dehydration, the sample was enclosed in a chamber containing a wet sponge that kept surrounding environment saturated with water vapor (Figure 2.1b). The chamber also had an inlet for gas flow so that the chamber's environment could have oxygen present or absent by purging the chamber with air or argon, respectively.

The temperature of the sample was maintained at 24 ± 1ºC (Omega HH059 thermocouple). Once the sample was in contact with the lower plate, a 15-minute interval was allowed for thermal equilibration before the linear storage modulus was measured at a frequency of 0.3 rad/s using an oscillatory stress amplitude of 30 Pa (in the linear regime). The storage modulus was measured every minute for 50 minutes, including 10 minutes prior to irradiation (to verify that gelation was complete), 30 minutes during irradiation and 10 minutes after cessation of irradiation (to determine if cross-linking continued, i.e., if there is significant "dark reaction"). Each condition was repeated at least 3 times to obtain the reported mean and standard deviation.

2.3 RESULTS

During the 30-minute irradiation period (3 mW/cm^2 at 370 nm), the average rate of change of the storage modulus, dG'/dt, of riboflavin samples was 27.2 ± 4.7 Pa/min in the presence of oxygen (in air) and decreased to being indistinguishable from zero in the absence of oxygen (in argon), or by addition of 100 mM sodium azide or 20 mM of ascorbic acid (Figure 2.2). Similarly, during irradiation (6 mW/cm^2 at 525 nm) of eosin Y samples, dG'/dt = 25.8 ± 5.1 Pa/min in air and indistinguishable from zero in argon (Figure 2.2a). In eosin Y samples, singlet oxygen scavengers reduce the rate of change of

modulus, but it remains distinguishable from zero in the presence of 100 mM sodium azide and 20 mM ascorbic acid. The greater effect of singlet oxygen quenchers on the rate of cross-linking in riboflavin samples is reinforced by the low concentration of sodium azide that reduces the rate to indistinguishable from zero (as little as 10mM sodium azide) and the substantial concentration of ascorbic acid that is required to effectively eliminate cross-linking in eosin Y samples (at least 100 mM ascorbic acid). In both riboflavin and eosin Y samples, ascorbic acid has a greater inhibitory effect than sodium azide.

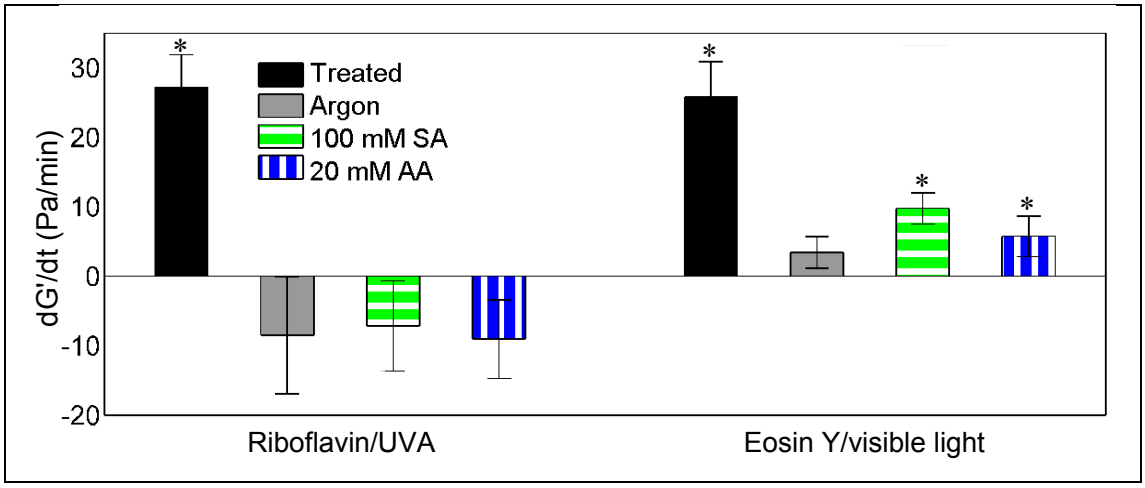

Figure 2.2. Average rate of change in storage modulus during 30-minute irradiation of collagen gels containing (left) 0.05% riboflavin (370 nm at 3 mW/cm^2) and (right) 0.02% eosin Y (530 ± 15 nm at 6 mW/cm^2). Four conditions are examined: under air (Treated), in the absence of oxygen (Argon), and under air with singlet oxygen quenchers: sodium azide (100 mM SA) and ascorbic acid (20 mM AA). The asterisk indicates a statistically significant rate that is distinguishable from 0 ($p < 0.05$). (N = 3 to 12)

2.4 DISCUSSION

Singlet oxygen mediates collagen cross-linking for both riboflavin and eosin Y – Riboflavin/UVA clinical treatment for keratoconus relies the formation of protein-protien cross-links in the cornea to enhance tissue strength and resist enzymatic degradation[34, 35]. Although there are contradictory reports in the literature[36], McCall, Kraft, *et al.*[37] found that corneal cross-linking induced by riboflavin/UVA proceeds via the singlet oxygen pathway. In accord with McCall *et al.* the present results indicate that riboflavin/UVA cross-linking requires oxygen and that singlet oxygen specifically mediates cross-linking (Figure 2.2).

Collagen cross-linking activated by eosin Y with visible light exhibits very similar behavior to riboflavin/UVA. In particular, oxygen is required for cross-linking and the addition of singlet oxygen quenchers (sodium azide and ascorbic acid) inhibits cross-linking (Figure 2.2). This is consistent with the fact that eosin Y generates singlet oxygen upon irradiation in the presence of molecular oxygen[38, 39], and that eosin photosensitized cross-linking of peptides mainly occurs through a process mediated by singlet oxygen[40].

Thus, the photosensitized cross-linking reactions for both riboflavin/UVA and eosin Y/visible proceed via the singlet oxygen pathway. It has been demonstrated that photodynamic reactions proceeding through the singlet oxygen pathway yield similar chemical modifications even when different sensitizers are used[41-43]. Based on this understanding, it is expected that the cross-links formed by eosin Y/visible light should be equivalent to the stable ones formed by riboflavin/UVA light. Collagen cross-links

induced by riboflavin/UVA are stable to chemical, heat, and enzymatic degradation, providing treatment efficacy that lasts for years[22].

Importance of histidine, arginine and lysine in collagen cross-linking by singlet oxygen – Considerable molecular insight into corneal collagen cross-linking can be gained by considering the literature on the reactions of singlet oxygen and proteins. Motivated by the importance of protein-protein cross-linking in aging, photodynamic therapy and tissue engineering, extensive studies have examined cross-linking induced by singlet oxygen in crystallins[9, 44, 45], ribonuclease A[10], spectrin[46], fibrin[47], fibrinogen[47], and collagen[48]. Photo-oxidation of susceptible amino acids is the primary photodynamic process; subsequent covalent cross-linking occurs via secondary, light independent reactions[12, 49]. There are only five amino acids that are susceptible to photo-oxidation: tryptophan, tyrosine, cysteine, methionine and histidine[13, 50, 51]. These photo-oxidized adducts of these amino acids can react with other amino acids; and some of these reactions produce covalent cross-links.

In relation to therapeutic cross-linking, the relative importance of each of the five photo-oxidizable amino acids can be evaluated based on their relative reactivity with singlet oxygen, their propensity to produce cross-links, and their relative abundance in the predominant protein present in the cornea and sclera—collagen type I (Table 2.1). While the amino acids that are very reactive with singlet oxygen are tryptophan and cysteine[52, 53], neither of these is present in collagen type I[54]. While methionine is reactive toward singlet oxygen and is present in collagen type I, it does not participate in the cross-linking reactions[10, 12, 55]. While tyrosines can be photo-oxidized to form cross-links[12, 36], the

presence of oxygen actually inhibits tyrosine modification and cross-linking (it occurs through a type I reaction pathway)[8, 36]. Furthermore, dityrosine formation was not observed in the cross-linking process mediated by singlet oxygen in proteins, peptides, or model tyrosine copolymers[10, 55, 56]. Therefore, among the five photo-oxidizable amino acid residues, tryptophan, cysteine, methionine, and tyrosine are not expected to be significant in the corneal and sclera cross-linking induced by the photosensitizers in this study. Therefore, we direct our attention to histidine.

Table 2.1. Rate constants for chemical reactions between singlet oxygen and photo-oxidizable amino acids and the quantity of each amino found in collagen type I.

Amino acid	$k_{^1O_2}$ x 10^{-7} $M^{-1}s^{-1}$	Mole %
Tryptophan	1.3-3	0
Cysteine	0.89	0
Methionine*	1.6	0.5
Tyrosine#	0.8	0.4
Histidine	3.2-3.4	0.6

*Methionine is not known to produce cross-links
#Tyrosine cross-linking is inhibited by oxygen

Table 2.2. The quantity of amino acid containing amine group(s) present in collagen type I.

Amino Acid	Mole %
Glutamine	0
Asparagine	0
Arginine	4.7
Lysine	2.8

Photo-oxidation of histidine via a singlet oxygen mediated process has been examined in free histidine amino acid[12, 42, 52, 57], histidine model compounds[10, 51], histidine in peptides[40, 52] and proteins[9, 10, 46, 55, 58]. Photo-oxidation of histidine can lead to cross-linking. Studies using rose bengal as a photosensitizer found histidine residues are necessary for cross-linking; blocking the histidine residues leads to a decrease in cross-link formation in crystallin[9] and ribonuclease A[9, 10]. Even though crystallin also

contains tryptophan and tyrosine and ribonuclease A also contains tyrosine, methionine, and cysteine, these amino acids have negligible roles in cross-linking mediated by singlet oxygen. Proteins without histidine (e.g. melittin and bovine pancreatic trypsin inhibitor) do not form cross-links in the presence of singlet oxygen[10]. Although the exact mechanism of cross-linking involving histidine is not well understood, cross-linking appears to occur through interaction between the photo-oxidized histidine and an amine group[10, 12, 40, 46, 55] or with another histidine[43, 51]. Model copolymers containing histidine can form photodynamic cross-links with other copolymers containing lysine[51] or histidine[43, 51] through the singlet oxygen pathway. Protecting the amine groups in protein inhibits photodynamic cross-linking[10, 43, 55].

Of the four amino acid residues that contain amine group(s), only two are present in collagen type I (Table 2.2). Based on their high abundance in collagen type I, a photo-oxidized histidine is most likely to react with an arginine or lysine. The specific rates of cross-linking reactions depend on the proximity of one of these amino acids to a photo-oxidized histidine and the degree of "exposure" of the side chains for reaction[13].

Peroxidic species are intermediate products in photodynamic cross-linking – Photo-oxidation of tryptophan and tyrosine residues has been investigated, establishing the structures of the peroxides intermediates formed and of some of their decomposition products[59-63]. However, tryptophan is not present in type I collagen; and tyrosine produces cross-links via a type I mechanism, which appears to be negligible in riboflavin/UVA and eosin Y/visible photodynamic cross-linking. Unfortunately, there is scant literature regarding the oxidation mechanism of histidine (or related compounds) in

aqueous media at physiological pH. Photolysis of N-benzoyl-His has been examined under basic conditions (pH 11), such that the imidazole ring is susceptible to nucleophilic attack (leading to formation of urea, N-benzoyl-Asp and N-benzoyl-Asn)[64, 65]. Oxidation of substituted imidazole derivatives in organic solvents gives rise to peroxidic species[66], which have been hypothesized to be intermediates in subsequent reactions, such as cross-linking of oxidized amino acids with unmodified residues[12, 43, 51].

Davies *et al.*[67] have performed the most thorough examination to date of the reactions of singlet oxygen with histidine, including comparison of multiple sensitizers and various histidine derivatives (free His amino acid, model compounds, and His in a peptide), examining the lifetimes and subsequent reactions of the peroxides that form, and solving the structures of some of the major photo-products. They performed detailed structural analysis of the radicals and relatively stable intermediate products formed via reactions of singlet oxygen with His, N-Ac-His, imidazole, 4(5)-methylimidazole and 3-(Imidazol-4-yl)propionic acid (IPA).

Using these solved structures, they searched for analogous adducts in a simple tripeptide, Gly-His-Gly (GHG), subjected to the same photo-oxidation conditions. Analysis of the reaction products by HPLC/MS revealed three fractions that could be resolved from GHG by HPLC, which differed in mass by the addition of two, three and five oxygen atoms, respectively; in contrast, only two added oxygens were present in the structures formed upon photo-oxidation of the model compounds. NMR spectra of the crude photo-oxidized-GHG solutions gave “weak, unidentified signals;” comparison with the spectral features of the established products of photo-oxidation of simpler compounds revealed no

evidence for the formation of analogous species. Davies speculates that peptide bond formation deactivates the lone pair on the nitrogen of the α-amino group, giving histidines in proteins a different reaction profile than the model compounds. To date, the structures formed during photo-oxidation of histidine in proteins are not known.

Potential role of favorable sensitizer-protein interactions – Eosin Y is commonly used as a staining agent since it binds to proteins. Its affinity to collagen is observed in how favorably it partitions into the cornea and sclera (Chapter 4). Specifically, Waheed *et al.*[68] found that histidine, lysine, and arginine residues bind electrostatically to eosin Y to produce a stable, water-soluble protein-dye complex. It is known that protein-binding of photosensitizers inhibits quenching of the singlet oxygen they produce during irradiation: for example, rose bengal binds to albumin and the addition of sodium azide only moderately reduces the rate of photo-oxidation of albumin by rose bengal (in contrast to the severely reduced rate observed for peptides that do not bind rose Bengal)[69]. A similar effect may be evident in the case of eosin Y bound to collagen (preferentially at histidine residues): singlet oxygen quenchers moderately suppress photo-oxidation of collagen by eosin Y (in contrast to the severely reduced rate observed with a photosensitizer that does not bind to collagen, Figure 2.2). Perhaps binding of eosin Y molecules to histidines increases the likelihood that a singlet oxygen generated during irradiation encounters a histidine before being quenched by sodium azide or ascorbic acid. For riboflavin, no such binding effect is present (Chapter 4), so singlet oxygen must diffuse through the quencher solution to reach histidine, consistent with the relative ease of preventing cross-link formation using singlet oxygen quenchers.

2.5 CONCLUSION

The present experimental results, along with prior literature, suggest collagen cross-linking induced by riboflavin/UVA and eosin Y/visible light are both mediated by singlet oxygen. In addition, histidine is the most likely amino acid to play a major role in the collagen cross-linking reactions in the cornea and sclera. Subsequent reactions with the photo-oxidized histidine residue are likely to involve an arginine, lysine, or another histidine. Cross-links formed via this pathway are found to be stable to chemical treatment using 2-mercaptoethanol, heat treatment by boiling in water for five minutes, and enzymatic degradation by pepsin[22]. These cross-links generated by riboflavin/UVA are found to be stable in the cornea for at least 5 years[20], and since eosin Y generates cross-links via the same reaction pathway they should be stable as well.

2.6 ACKNOWLEDGEMENTS

This work includes contributions from Alex Wang and Dr. Matthew Mattson. Undergraduate Alex Wang assisted in collagen gel preparation and data collection. Dr. Matthew Mattson built the rheometer light unit.

2.7 BIBLIOGRAPHY

1. Henderson, B. W., *Photodynamic Therapy: Basic Principles and Clinical Applications*. 1992: Taylor & Francis, Inc.
2. Henderson, B.W., Dougherty, T.J., *How Does Photodynamic Therapy Work?* Photochemistry and Photobiology, 1992. **55**(1): p. 145.
3. Khurana, M., H.A., Collins, A., Karotki, H.L., Anderson, D.T., Cramb B.C., Wilson, *Quantitative In Vitro Demonstration of Two-Photon Photodynamic Therapy Using Photofrin and Visudyne.* Photochemistry and Photobiology, 2007. **83**(6): p. 1441.
4. Chan, B.P., T.Y., Hui, O.C., Chan, K.F., So, W., Lu, K.M., Cheung*, et al.*, *Photochemical Cross-linking for Collagen-based Scaffolds: A Study on Optical Properties, Mechanical Properties, Stability, and Hematocompatibility.* Tissue Engineering, 2007. **13**(1): p. 73.
5. Chan, B.P., K.F., So, *Photochemical Crosslinking Improves the Physicochemical Properties of Collagen Scaffolds.* Journal of Biomedical Materials Research - Part A, 2005. **75A**(3): p. 689.
6. Spoerl, E., Huhle, M., Seiler, T., *Induction of cross-links in corneal tissue.* Experimental Eye Research, 1998. **66**(1): p. 97-103.
7. Wollensak, G., Spoerl, E., *Collagen Crosslinking of Human and Porcine Sclera.* Journal of Cataract and Refractive Surgery, 2004. **30**(3): p. 689-695.
8. Webster, A., Britton, D., Apap-Bologna, A., Kemp, G., *A Dye-photosensitized Reaction that Generates Stable Protein-Protein Crosslinks.* Analytical Biochemistry, 1989. **179**(1): p. 154.

9. Balasubramanian, D., Du, X., Zigler, J.S., *The Reaction of Singlet Oxygen with Proteins, with Special Reference to Crystallins.* Photochemistry and Photobiology, 1990. **52**(4): p. 761.

10. Shen, H.R., Spikes, J.D., Kopecková, P. , Kopecek, J., *Photodynamic Crosslinking of Proteins II. Photocrosslinking of a Model Protein-Ribonuclease A.* Journal of Photochemistry and Photobiology B - Biology, 1996. **35**(3): p. 213.

11. Foote, C.S., *Definition of Type I and Type II Photosensitized Oxidation.* Photochemistry and Photobiology, 1991. **54**(5): p. 659.

12. Verweu, H., Steveninck, J.V., *Model Studies on Photodynamic Cross-linking.* Photochemistry and Photobiology, 1982. **35**(2): p. 265.

13. Spikes, J.D., MacKnight, M.L., *Dye-Sensitized Photooxidation of Proteins.* Annals of the New York Academy of Sciences, 1970. **171**(1 International): p. 149.

14. Rabinowitz, Y.S., *Keratoconus.* Survey of Ophthalmology, 1998. **42**(4): p. 297-319.

15. Krachmer, J.H., Feder, R.S., Belin, M.W., *Keratoconus and Related Noninflammatory Corneal Thinning Disorders.* Survey of Ophthalmology, 1984. **28**(4): p. 293-322.

16. Randleman, J.B., *Post-laser in-situ Keratomileusis Ectasia: Current Understanding and Future Directions.* Current Opinion in Ophthalmology, 2006. **17**(4): p. 406.

17. Binder, P.S., *Ectasia After Laser in situ Keratomileusis.* Journal of Cataract and Refractive Surgery, 2003. **29**(12): p. 2419-29.

18. Curtin, B.J., *The Myopias: Basic Science and Clinical Management*. 1985: Harpercollins College Div.

19. McBrien, N. A., Gentle, A., *Role of the sclera in the development and pathological complications of myopia.* Progress In Retinal And Eye Research, 2003. **22**(3): p. 307-338.

20. Wollensak, G., *Crosslinking Treatment of Progressive Keratoconus: New Hope.* Current Opinion in Ophthalmology, 2006. **17**(4): p. 356.

21. Raiskup-Wolf, F., Hoyer, A., Spoerl, E., Pillunat, L.E., *Collagen Crosslinking with Riboflavin and Ultraviolet-A light in Keratoconus: Long-term Results.* Journal of Cataract and Refractive Surgery, 2008. **34**(5): p. 796.

22. Wollensak, G., Redl, B., *Gel Electrophoretic Analysis of Corneal Collagen After Photodynamic Cross-linking Treatment.* Cornea, 2008. **27**(3): p. 353.

23. Kao, W.W.Y., Vergnes, J.P. , Ebert, J. , Sundar-Raj, C.V. , Brown, S.I., *Increased Collagenase and Gelatinase Activities in Keratoconus.* Biochemical and Biophysical Research Communications, 1982. **107**(3): p. 929.

24. Ihalainen, A., Salo, T., Forsius, H. , Peltonen, L., *Increase in Type I and Type IV Collagenolytic Activity in Primary Cultures of Keratoconus Cornea.* European Journal of Clinical Investigation, 1986. **16**(1): p. 78.

25. Wollensak, G., Iomdina, E., *Long-term Biomechanical Properties of Rabbit Sclera After Collagen Crosslinking Using Riboflavin and Ultraviolet A (UVA).* Acta Ophthalmologica, 2009. **87**(2): p. 193-198.

26. Tano, Y., *Pathologic Myopia: Where Are We Now?* American Journal of Ophthalmology, 2002. **134**(5): p. 645-60.

27. Kymionis, G. D., Diakonis, V.F., Kalyvianaki, M., Portaliou, D., Siganos, C., Kozobolis, V.P.*, et al.*, *One-Year Follow-up of Corneal Confocal Microscopy After Corneal Cross-Linking in Patients With Post Laser In Situ Keratosmileusis Ectasia and Keratoconus.* American Journal of Ophthalmology, 2009. **147**(5): p. 774.

28. Wollensak, G., Iomdina, E., Dittert, D., Salamatina, O., Stoltenburg G, *Crosslinking of Scleral Collagen in the Rabbit Using Riboflavin and UVA.* Acta Ophthalmologica Scandinavica, 2005. **83**(4): p. 477.

29. Mazzotta, C., Balestrazzi, A., Traversi, C., Baiocchi, S., Caporossi, T., Tommasi, C.*, et al.*, *Treatment of Progressive Keratoconus by Riboflavin-UVA-induced Cross-linking of Corneal Collagen: Ultrastructural Analysis by Heidelberg Retinal Tomograph II In Vivo Confocal Microscopy in Humans.* Cornea, 2007. **26**(4): p. 390.

30. Wollensak, G., Spörl, E., Reber, F., Pillunat, L., Funk, R., *Corneal Endothelial Cytotoxicity of Riboflavin/UVA Treatment In Vitro.* Ophthalmic Research, 2003. **35**(6): p. 324.

31. Wollensak, G., Iomdina, E., *Biomechanical and Histological Changes After Corneal Crosslinking with and without Epithelial Debridement.* Journal of Cataract & Refractive Surgery, 2009. **35**(3): p. 540-546.

32. Ashwin, P.T., McDonnell, P.J., *Collagen Cross-linkage: A Comprehensive Review and Directions for Future Research.* British Journal of Ophthalmology, 2010. **94**(8): p. 965.

33. Khan, S.A., Plitz, I.M., Frantz, R.A., *In Situ Technique for Monitoring the Gelation of UV Curable Polymers.* Rheologica Acta, 1992. **31**(2): p. 151.

34. Kohlhaas, M., Spoerl, E., Schilde, T., Unger, G., Wittig, C. Pillunat, L.E., *Biomechanical Evidence of the Distribution of Cross-links in Corneas Treated with Riboflavin and Ultraviolet A Light.* Journal of Cataract & Refractive Surgery, 2006. **32**(2): p. 279.

35. Spoerl, E., Wollensak, G., Seiler, T., *Increased Resistance of Crosslinked Cornea Against Enzymatic Digestion.* Current Eye Research, 2004. **29**(1): p. 35.

36. Kato, Y., Uchida, K., Kawakishi, S., *Aggregation of Collagen Exposed to UVA in the Presence of Riboflavin: A Plausible Role of Tyrosine Modification.* Photochemistry and Photobiology, 1994. **59**(3): p. 343.

37. McCall, A.S., S., Kraft, H.F., Edelhauser, G.W., Kidder, R.R., Lundquist, H.E., Bradshaw*, et al.*, *Mechanisms of Corneal Tissue Cross-linking in Response to Treatment with Topical Riboflavin and Long-Wavelength Ultraviolet Radiation (UVA).* Investigative Ophthalmology & Visual Science. **51**(1): p. 129.

38. Hall, R.D., C.F., Chignell., *Steady-state Near infrared Detection of Singlet Molecular Oxygen: A Stern-Volmer Quenching Experiment with Sodium Azide* Photochemistry and Photobiology, 1987. **45**(4): p. 459.

39. Amat-Guerri, F., López-González, M.M.C., Martínez-Utrilla, R., Sastre, R., *Singlet Oxygen Photogeneration By Ionized and Un-ionized Derivatives of Rose Bengal and Eosin Y in Diluted Solutions.* Journal of Photochemistry and Photobiology A - Chemistry, 1990. **53**(2): p. 199-210.

40. Miskoski, S., Garca, N.A., *Influence of the Peptide Bond on the Singlet Molecular Oxygen-mediated (O_2[g]) Photooxidation of Histidine and Methionine Dipeptides. A Kinetic Study.* Photochemistry and Photobiology, 1993. **57**(3): p. 447-452.

41. Foote, C.S., Wexler, S., *Singlet Oxygen. A Probable Intermediate in Photosensitized Autoxidations.* Journal of the American Chemical Society, 1964. **86**(18): p. 3880.

42. Matheson, I.B.C., Lee, J., *Chemical Reaction Rates of Amino Acids with Singlet Oxygen.* Photochemistry and Photobiology, 1979. **29**(5): p. 879.

43. Shen, H.R., J.D., Spikes, Smith, C.J., Kopecek, J., *Photodynamic Cross-linking of Proteins IV. Nature of the His-His Bond(s) Formed in the Rose Bengal-photosensitized Cross-linking of N-benzoyl-histidine.* Journal of photochemistry and Photobiology A - Chemistry, 2000. **130**(1): p. 1.

44. Criado, S., Soltermann, A.T., Marioli, J.M., García, N.A., *Sensitized Photooxidation of Di- and Tripeptides of Tyrosine.* Photochemistry and Photobiology, 1998. **68**(4): p. 453.

45. Zigler, J. S., Jernigan, H.M., Perlmutter, N.S., Kinoshita, J.H., *Photodynamic Cross-linking of Polypeptides in Intact Rat Lens.* Experimental Eye Research, 1982. **35**(3): p. 239-249.

46. Verweij, H., Dubbelman, T.M.A.R., Stevenincka, J.V., *Photodynamic Protein Cross-linking.* Biochimica et Biophysica Acta - Biomembranes, 1981. **647**(1): p. 87.

47. Hemmendorff, B., Brandt, J., Andersson, L.O., *Photosensitized Labeling of Solvent-exposed Parts of Proteins. Studies on Fibrinogen and the Fibrinogen-fibrin Conversion.* Biochimica et Biophysica Acta - Protein Structure, 1981. **667**(1): p. 15.

48. Ramshaw, J.A.M., Stephens, L.J., Tulloch, P.A., *Methylene Blue Sensitized Photo-oxidation of Collagen Fibrils.* Biochimica et Biophysica Acta - Protein Structure and Molecular Enzymology, 1994. **1206**(2): p. 225.

49. Dubbelman, T.M., Haasnoot, C., Steveninck, J.V., *Temperature Dependence of Photodynamic Red Cell Membrane Damage.* Biochimica et Biophysica Acta, 1980. **601**(1): p. 220-7.

50. Michaeli, A., Feitelson, J., *Reactivity of Singlet Oxygen Toward Large Peptides.* Photochemistry and Photobiology, 1995. **61**(3): p. 255.

51. Shen, H.R., Spikes, J.D., Kopeceková, P., Kopecek, J., *Photodynamic Crosslinking of Proteins I. Model Studies Using Histidine-and Lysine-containing N-(2-hydroxypropyl) Methacrylamide Copolymers.* Journal of Photochemistry and Photobiology B - Biology, 1996. **34**(2-3): p. 203.

52. Michaeli, A., Feitelson, J., *Reactivity of Singlet Oxygen Toward Amino Acids and Peptides.* Photochemistry and Photobiology, 1994. **59**(3): p. 284.

53. Davies, M. J., *Singlet Oxygen-mediated Damage to Proteins and Its Consequences.* Biochemical and Biophysical Research Communications, 2003. **305**(3): p. 761.

54. Eastoe, J. E., *Amino Acid Composition of Mammalian Collagen and Gelatin* Biochemical Journal, 1955. **61**(4): p. 589-600.

55. Dubbelman, T., Goeij, A.F. , J.V., Steveninck, *Photodynamic Effects of Protoporphyrin on Human Erythrocytes. Nature of the Cross-linking of Membrane Proteins.* Biochimica et Biophysica Acta - Biomembranes, 1978. **511**(2): p. 141.

56. Spikes, J.D., Shen, H.R., Kopecková, P., Kopecek, J., *Photodynamic Crosslinking of Proteins III. Kinetics of the FMN-and Rose Bengal-sensitized Photooxidation and Intermolecular Crosslinking of Model Tyrosine-containing N-(2-hydroxypropyl) Methacrylamide Copolymers.* Photochemistry and Photobiology, 1999. **70**(2): p. 130.

57. Nilsson, R., Merkel, P.B., Kearns, D.R., *Unambiguous Evidence for the Participation of Singlet Oxygen (1) in photodynamic oxidation of amino acids.* Photochemistry and Photobiology, 1972. **16**(2): p. 117.

58. Miranda, M.A., Castell, J.V., Hernández, D., Gómez-Lechón, M.J., Bosca, F., Morera, I.M.*, et al.*, *Drug-Photosensitized Protein Modification: Identification of the Reactive Sites and Elucidation of the Reaction Mechanisms with Tiaprofenic Acid/Albumin as Model System.* Chemical Research in Toxicology, 1998. **11**(3): p. 172.

59. Wright, A., Bubb, W.A., Hawkins, C.L., Davies, M.J., *Singlet Oxygen-mediated Protein Oxidation: Evidence for the Formation of Reactive Side Chain Peroxides on Tyrosine Residues.* Photochemistry and Photobiology, 2002. **76**(1): p. 35-46.

60. Wright, A., Hawkins, C.L., Davies, M.J., *Singlet Oxygen-mediated Protein Oxidation: Evidence for the Formation of Reactive Peroxides.* Redox Report, 2000. **5**(2-3): p. 159-161.

61. Nakagawa, M., Watanabe, H., Kodato, S., Okajima, H., Hino, T., Flippen, J.L.*, et al.*, *Valid Model for Mechanism of Oxidation of Tryptophan to Formylkynurenine - 25 Years Later.* Proceedings of the National Academy of Sciences, 1977. **74**(11): p. 4730-4733.

62. Saito, I., Matsuura, T., Nakagawa, M., Hino, T., *Peroxidic Intermediates in Photosensitized Oxygenation of Tryptophan Derivatives.* Accounts of Chemical Research, 1977. **10**(9): p. 346-352.

63. Langlois, R., Ali, H., Brasseur, N., Wagner, J. R., Vanlier, J. E., *Biological-activities of Phthalocyanines-IV. Type-II Sensitized Photo-oxidation of L-Tryptophan and Cholesterol by Sulfonated Metallo Phthalocyanines.* Photochemistry and Photobiology, 1986. **44**(2): p. 117-123.

64. Tomita, M., Irie, M., Ukita, T., *Sensitized Photooxidation of Histidine and Its Derivatives. Products and Mechansim of Reaction.* Biochemistry, 1969. **8**(12): p. 5149-&.

65. Tomita, M., Irie, M., Ukita, T., *Sensitized Photooxidation of N-benzoyl Histidine.* Tetrahedron Letters, 1968(47): p. 4933-&.

66. Kang, P., Foote, C.S., *Photosensitized Oxidation of C-13,N-15-labeled Imidazole Derivatives.* Journal of the American Chemical Society, 2002. **124**(32): p. 9629-9638.

67. Agon, V.V., Bubb, W.A., Wright, A., Hawkins, C.L., Davies, M.J., *Sensitizer-mediated Photooxidation of Histidine Residues: Evidence for the Formation of Reactive Side-chain Peroxides.* Free Radical Biology and Medicine, 2006. **40**(4): p. 698-710.

68. Waheed, A.A., Rao, K.S., Gupta, P.D., *Mechanism of Dye Binding in the Protein Assay Using Eosin Dyes.* Analytical Biochemistry, 2000. **287**(1): p. 73.

69. Alarcon, E., Edwards, A.M., Aspee, A., Borsarelli, C.D., Lissi, E.A., *Photophysics and Photochemistry of Rose Bengal Bound to Human Serum Albumin.* Photochemical & Photobiological Sciences, 2009. **8**(7): p. 933-943.

Chapter 3

Collagen Cross-linking Kinetics

3.1 INTRODUCTION

Keratoconus is a corneal ectasia associated with progressive corneal thinning and protrusion resulting in a conical shaped cornea. This disease has a prevalence of 1 in 2,000 with no race or gender bias[1]. Pioneering research of Wollensak, Seiler, and Spoerl demonstrated that photodynamic corneal collagen cross-linking using riboflavin and UVA can halt the progression of keratoconus[2]. The concept underlying the treatment is revolutionary, however, the phototoxicity of riboflavin and UVA results in certain limitations and drawbacks. The combination of riboflavin and UVA is toxic to both keratocytes and endothelial cells[3, 4]. The endothelium is responsible for maintaining corneal transparency and the cells do not regenerate in humans. Therefore, the treatment parameters (riboflavin concentration, duration of drug delivery prior to irradiation and frequent reapplication of riboflavin during irradiation) are carefully designed to restrict toxicity to the anterior 350 μm of the stroma[5].

In the current clinical protocol, topical application the drug solution (0.1% riboflavin with 20% dextran) to the cornea is repeated every 2 minutes for 30 minutes before irradiating,

and every 5 minutes during the 30 minute irradiation with 3 mW/cm^2 UVA. The high riboflavin concentration is necessary to prevent significant UVA light from penetrating more than 350 µm. Thirty minutes of topical application prior to irradiation is required to establish the protective riboflavin concentration in the stroma[5]. The treatment cannot be used with corneas under 400 µm because it then results in "significant necrosis and apoptosis of endothelial cells"[4]. Almost all of the keratocytes in the anterior 300-350 µm of the stroma undergo apoptosis, which results in corneal edema[3, 6-8]. The resulting stromal haze persists for weeks to months after treatment; full recovery of the keratocyte population requires 6 to 12 months[8, 9].

To retain the benefits of corneal cross-linking and reduce the toxicity of the treatment, it has been suggested that a photosensitizer that is activated by visible light might be used[10]. *In vitro* results suggest that Eosin Y (a photosensitizer with an absorption peak at 514 nm) can produce cross-linking in the cornea (Chapter 6) and sclera[11], comparable to riboflavin/UVA treatment. Eosin Y has been approved by the US-FDA for use in the body[12]. Safety studies of eosin Y activated by green light in a rabbit model show little keratocyte apoptosis, using eosin Y concentration and irradiation conditions that produce comparable cross-linking to the riboflavin/UVA treatment for keratoconus (Chapter 6). No endothelial toxicity was observed with eosin Y/visible light, opening the way to treating patients whose cornea is less than 400 µm thick due to advanced keratoconus or other conditions, such as post-LASIK ectasia[13]. In relation to the application of collagen cross-linking to treat degenerative myopia[14, 15], *in vivo* studies of eosin Y activated by visible light showed no retinal toxicity in a guinea pig model[11], in contrast to early *in vivo* results with riboflavin/UVA[4].

Here we examine the relative rates of cross-linking produced by both the clinical therapy (riboflavin/UVA) and the pre-clinical therapy (eosin Y/visible light). The rate of change of the apparent shear modulus is measured as a function of photosensitizer concentration and irradiation intensity using photorheology, which is widely used to study photopolymerization kinetics[16-18]. Collagen gel is used as a substrate because of its excellent uniformity and reproducibility.

3.2 METHODS

Collagen Gel Preparation – Similar method used in Chapter 2 was used for preparing gel. Briefly, a mixture of 2.5 g gelatin from bovine skin and 6.5 mL dulbecco's phosphate buffered saline (DPBS) was heated at 75°C for 30 ± 1 minutes to dissolve all the gelatin. After the gelatin solution was removed from the heat bath, 1 mL of an eosin Y or riboflavin stock solution having 10 times the final desired concentration was added to the 9 mL gelatin solution. The final mixture contained 25% w/w gelatin and the desired concentration of eosin Y or riboflavin. Six concentrations of eosin Y (0.005, 0.01, 0.02, 0.04, 0.1 and 0.2%) and 8 concentrations of riboflavin (0.005, 0.01, 0.03, 0.05, 0.07, 0.1, 0.3, and 0.5%) were examined as well as controls without photosensitizers.

To produce a uniform layer of gel, a mold was prepared using a Teflon spacer between two Plexi-glass plates, which were held together with clamps (Figure 3.1a). The Teflon spacer provided a controlled gap with the desired gel thickness; four spacer thicknesses were used (250, 500, 1000 and 1500 μm). The warm solution was dispensed into the warm mold; then the filled mold was wrapped in aluminum foil to prevent dehydration

and stored at ~4°C for at least 8 hours to form a solid gel. All samples were measured within 48 hours of the beginning of gel preparation.

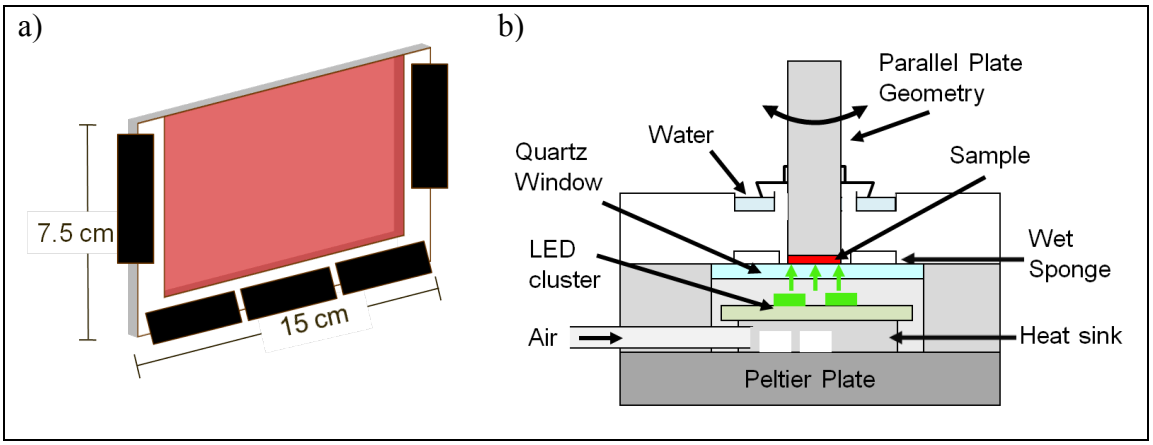

Figure 3.1. a) Forming a gel in a mold made of two Plexi-glass plates and a Teflon spacer all held together by clamps. **b)** A schematic of the photorheology set up for measuring real-time changes in sample modulus. The chamber with the sponge and water at the top sealed off by a cap prevented sample dehydration. LEDs below the quartz window provided light for sample irradiation.

Photorheology Apparatus – The same apparatus was used as in Chapter 2. Briefly, Collagen gel photorheology was performed on a stress-controlled shear rheometer (TA Instrument AR1000). The lower, stationary tool was modified to deliver light to the sample. The lower plate was replaced with an aluminum plate with a 50-mm diameter quartz window positioned at the center allowing the transmission of both visible and ultraviolet (UV) light. The light intensity (0-6 mW/cm^2) was controlled by adjusting the input voltage (0-16 V) provided by a power supply. The intensity profile as a function of position at the top of the quartz window was found to vary less than 5% from the value at the center of the 8-mm diameter sample area.

Oscillatory Shear Storage Modulus Measurement – An 8-mm diameter sample was cut from the gel sheet. The sample was placed onto the upper tool (8-mm aluminum parallel plate) to ensure proper alignment. Then the upper tool was lowered to bring the sample in contact with the lower plate. To ensure good contact between the specimen and the tools, the gap was reduced to 90% of the nominal sample thickness. To prevent gel dehydration, the sample was enclosed in a chamber containing a wet sponge that kept surrounding air saturated with water vapor (Figure 3.1b).

The temperature of the sample was maintained at 24 ± 1ºC (Omega HH059 thermocouple). Once the sample was in contact with the lower plate, a 15-minute interval was allowed for thermal equilibration before the linear storage modulus was measured at a frequency of 0.3 rad/s using an oscillatory stress amplitude of 30 Pa (in the linear regime). The storage modulus was measured for 50 minutes, including 10 minutes prior to irradiation (to verify that gelation was complete), 30 minutes during irradiation and 10 minutes after cessation of irradiation (to determine if cross-linking continued, i.e., if there is significant "dark reaction"). Each condition was repeated at least 3 times to obtain the reported mean and standard deviation.

3.3 RESULTS

The initial modulus was in the range of 3610 ± 760 Pa and, during the ten minutes prior to irradiation, G' typically decreased slightly, by 50 to 200 Pa (see Appendix for individual G' curves). The change of the storage modulus G' during and after irradiation relative to its value at the beginning of irradiation (i.e., end of the first ten minutes, G'_{10}) is

$$\Delta G' = G'_t - G'_{10} \qquad \text{Equation 1}$$

where G'_t is the modulus at time t. For example, the storage modulus of a sample containing 0.02% eosin Y increased 793 ± 118 Pa while exposed to 6 mW/cm^2 at 530 ± 15 nm (Figure 3.2a). A similar change in modulus (819 ± 85 Pa) was observed in the gelatin containing 0.1% riboflavin sample over the 30-minute irradiation with 3 mW/cm^2 at 370 ± 12 nm (Figure 3.2b).

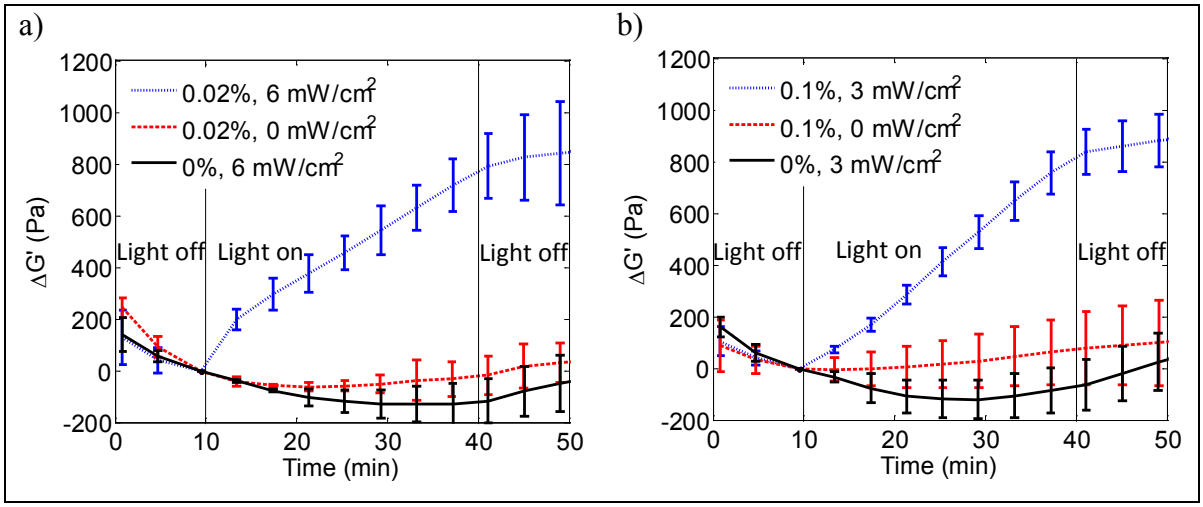

Figure 3.2. Change in storage modulus where $\Delta G' = G'_t - G'_{10}$ as a function of time for 450 µm thick gel samples with **a)** eosin Y and **b)** riboflavin. Samples containing eosin Y were irradiated with green light at 530 ± 15 nm and those containing riboflavin were irradiated with UV light at 370 ± 15 nm. The presence of both drug and light are necessary for enhancing the storage modulus. (N = 3 to 6)

Negligible modulus change was observed over the 30-minute period in controls that either received no light or that contained no sensitizer: without irradiation $\Delta G'$ was -23 ± 76 Pa for (0.02% eosin Y, 0 mW/cm^2) and 72 ± 136 Pa for (0.1% riboflavin, 0 mW/cm^2); and without sensitizer $\Delta G'$ was -125 ± 80 Pa for (0% eosin Y, 6 mW/cm^2) and -74 ± 95 Pa for (0% riboflavin, 3 mW/cm^2). This demonstrates that both sensitizer and irradiation

are necessary to produce the collagen cross-linking that underlies the increase in the storage modulus.

During the 10 minutes after cessation of irradiation, the modulus changes were small and indistinguishable (p-values were > 0.05 for all conditions with respect to the average of all of them together) for all six conditions: 61 ± 136 Pa for (0.02% eosin Y, 6 mW/cm^2), 59 ± 34 Pa for (0.02% eosin Y, 0 mW/cm^2), 84 ± 34 Pa for (0% eosin Y, 6 mW/cm^2), 70 ± 19 Pa for (0.1% riboflavin, 3 mW/cm^2), 32 ± 36 Pa for (0.1% riboflavin, 0 mW/cm^2), and 112 ± 30 Pa for (0% riboflavin, 3 mW/cm^2). Therefore, negligible cross-linking occurs after cessation of irradiation in either system.

Since the presence of both drug and light are necessary for enhancing the gel's modulus, it is of interest to examine how each of these two factors affects the rate of change of G'. The rate of increase was nearly constant throughout the irradiation period. Therefore, the rate of change of G', denoted dG'/dt, was estimated by simply dividing the overall change in G' during irradiation by the irradiation time:

$$\frac{dG'}{dt} = \frac{G'(t_f) - G'(t_i)}{t_f - t_i} \qquad \text{Equation 2}$$

where t_i = 10 minute and t_f = 40 minutes correspond to the beginning and the end of the irradiation period. At a given photosensitizer concentration and sample thickness, the cross-linking rate (manifested by dG'/dt) increases monotonically with irradiation intensity for both eosin Y and riboflavin, approaching a plateau rate (Figure 3.3a).

For a fixed sample thickness that is similar to the thickness of the cornea (450 µm) and a light intensity that saturates the cross-linking rate (6 mW/cm^2 for eosin Y and 3 mW/cm^2 for riboflavin), there is a distinct maximum in *dG′/dt* as a function of photosensitizer concentration for both eosin Y and riboflavin. The peak values are similar for the two sensitizers (dG'/dt_{max} = 27 ± 4.1 Pa/min for eosin Y, and dG'/dt_{max} = 33 ± 4.6 Pa/min for riboflavin). The optimal concentrations, 0.02% eosin Y and 0.05% for riboflavin, correlate with the molar absorptivity of the two compounds (below). The shapes of the peaks in *dG′/dt* as a function of concentration are very similar for eosin Y and riboflavin. For a photosensitizer concentration near the optimal value for a 450 µm thick specimen, *dG′/dt* decreased with increasing sample thickness over the range from 225 to 1350 µm for both eosin Y and riboflavin (Figure 3.3c).

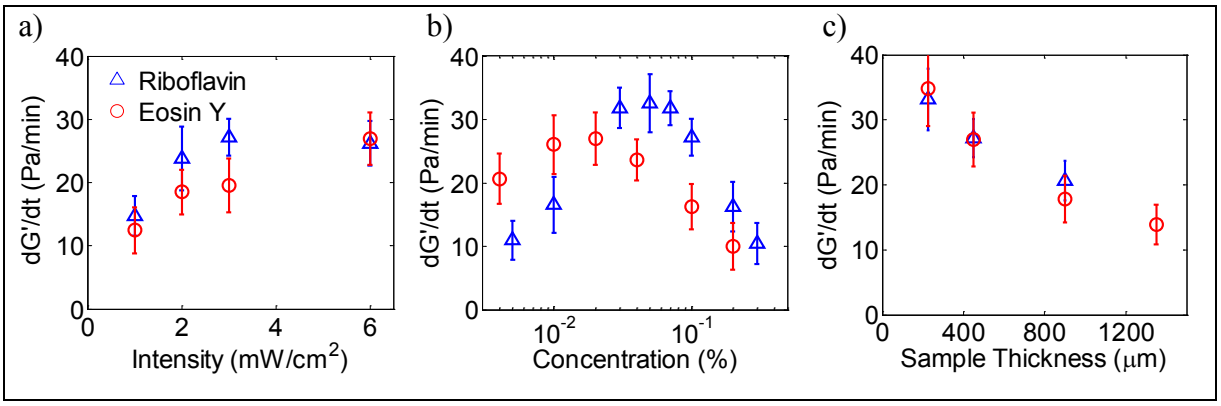

Figure 3.3. Rate of change of the apparent storage modulus **a)** as a function of irradiation intensity at a fixed sample thickness (450 µm) and fixed photosensitizer concentration (0.02% eosin Y, 0.1% riboflavin) **b)** as a function of photosensitizer concentration at fixed sample thickness (450 µm) and fixed irradiation intensity (6 mW/cm^2 for eosin Y, 3 mW/cm^2 for riboflavin) and **c)** as a function of sample thickness at fixed photosensitizer concentration (0.02% for eosin Y and 0.1% for riboflavin) and irradiation intensity (6 mW/cm^2 for eosin Y and 3 mW/cm^2 for riboflavin). Samples containing eosin Y were irradiated with green light at 530 ± 15 nm and those containing riboflavin were irradiated with green light at 370 ± 12 nm. (N = 4 to 14)

3.4 DISCUSSION

Collagen gel photorheology can be used to efficiently characterize the effects of irradiation intensity, photosensitizer concentration, and sample thickness on the rate of collagen cross-linking. Consistent with previous results, collagen can be cross-linked in the presence of a photosensitizer (e.g. riboflavin[19-21], eosin Y[22, 23], rose bengal[19, 24-26], methylene blue[27], and brominated 1,8-naphthalimide[28]) upon irradiation and no cross-linking was observed in the absence of either the sensitizer or irradiation[25, 26].

Collagen cross-linking can also be achieved through non-photo-activated chemical or physical techniques. Chemical agents such as glutaraldehyde and formaldehyde are very effective in cross-linking collagen but they are cytotoxic[25, 26]. Other chemical agents such as carbodiimide and its derivatives are more biocompatible but the reactions are very slow[25]. Collagen cross-linking with physical techniques such as heat, UV irradiation, and gamma irradiation do not form stable cross-links[26]. Photo-activated cross-linking has been demonstrated to be biocompatible[19, 26]. Using photo-activated molecules decouples reaction and diffusion and confers spatial control of cross-linking. Diffusion can occur, then reaction can be initiated by light. Treatment can be targeted to specific locations by delivering the drug and then irradiating selected locations to avoid cross-linking adjacent tissues which can lead to adverse effects. Light activation of the drug also enables control over the depth of cross-linking inside the tissue. The photosensitizing drug can be delivered then allowing time for diffusion to achieve a desirable drug concentration profile before irradiating. In addition, the use of light activation also enables control over the extent of cross-linking by selecting irradiation

parameters (intensity and duration). Photo-activated corneal cross-linking efficacy depends on the collagen cross-linking rate.

The non-monotonic concentration dependence of photo-activated reactions is well known in systems ranging from photodynamic therapy to curing polymers via photopolymerization[29-32]. The optimal concentration reflects the trade-off between the number of sensitizer molecules present and the attenuation of light by the sensitizer: at low concentration, the reaction is limited by the amount of photosensitizer present; beyond the optimal concentration, the reaction is limited by the penetration depth of the irradiation.

The fraction of the sample that receives irradiation of the order of that incident on its surface is characterized by Λ, the ratio of the optical penetration depth (L_p, at which the intensity has been attenuated by $1/e$) to the sample thickness (L), which decreases with increasing photosensitizer concentration in the sample:

$$\Lambda = \frac{L_p}{L} \qquad \text{Equation 3}$$

The light intensity profile in a sample with uniform concentration C of photosensitizer is given by:

$$I(z) = I_o e^{-(\mu + C\varepsilon)z} \qquad \text{Equation 4}$$

where $I(z)$ is the intensity at depth z, I_o is the incident intensity, μ is the sample's absorptivity, and ε is the photosensitizer's molar absorptivity. The normalized cross-

linking rate characterized by $(dG'/dt)/(dG'/dt)_{max}$ initially increases as Λ increases by decreasing concentration at fixed sample thickness until more than half the thickness of the sample receives intensity greater than I_o/e (i.e., until $\Lambda > ½$), where a maximum rate occurs at approximately $\Lambda_{max} = 0.6$ to 0.7 for both eosin Y and riboflavin (Figure 3.4a). Beyond Λ_{max} the rate decreases with increasing Λ, reflecting the loss of efficacy at low sensitizer concentration. When Λ is increased by decreasing sample thickness, $(dG'/dt)/(dG'/dt)_{max}$ increases until it saturates at the value associated with uniform light intensity throughout the sample.

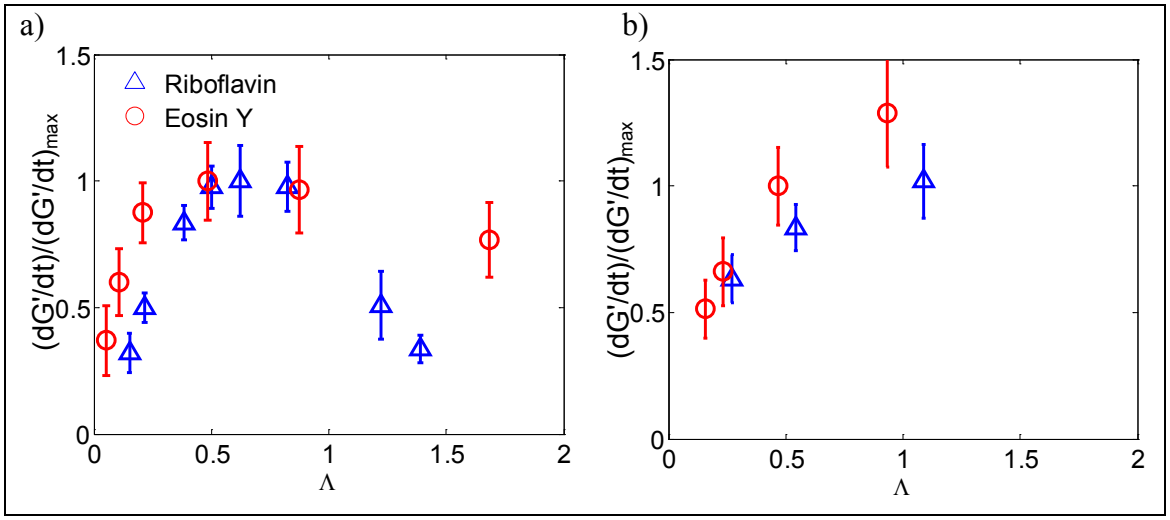

Figure 3.4. Normalized rate of change in modulus $(dG'/dt)/(dG'/dt)_{max}$ as a function of the normalized optical penetration depth evaluated using **a)** data obtained with a fixed sample thickness (450 µm, Figure 3.3b) and **b)** data obtained using a fixed photosensitizer concentration (0.02% eosin Y and 0.1% riboflavin, Figure 3.3c). Eosin Y samples were irradiated with 530 ± 15 nm light at 6 mW/cm^2 and riboflavin samples were irradiated with 370 ± 12 nm light at 3 mW/cm^2. (N = 4 to 14)

The keratoconus treatment protocol approved for clinical use in Europe and undergoing clinical trials in the United States uses 0.1% riboflavin concentration and 3 mW/cm^2 at 370 nm. The drug is applied topically every 2 minutes for 30 minutes followed by UV

irradiation for 30 minutes while applying drops every five minutes. Using the riboflavin diffusion coefficient (D = 79 μm^2/s) obtained in Chapter 4, the concentration profile after 30 minutes of drug application yields a relatively uniform concentration throughout the thickness of the cornea, similar to the situation in the collagen gel experiments. Using the riboflavin partition coefficient (k = 1.7) obtained in Chapter 4, the average concentration of riboflavin in the cornea is predicted to be 0.12% (varying from 0.17% at the anterior surface to 0.06% at the posterior surface, Figure 3.5a). In collagen gel samples with 0.1% riboflavin, the rate increases with intensity up to 3 mW/cm^2 and then saturates (Figure 3.3a). Thus, the clinical irradiation intensity (3 mW/cm^2) corresponds to the lowest value which induces the highest cross-linking rate. The clinical protocol uses a riboflavin concentration that is not optimal (by interpolation, 0.12% riboflavin concentration yields a cross-linking rate that is approximately 78% of the optimal rate that would be achieved using 0.05% riboflavin, see Figure 3.3b). The selection of a greater-than-optimal concentration of riboflavin may be due to the toxicity of riboflavin and UVA light: the riboflavin concentration is chosen based on the need to attenuate UVA light to a safe level, protecting the endothelium in patients with stromal thickness greater than 400 μm[2, 4, 9, 33]; patients with stromal thickness less than 400 μm are excluded from treatment[2].

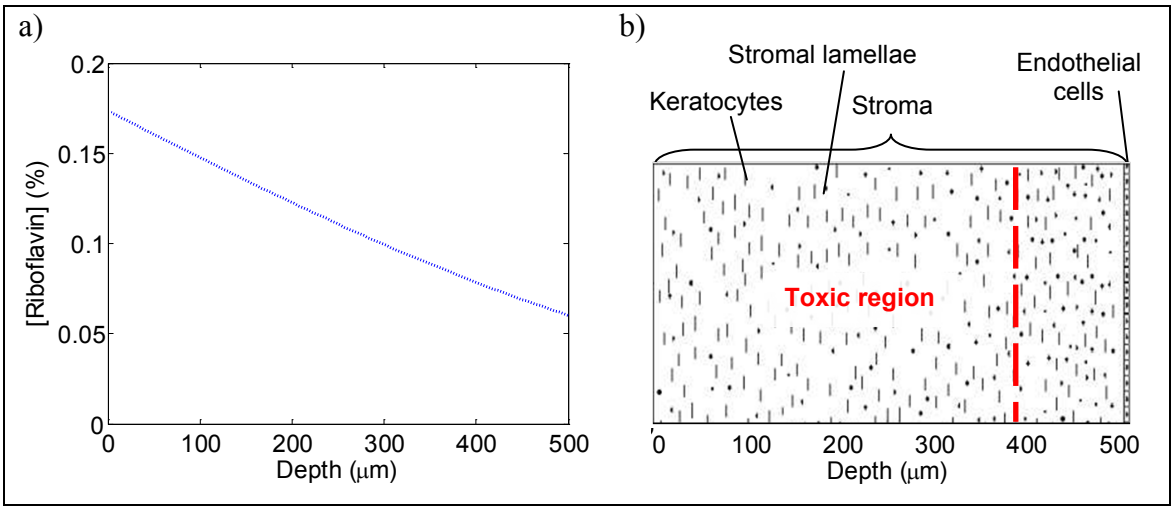

Figure 3.5. a) Riboflavin concentration profile inside corneal tissue after 30 minutes of applying drug using the clinical dose of 0.1%. **b)** Keratocyte toxicity is observed in the anterior 300-350 μm of the corneal stroma after riboflavin/UVA treatment. (Image adopted from lasikcomplications.com)

Unlike riboflavin/UVA treatment, collagen cross-linking activated by eosin Y using visible light has relatively low toxicity (Chapter 6). Therefore, the combination of eosin Y and visible light can be optimized for efficacy (Chapter 5). The low cytotoxicity of eosin Y and visible light may expand the range of patients who can safely receive corneal cross-linking treatment to include cases of advanced keratoconus or post-LASIK ectasia, in which corneal thickness is frequently less than 400 μm[13].

3.5 CONCLUSION

Photorheology can be used to efficiently characterize the effects of treatment parameters (including photosensitizer concentration and irradiation intensity) on the cross-linking rate of therapeutic collagen cross-linking. In the specific case of eosin Y activated by green light, photorheology indicates that the rate and extent of collagen cross-linking can

match those of riboflavin activated by UVA at the conditions that have proven to be clinically efficacious. The kinetic data provided by photorheology can be used in a predictive model of collagen cross-linking to anticipate the safety and efficacy of proposed treatment protocols (Chapter 5).

3.6 APPENDIX

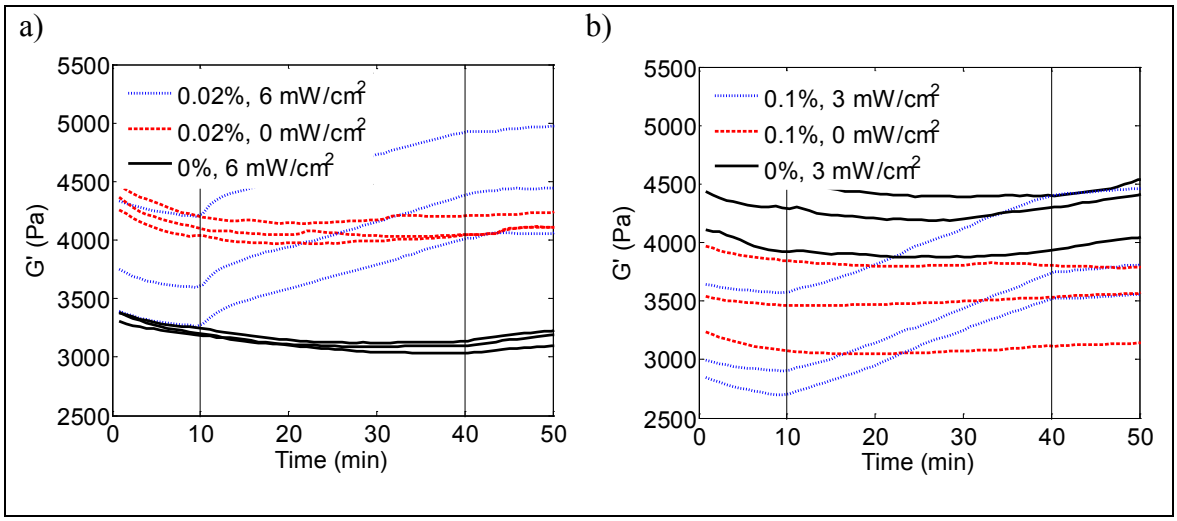

Figure 3.6. Storage modulus as a function of time for 450 µm thick gel samples with **a)** eosin Y and **b)** riboflavin. Samples containing eosin Y were irradiated with green light at 530 ± 15 nm and those containing riboflavin were irradiated with UV light at 370 ± 15 nm. The presence of both drug and light are necessary for enhancing the storage modulus. (To avoid over-crowding of the figures, only three samples are shown for each condition.)

3.7 ACKNOWLEDGEMENTS

This work includes contributions from Viet Anh Nguyen Huu and Dr. Matthew Mattson. Undergraduate Viet Anh Huu assisted in collagen gel preparation and data collection. Dr. Matthew Mattson built the rheometer light unit.

3.8 BIBLIOGRAPHY

1. Rabinowitz, Y.S., *Keratoconus.* Survey of Ophthalmology, 1998. **42**(4): p. 297-319.
2. Wollensak, G., *Crosslinking Treatment of Progressive Keratoconus: New Hope.* Current Opinion in Ophthalmology, 2006. **17**(4): p. 356.
3. Mazzotta, C., Balestrazzi, A., Traversi, C., Baiocchi, S., Caporossi, T., Tommasi, C*., et al.*, *Treatment of Progressive Keratoconus by Riboflavin-UVA-induced Cross-linking of Corneal Collagen: Ultrastructural Analysis by Heidelberg Retinal Tomograph II In Vivo Confocal Microscopy in Humans.* Cornea, 2007. **26**(4): p. 390.
4. Wollensak, G., Spoerl, E., Wilsch, M., Seiler, T., *Endothelial Cell Damage After Riboflavin-ultraviolet-A Treatment in the Rabbit.* Journal of Cataract & Refractive Surgery, 2003. **29**(9): p. 1786-90.
5. Spoerl, E., Mrochen, M., Sliney, D., Trokel, S., Seiler, T., *Safety of UVA-riboflavin Cross-linking of the Cornea.* Cornea, 2007. **26**(4): p. 385.
6. Wollensak, G., Spoerl, E., Seiler, T., *Riboflavin/ultraviolet-a-induced Collagen Crosslinking for the Treatment of Keratoconus.* American Journal of Ophthalmology, 2003. **135**(5): p. 620-627.
7. Wollensak, G., Spoerl, E., Reber, F., Seiler, T., *Keratocyte Cytotoxicity of Riboflavin/UVA-treatment In Vitro.* Eye, 2004. **18**(7): p. 718.
8. Mazzotta, C., Balestrazzi, A., Baiocchi, S., Traversi, C., Caporossi, A., *Stromal Haze After Combined Riboflavin/UVA Corneal Collagen Cross-linking in*

Keratoconus: In Vivo Confocal Microscopic Evaluation. Clinical & Experimental Ophthalmology, 2007. **35**(6): p. 580.

9. Kolli, S., Aslanides, I.M., *Safety and Efficacy of Collagen Crosslinking for the Treatment of Keratoconus.* Expert Opinion on Drug Safety. **9**(6): p. 949.
10. Ashwin, P.T., P.J., McDonnell, *Collagen Cross-linkage: A Comprehensive Review and Directions for Future Research.* British Journal of Ophthalmology, 2010. **94**(8): p. 965.
11. Mattson, M., *Understanding and Treating Eye Diseases: Mechanical Characterization and Photochemical Modification of the Cornea and Sclera.* Dissertation (Ph.D), California Institute of Technology, 2008.
12. Alleyne, C.H., Cawley, C.M., Barrow, D.L., Poff, B.C., Powell, M.D., Sawhney, A.S*., et al.*, *Efficacy and Biocompatibility of a Photopolymerized, Synthetic, Absorbable Hydrogel as a Dural Sealant in a Canine Craniotomy Model.* Journal of Neurosurgery, 1998. **88**(2): p. 308.
13. Bilgihan, K., Ozdek, SC., Sari, A., Hasanreisoğlu, B., *Excimer Laser-assisted Anterior Lamellar Keratoplasty for Keratoconus, Corneal Problems After Laser In Situ Keratomileusis, and Corneal Stromal Ppacities.* Journal of Cataract & Refractive Surgery, 2006. **32**(8): p. 1264.
14. Wollensak, G., Spoerl, E., *Collagen Crosslinking of Human and Porcine Sclera.* Journal of Cataract & Refractive Surgery, 2004. **30**(3): p. 689-695.
15. Wollensak, G., Iomdina, E., Dittert, D., Salamatina, O., Stoltenburg G, *Crosslinking of Scleral Collagen in the Rabbit Using Riboflavin and UVA.* Acta Ophthalmologica Scandinavica, 2005. **83**(4): p. 477.

16. Khan, S.A., Plitz, I.M., Frantz, R.A., *In Situ Technique for Monitoring the Gelation of UV Curable Polymers.* Rheologica Acta, 1992. **31**(2): p. 151.

17. Cook, W.D., Chausson, S., Chen, F., Pluart, L.L., Bowman, C.N. Scott, T.F., *Photopolymerization Kinetics, Photorheology and Photoplasticity of Thiol-ene-allylic Sulfide Networks.* Polymer International, 2008. **57**(3): p. 469.

18. Schmidt, L.E., Leterrier, Y., Vesin, J., Wilhelm, M., Månson, J.E., *Photorheology of Fast UV-Curing Multifunctional Acrylates.* Macromolecular Materials and Engineering, 2005. **290**(11): p. 1115.

19. Ibusuki, S., G.J., Halbesma, M.A., Randolph, R.W., Redmond, I.E., Kochevar T.J., Gill, *Photochemically Cross-linked Collagen Gels as Three-dimensional Scaffold for Tissue Engineering.* Tissue Engineering, 2007. **13**(8): p. 1995.

20. Kato, Y., Uchida, K., Kawakishi, S., *Aggregation of Collagen Exposed to UVA in the Presence of Riboflavin: A Plausible Role of Tyrosine Modification.* Photochemistry and Photobiology, 1994. **59**(3): p. 343.

21. Wollensak, G., Redl, B., *Gel Electrophoretic Analysis of Corneal Collagen After Photodynamic Cross-linking Treatment.* Cornea, 2008. **27**(3): p. 353.

22. Brinkman, W. T., *Photo-cross-linking of Type I Collagen Gels in the Presence of Smooth Muscle Cells: Mechanical Properties, Cell Viability, and Function.* Biomacromolecules, 2003. **4**(4): p. 890.

23. Nakayama, Y., Kameoa, T., Ohtakaa, A., Hiranob, Y., *Enhancement of Visible Light-induced Gelation of Photocurable Gelatin by Addition of Polymeric Amine.* Journal of Photochemistry and Photobiology A - Chemistry, 2006. **177**(2-3): p. 205.

24. Son, T., Sakuragi, M., Takahashi, S., Obuse, S., Kang, J., Fujishiro, M.*, et al.*, *Visible Light-induced Crosslinkable Gelatin.* Acta Biomaterialia. **6**(10): p. 4005-4010.

25. Chan, B.P., So, K.F., *Photochemical Crosslinking Improves the Physicochemical Properties of Collagen Scaffolds.* Journal of Biomedical Materials Research - Part A, 2005. **75A**(3): p. 689.

26. Chan, B.P., T.Y., Hui, O.C., Chan, K.F., So, W., Lu, K.M., Cheung*, et al.*, *Photochemical Cross-linking for Collagen-based Scaffolds: A Study on Optical Properties, Mechanical Properties, Stability, and Hematocompatibility.* Tissue Engineering, 2007. **13**(1): p. 73.

27. Ramshaw, J.A.M., Stephens, L.J., Tulloch, P.A., *Methylene Blue Sensitized Photo-oxidation of Collagen Fibrils.* Biochimica et Biophysica Acta - Protein Structure and Molecular Enzymology, 1994. **1206**(2): p. 225.

28. Judy, M.M., Fuh, L., Matthews, J.L., Lewis, D.E., Utecht, R.E. *Gel electrophoretic Studies of Photochemical Cross-linking of Type I Collagen with Brominated 1, 8-naphthalimide Dyes and Visible Light*. in *Proceedings of SPIE*. 1994.

29. Bown, S.G., Tralau, C.J., Smith, P.D., Akdemir, D., Wieman, T.J., *Photodynamic Therapy with Porphyrin and Phthalocyanine Sensitisation: Quantitative Studies in Normal Rat Liver.* British Journal of Cancer, 1986. **54**(1): p. 43.

30. Wilson, B.C., Patterson, M.S., Burns, D.M., *Effect of Photosensitizer Concentration in Tissue on the Penetration Depth of Photoactivating Light.* Lasers in Medical Science, 1986. **1**(4): p. 235.

31. Terrones, G., Pearlstein, A.J., *Effects of Optical Attenuation and Consumption of a Photobleaching Initiator on Local Initiation Rates in Photopolymerizations.* Macromolecules, 2001. **34**(10): p. 3195.

32. Lee, J.H., Prud'Homme, R.K., Aksay, I.A., *Cure Depth in Photopolymerization: Experiments and Theory.* Journal of Materials Research, 2001. **16**(12): p. 3536.

33. Wollensak, G., Spöerl, E., Reber, F., Pillunat, L., Funk, R., *Corneal Endothelial Cytotoxicity of Riboflavin/UVA Treatment In Vitro.* Ophthalmic Research, 2003. **35**(6): p. 324.

Chapter 4

Transcorneal and Transcleral Transport of Eosin Y and Riboflavin

4.1 INTRODUCTION

Topical drug delivery is the dominant route for ocular drug delivery due to the accessibility of the front of the eye, the minimal risk of infection, and the ability to transfer drug into the ocular coat (cornea and sclera), anterior chamber and its associated tissues[1-4]. To reach any of these tissues, topically applied drug must penetrate the ocular coat; therefore, it is important to understand the transport across these tissues. Here, we focus on the transport of drugs through the ocular coat with specific interest in treating diseases associated with progressive thinning and weakening of the ocular coat, including keratoconus, post-LASIK ectasia and degenerative myopia. Photo-activated cross-linking treatments have been proposed for halting the progression of these diseases by strengthening the weakened tissue[5-10]. The safety and efficacy of cross-linking treatments depend on the local drug concentration and light intensity as a function of depth into the tissue. This study aims to characterize the transport of both riboflavin, which is currently being used clinically, and eosin Y, which is a less toxic photosensitizer

(Chapter 6). The development of less toxic routes to tissue cross-linking would enable treatment of patients with post-LASIK ectasia and degenerative myopia, in addition to keratoconus.

Keratoconus is a bilateral corneal thinning disorder with a prevalence of 1 out of 2,000[11]. This eye disease is characterized by progressive corneal thinning and protrusion[11-13]. Post-LASIK ectasia is a complication of refractive surgery that results in corneal thinning and protrusion, similar to keratoconus[14-16]. Post-LASIK ectasia has an incidence of 1 out of 2,500 LASIK surgical procedures[17]. Degenerative myopia is associated with the progressive thinning and stretching of the posterior sclera[18, 19]. It is the leading cause of blindness in Asia and is ranked 7th in the United States[20].

Therapeutic cross-linking using riboflavin activated by UVA irradiation pioneered by Wollensak, Spoerl, and Sieler has been shown to be promising for halting the progression of keratoconus[6, 21]. Riboflavin/UVA treatment has not yet been successfully demonstrated in treating corneal ectasia for patients with cornea thinner than 400 μm[6, 22, 23] or degenerative myopia[10, 24]. Motivated by the need for a safer cross-linking treatment, we have investigated eosin Y, a visible light activated photosensitizer that has been approved by the FDA for use in the body[25].

Even though riboflavin/UVA treatment has been performed on keratoconus patients for almost a decade[26], the transport of riboflavin into the corneal stroma has not yet been quantified. Although two studies examine the concentration profile of riboflavin as a function of depth in the cornea, Sondergaard *et al*.[27] using confocal fluorescence microscopy and Cui *et al*.[28] using two-photon excited fluorescence technique, the

reported maximum concentration of riboflavin in the tissue differs by two orders of magnitude. There is also a discrepancy in the reported shapes of the concentration distribution of riboflavin along the tissue depth.

Fundamentally, knowledge of the diffusion and partition coefficient of the molecule in the tissue is needed to predict the time evolution of the amount and distribution of drug transferred into the tissue. We were unable to find any literature on the diffusion and partition coefficient of riboflavin in the cornea or sclera. Riboflavin has a similar molecular structure and molecular weight to fluorescein, a compound used extensively in ophthalmology, so its diffusion and partition coefficient has been measured in various studies[29-31]. A theoretical concentration profile of riboflavin in the cornea has been predicted before using fluorescein's diffusion coefficient (D = 65 $\mu m^2/s$) and assuming a partition coefficient of 1[32].

Transport through the ocular coat tissues has been commonly studied using an Ussing chamber to determine the permeability of the compounds of interest across the cornea or sclera[33-35]. Permeability is the product of the partition coefficient and diffusivity divided by the tissue thickness[36]. Other techniques have been developed to determine the partition coefficient and diffusivity. One technique involves applying drug to the end of a strip of cornea or sclera and monitoring the concentration at various positions along the strip as a function of time either by measuring the tissue fluorescence or sectioning the tissue and performing extraction. The concentration profile was fit to a 1-dimensional diffusion model[30, 31, 37, 38] to determine the partition and diffusion coefficient. Another technique entails immersing a cross-section of the sclera in a solution to saturate the

tissue, then transferring the cross-section into a solute-free solution and measures the rate of solute leaving the cross-section and then fitting the data to a diffusion model to determine the diffusion coefficient[37].

Our study examined the transport of molecules into an intact globe, which mimics *in vivo* conditions and avoids damaging the tissue structure from cutting. After drug was delivered to the eye, the cornea or sclera was isolated to extract the molecules delivered to the tissue as a function of contact time with the drug solution. We then applied a diffusion model to fit the data. From this, we were able to determine the partition coefficient, k and diffusion coefficient, D. Absorbance measurements of the tissue cross-sections were performed to check for consistency with the extraction measurements. The absorbance method for quantifying the amount of drug delivered was also used to compare different delivery techniques (drops and different formulations of viscous gels) to determine which would be worthy of pre-clinical evaluation.

4.2 METHODS

Drug diffusion into the cornea – Sierra for Medical Science supplied porcine eyes from 3-4 month old swine. Eyes were stored in ocular balanced saline solution on ice until use within 48 hours post mortem. Corneal tissues were all clear with no signs of edema. The epithelial cell layer was removed by scraping with a scalpel. Each eye was immersed in 30 mL of drug solution, either 0.289 mM (0.02%) eosin Y (Sigma Aldrich E6003) solution in Dulbecco's phosphate buffered saline (DPBS, Sigma D8662) or 0.289 mM (0.0138%) riboflavin 5'-monophosphate sodium salt (riboflavin, Fluka 77623) solution in DPBS. The drug solution containing the eye was gently agitated using a rocker for a

specified "drug contact time" ($t_{c,cornea}$ ranging from 0 to 4 hours). After the drug contact time, the eye was removed from the drug solution, and excess solution on the cornea was dabbed away with a Kimwipe (Figure 4.1a). The eye was dissected using a scalpel blade and a pair of scissors to cut around the corneoscleral limbus to separate out the cornea (Figure 4.1b). The tissue section was placed onto a trephine punch to cut out a 9.5-mm diameter corneal cross-section (Figure 1c). The sizes of the cross-sections were very consistent with mass of 95 ± 12 mg for eyes with $t_{c,cornea}$ = 0 hr.

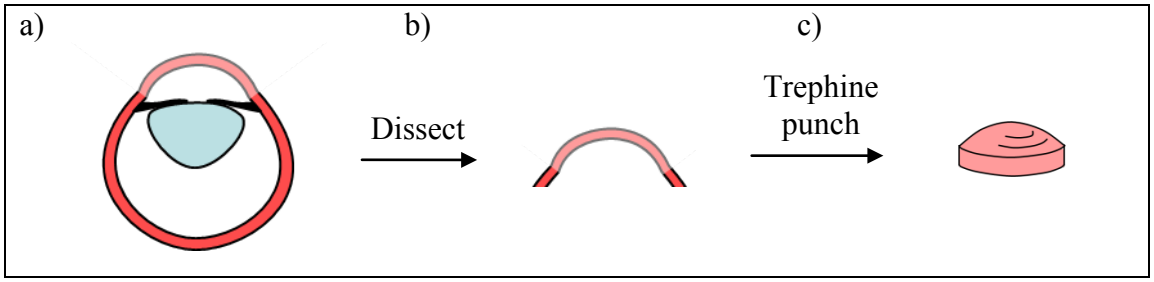

Figure 4.1. a) Eye removed from eosin Y solution when contact time completed. **b)** Dissection to separate the cornea. **c)** Trephine punch used to cut out a 9.5-mm diameter cross-section of the cornea.

Drug diffusion into the sclera – Orbital tissues were removed with scissors to expose the sclera. Each eye was placed into 30 mL of a drug solution (either Eosin Y or riboflavin) and gently agitated using a rocker for a specified contact time ($t_{c,sclera}$ ranging from 0 to 120 hours). After the contact time, the eye was removed from the drug solution, and excess solution on the sclera was dabbed away with a Kimwipe. The eye was dissected using a scalpel blade and a pair of scissors to obtain a posterior scleral section on the temporal side near the optic nerve (Figure 4.2b). The tissue section was placed onto a trephine punch to cut out a 9.5-mm diameter cross-section (Figure 4.2c).

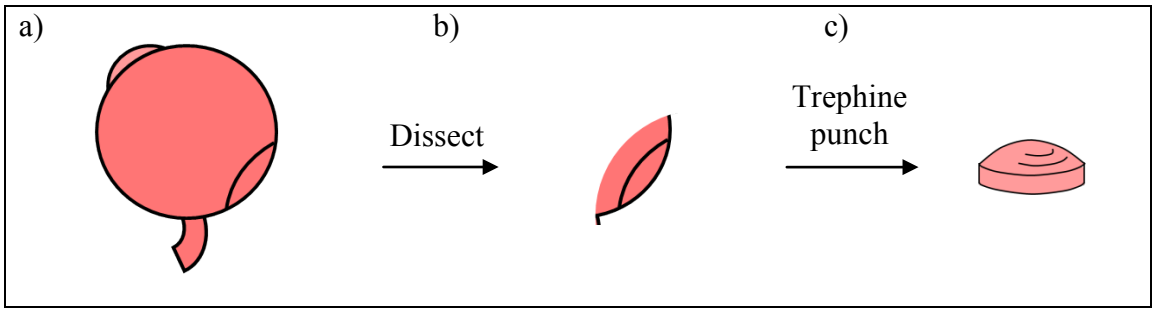

Figure 4.2. a) Eye removed from eosin Y solution when contact time completed. **b)** Dissection to separate the sclera section near the optic nerve. **c)** Trephine punch used to cut out a 9.5-mm diameter cross-section of the sclera.

Quantitative assay of the amount of drug delivered – Experiments were performed for five drug contact times (four samples each): for the cornea, $t_{c,cornea}$ = 0.25, 0.5, 1, 2, and 4 hrs, and for the sclera, $t_{c,sclera}$ = 0.5, 2, 4, 7.5, and 120 hrs. Each experiment was repeated four times. For each experiment, the 9.5-mm diameter tissue cross-section obtained as described above was placed into a 50 mL centrifuge tube and immersed in 50 mL of extractant (doubled-distilled water for cornea or DPBS for sclera) then placed on a rocker to extract the drug molecules (Figure 4.3). DPBS was used instead of water to extract drug from the sclera because eosin Y did not partition favorably from the sclera into water. After a first extraction time $t_{e,1}$ of 8 hours, the tissue specimen was then transferred into another 50 mL of fresh extractant and the extract was retained for analysis.

The concentration of the drug in the extract was determined using fluorimetry. Eosin Y was excited at 514 nm and the fluorescence was detected at 534 nm; for riboflavin, the excitation wavelength was 466 nm and detection wavelength was 523 nm. The fluorescence of each extract was measured and concentration was determined based on calibration curves prepared for each compound using a series of solutions with known

concentrations. The extraction process was repeated using successively longer extraction times until there was no detectable fluorescence in the supernatant. For the cornea, three extractions were sufficient, with $t_{e,1} = 8$, $t_{e,2} = 24$ and $t_{e,3} = 48$ hours (a total extraction time of 48 hours). For the sclera, five extractions were required with $t_{e,1} = 8$, $t_{e,2} = 24$, $t_{e,3} = 48$, $t_{e,4} = 72$, $t_{e,5} = 96$, and $t_{e,6} = 120$ hours (a total extraction time of 120 hours). The final extraction time was only needed for sclera specimens that had been kept in contact with eosin Y for $t_{c,sclera} = 120$ hours.

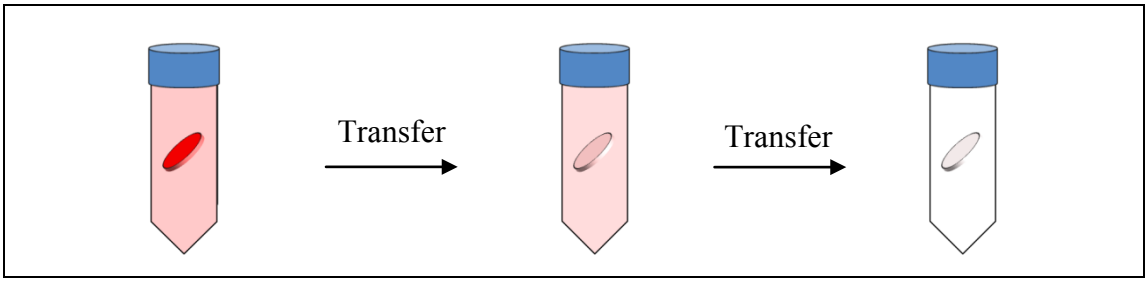

Figure4. 3. Quantitative assay of the amount of molecules transferred to the tissue cross-section. The section was placed into 50 mL of double-distilled water for 8 hours, then transferred to a new 50 mL of double-distilled after 24 hours, then transferred again after 48 hours.

Assessing residual eosin Y remaining in tissue after extraction – Eosin Y is known to bind to collagen[39, 40] which makes up more than 68% of the cornea's dry mass[36] and more than 80% of the sclera's dry mass[36]. Therefore, light absorption measurements were performed to exclude the possibility that a significant amount of eosin Y remained in the tissue after extraction. One cornea specimen was prepared as above for each of the following drug contact times: $t_{c,cornea} = 0.25$, 1, and 4 hrs. Before placing the corneal cross-section into the first extractant, its UV-vis absorption spectrum was measured. There was a distinct peak at 525 nm with absorbance value greater than 2 for all samples

(i.e., transmitted intensity was < 0.01 of the incident intensity). Eosin Y was then extracted from the corneal cross-sections into double distilled water using three successive extractions with $t_{e,1}$ = 8, $t_{e,2}$ = 24 and $t_{e,3}$ = 48 hrs as described above. After the last extraction, UV-vis absorption spectrum of the corneal cross-section was measured again. Even though the corneas were cloudy after the extraction process, the absorbance values were ~1.2 (i.e. transmitted intensity was ~5% of the incident intensity), and the peak at 525 nm was no longer present in any of the three cornea specimen. This demonstrates the amount of eosin Y remaining in the tissue specimen after the extraction procedure is negligible compared to the amount extracted. Riboflavin does not bind to collagen; therefore, none is expected to remain in the tissue after extract is complete.

Absorbance measurement to determine the amount of drug delivered – The extraction method provides a quantitative measure of the number of drug molecules delivered; however, the procedure requires 48 hours to 120 hours. For determining the number of molecules transferred to the cornea as a function of the delivery protocol and delivery vehicle, light absorption measurements suffice to characterize the number of drug molecules delivered to the cornea. Once the drug delivery step is complete, a 9.5-mm diameter cross-section of the central cornea was obtained as described above (Figure 4.4). After taking a "blank" absorbance reading with the empty cuvette, the corneal section is placed into the cuvette and the sample's absorbance was measured at the wavelength of the maximum absorbance of the drug (e.g., at 525 nm for eosin Y) in the tissue. Using the calibration curves described above, the amount of drug delivered was calculated from the absorbance of the corneal section.

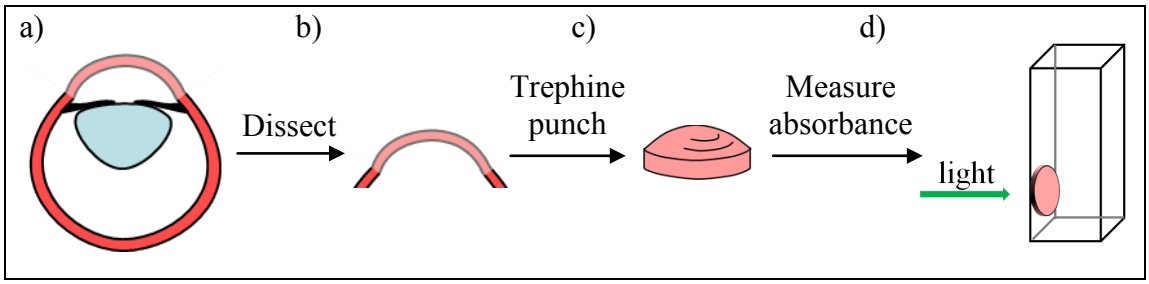

Figure 4.4. a) Eye removed from eosin Y solution when contact time completed. **b)** Dissection to separate the cornea. **c)** Trephine punch used to cut out a 9.5-mm diameter cross-section of the cornea. **d)** The section was placed into a cuvette to measure the absorbance.

Number of molecules delivered to each cornea was calculated from the absorbance using the following equations

$$A_o = \varepsilon_o \cdot L \qquad \text{Equation 1}$$

where A_o is the apparent absorbance of the control sample soaked in DPBS for 5 minutes, $\boldsymbol{\varepsilon}_o$ is the extinction coefficient of the cornea, and L is the thickness of the sample.

$$A = \varepsilon_o \cdot L + \varepsilon_{EY} \cdot C \cdot L \qquad \text{Equation 2}$$

where A is the absorbance of the sample with eosin Y and $\boldsymbol{\varepsilon}_{EY}$ is the extinction coefficient of eosin Y, C is the of eosin Y concentration inside the tissue. Subtracting Equation 1 from Equation 2 and rearranging yields

$$C \cdot L = \frac{A - A_o}{\varepsilon_{EY}} \qquad \text{Equation 3}$$

The product of concentration and sample thickness is the number of drug molecules delivered per unit area.

This method was used to compare different drug delivery techniques *in vitro* to determine which would be worthy of preclinical evaluation *in vivo*: 1) immersion in drug solution, 2) topical drops of drug solution, and 3) topical application of a gel. These three drug delivery techniques were examined using porcine eyes from 3-4 month old swine (Sierra for Medical Science) stored in saline on ice until use within 48 hours post mortem. The epithelial cell layer was removed from the cornea by scraping with a scalpel. Drug was delivered to the cornea using one of the following techniques (or the corresponding control):

1) Immersion: Each eye was immersed in 30 mL of 0.289 mM (0.02%) eosin Y solution that was gently agitated using a rocker. After 5 minutes, the eye was removed from the eosin Y solution, and excess solution on the cornea was dabbed away with a Kimwipe. Control eyes were placed in 30 mL of DPBS solution instead of eosin Y solution.

2) Topical drops: Drops of 0.289 mM eosin Y in DPBS solution were applied to the cornea every minute for 5 minutes. Excess solution on the cornea was dabbed away with a Kimwipe.

3) Topical gel: Four different viscosity enhancers were examined, each at a concentration such that the gel would remain on the cornea for 5 minutes: 2% hyaluronic acid (HA), 3% carboxymethylcellulose (CMC), 3% sodium alginate (SA), and 3% methylcellulose (MC) each in DPBS. Approximately 0.5 mL of 0.289 mM eosin Y gel was applied to the cornea using a syringe and then the gel was spread evenly over the cornea and limbus using a spatula. Hyaluronic acid provided a gel that was free of bubbles, but it was somewhat difficult to spread into an even layer. Sodium alginate and methylcellulose gels

were easy to spread, but retained air bubbles. Carboxymethylcellulose provided a gel free of bubbles that spread easily with a spatula. After 5 minutes, the gel was removed from the cornea with a spatula and the site was quickly rinsed with ~2 mL of DPBS. Excess solution was then dabbed away with a Kimwipe

4.3 RESULTS

Cornea samples required two extracts to remove the delivered drug molecules (Figure 4.5). For all contact times examined (0.25, 1, 2, and 4 hours), the second extract contained much less drug than the first (for eosin Y, 3 to 6% and for riboflavin, 1.6 to 2.5% of the first extract) and the third extract had negligible drug (fluorescence value was similar to that of doubled-distilled water, indicating a drug concentration less than 1% of the first extract). Therefore, we approximate the total number of drug molecules delivered to the cornea during t_c as the sum of the number of drug molecules in the three extracts (Figure 4.6a).

Sclera samples required more extractions than cornea samples, particularly for eosin Y. For all contact times examined (0.5, 2, 4, 7.5, 30, and 120 hours), the amount of eosin Y in the second extract was a substantial fraction of that in the first extract, between 10 to 45% (e.g., for 2 hours contact time, the second extract contained approximately 20% as much as the first extract, Figure 4.5b). As the duration of the extraction step increased, the ratio of the content of eosin Y in the successive extracts approached a constant value of approximately 1/3; specifically, relative to the first extract, the amount of eosin Y in the subsequent extracts was between 3 to 22% in the 3^{rd}, between 2 to 8% in the 4^{th}, between 0-2% in the 5^{th} and $\leq$ 1% in the 6^{th}. Riboflavin was much more readily extracted

from the sclera: relative to the first extract, the second extract contained only 3 to 6%, the 3rd extract contained between 1 to 3%, and the 4th extract ≤ 1%. Therefore, we also approximate the total number of drug molecules delivered to the sclera during t_c as the sum of the number of drug molecules in all the extracts (Figure 4.6b).

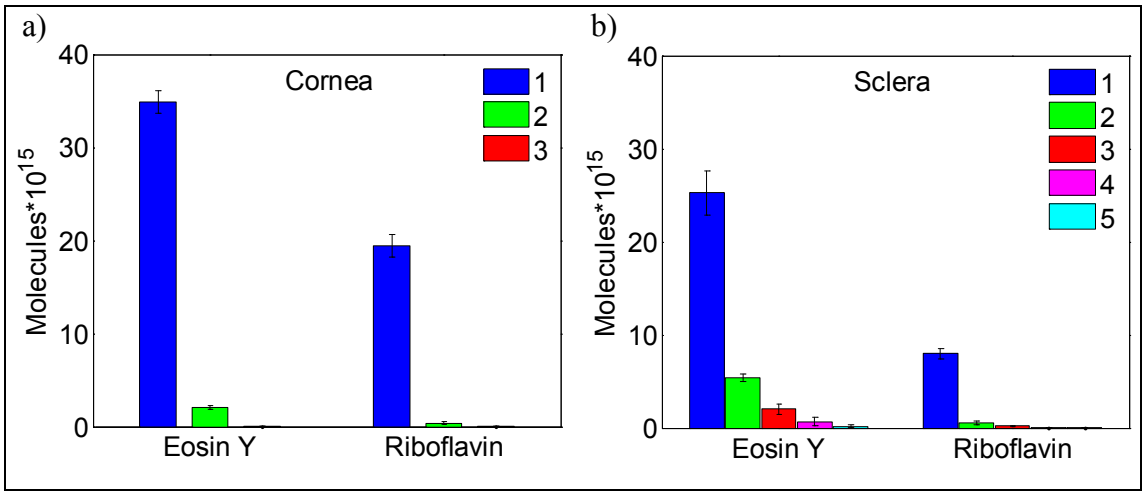

Figure 4.5. Number of drug molecules, eosin Y and riboflavin, in successive extracts from tissue specimens given a 2 hours contact time for the **a)** cornea and **b)** sclera. Approximately all of the extractable molecules were removed from the cornea after 3 extractions, and from the sclera after 5 extractions. Therefore, the sum of the number of drug molecules in all the extracts is a good approximation of all the drug molecules that had been transferred into the tissue cross-section. (N = 4)

The total drug delivered per unit area of contact, estimated as the sum of the number of drug molecules in all extracts, normalized by the cross-sectional area of the sample, increases with drug contact time (Figure 4.6). The value levels off at long time as the system approaches equilibrium partitioning of drug between the tissue and the solution. For the cornea, the initial increase with drug contact time levels off at 2 hours for both eosin Y and riboflavin, indicating that the two molecules have similar diffusivities in the cornea; the long time asymptotes show that the eosin Y partitions more favorably into the

cornea than riboflavin does, by approximately a factor of 2 (Figure 4.6a). For the sclera, much longer time was required for the concentration to level off (note different time scales for part a and b of Figure 4.6). Furthermore, the time scales were *not* the same for the two drugs (approximately 30 hours for eosin Y and approximately 7.5 hours for riboflavin); the sclera also showed a more dramatic difference in affinity for eosin Y and riboflavin – approximately 7-fold greater for eosin Y than riboflavin at the long time asymptotes (Figure 4.6b).

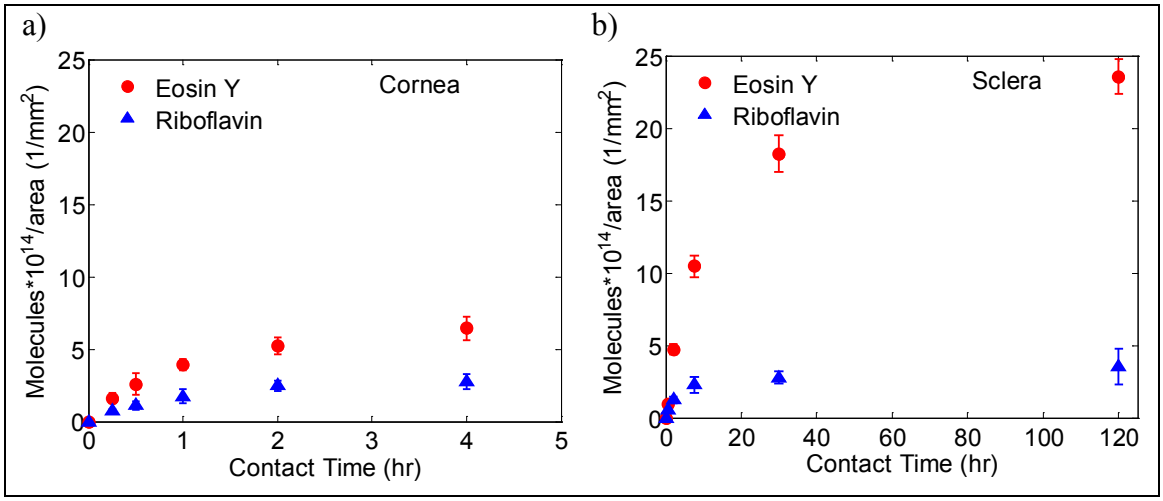

Figure 4.6. Total number of drug molecules delivered as a function of drug contact time for both eosin Y and riboflavin in **a)** the cornea and **b)** the sclera. Note: all data points have associated error bars, however some error bars are too small to visible on the graph. (N = 4)

The equilibrium partitioning of riboflavin between the drug solution and the tissue was quite similar for the cornea and the sclera. There is a pronounced difference in the equilibrium partitioning of eosin Y for the cornea and sclera with the sclera being much more favorable than the corneal stroma. Despite the much greater affinity of the sclera for eosin Y, the rapid rate of transport into the cornea led to greater eosin Y uptake by the

cornea than the sclera at short contact times (0.5 and 2 hours). The situation reversed at long contact times (4 hours in the cornea and 120 hours in the sclera), when significantly more eosin Y was absorbed by the sclera than the cornea. In contrast, approximately the same amount of riboflavin was absorbed by both of these tissues at long contact times.

Evaluation of Partition Coefficients and Diffusion Coefficients

A quantitative description of the number of drug molecules delivered to targeted tissue is crucial in the drug delivery aspect of developing safe and effective therapeutics. In addition to the quantity of drug delivered, photo-activated therapy is sensitive to the distribution of drug inside the tissues. Following Maurice[29], Nagataki *et al*.[30, 31], Prausnitz *et al.*[38, 41] we find that a simplified diffusion model provides a good description of the experiment results (see below) and, therefore, we it use to evaluate the partition and diffusion coefficients. The observed accord between the model and the present experimental results also indicates that the model can be used to predict the drug concentration profile inside the tissue as a function of treatment parameters (i.e. drug concentration, drug contact time, and the delay time from the drug application to drug activation via irradiation, which is discussed in Chapter 5).

Porcine eyes closely resemble a sphere with diameter ~25 mm. The cornea and sclera are the targeted tissues and both have thicknesses that are on the order of 1 mm. Since these tissue thicknesses are less than a tenth of the diameter of the eye, they are modeled as semi-infinite slabs. Each tissue is approximated as a uniform material. Fick's diffusion equation is given by

$$\frac{\partial C(z)}{\partial t} = D\frac{\partial^2 C(z)}{\partial z^2} \qquad \text{Equation 4}$$

where *C(z,t)* is the drug concentration inside the tissue, I is the time since the exterior surface of the tissue was placed in contact with the drug solution, *z* is the distance into the tissue from its exterior surface, and *D* is the diffusion coefficient. An initial condition and two boundary conditions are needed: the initial condition has no drug in the tissue, the concentration just inside the tissue (at *z = 0*) is given by the product of the partition coefficient and the concentration of the drug in the solution, and the concentration falls to zero far from the surface of the tissue. For short contact times, the concentration falls to zero before the profile reaches the endothelium. For longer contact times, the boundary condition that the concentration falls to zero far into the system is still used as a first approximation (neglecting the change in material properties at the endothelium and neglects different transport processes in the aqueous or vitreous).

Initial condition at $t = 0,\ C = 0$ for all $z \geq 0$ Equation 5.1

Boundary condition at $z = 0, C = k \cdot C_{drug}$ for $t > 0$ Equation 5.2

Boundary condition at $z = \infty, C = 0$ for all t Equation 5.3

where *k* is the partition coefficient and C_{drug} is the concentration of the drug solution applied. Applying the initial and boundary conditions to the diffusion equation, the concentration profile is given by

$$C(t,z) = k \cdot C_{drug} \cdot erfc\left(\frac{z}{\sqrt{4Dt}}\right) \qquad \text{Equation 6}$$

where *erfc* is the complementary error function. Using this theoretical concentration profile, the total number of drug molecules present in the tissue can be calculated by integrating over the thickness of interest

$$\frac{molecules}{area} = \int_0^L k \cdot C_{drug} \cdot erfc\left(\frac{z}{\sqrt{4Dt}}\right) \cdot dz \qquad \text{Equation 7}$$

where *area* represents the cross-sectional area of the tissue sample and *L* is the thickness of the tissue sample. At long drug contact time, the predicted concentration changes very slowly and approaches a value governed by the partition coefficient. At short drug contact times, the rate of change is strong and largely determined by the diffusivity. The measured number of molecules delivered per area is compared to the model to deduce the values *k* and *D* that minimize the mean-square deviation, *S*, between the predicted and observed values for a given drug-tissue pair:

$$S = \sum_{i=1}^{N} \left[\left(\frac{molecules}{area}\right)_i - \left(\frac{molecules}{area}\right)_{measured,i} \right]^2 \qquad \text{Equation 8}$$

with *i* being the individual data point and *N* being the total data points used for the fit. Data fitting was performed by writing a program in MATLAB software. The quality of fit provided by the resulting values of *k* and *D* (Table 4.1) is good (all predicted values are within 15% of the average measured values), suggesting that the approximations made are acceptable (Figure 4.7).

Table 4.1. Values of diffusivity, D and partition coefficient, k for eosin Y and riboflavin penetrating into the cornea and sclera from DPBS.

		D (μm^2/s)	k
Cornea	Eosin Y	62 ± 22	4.3 ± 0.7
	Riboflavin	79 ± 22	1.7 ± 0.2
Sclera	Eosin Y	6.2 ± 1.7	13.0 ± 1.1
	Riboflavin	27 ± 8.4	1.5 ± 0.6

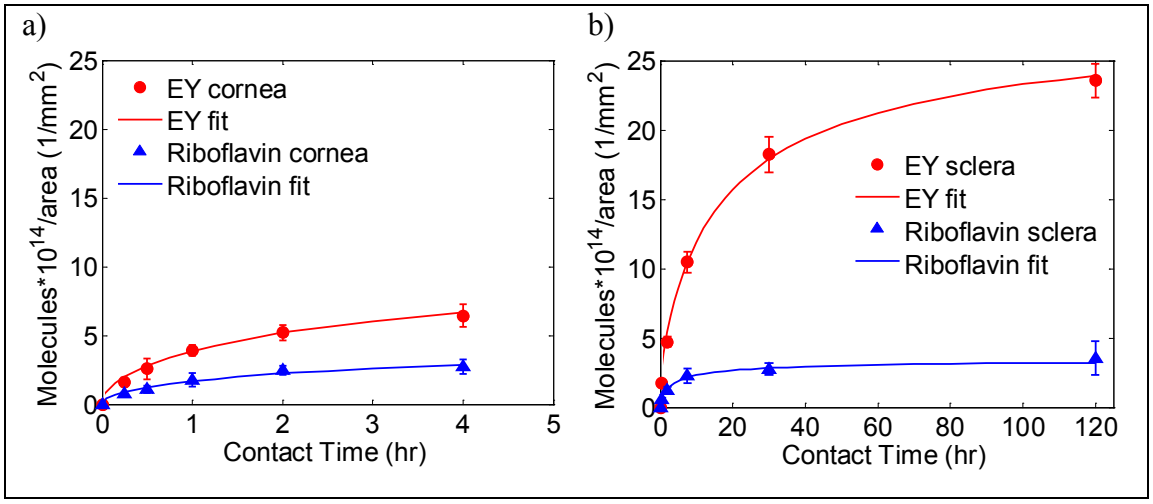

Figure 4.7. Total number of drug molecules delivered as a function of drug contact time for both eosin Y and riboflavin in **a)** the cornea and **b)** the sclera. The "best fit" curves were generated using a diffusion model with values of k and D given in Table 4.1.

For the cornea, eosin Y's partition coefficient is greater than that of riboflavin ($k_{c,EY}$ = 4.3, $k_{c,R}$ = 1.7), in accord with the difference noted above in their concentrations observed at long time. Eosin Y's diffusion coefficient in the corneal stroma is similar to that of riboflavin ($D_{c,EY}$ = 62 μm^2/s, $D_{c,R}$ = 79 μm^2/s), in accord with the similar time course for sorption noted above.

In contrast to the cornea, the difference in behavior between the two drugs is pronounced in the sclera. The partition coefficient for eosin Y is almost ten-times greater than that of riboflavin ($k_{s,EY}$ = 13, $k_{s,R}$ = 1.5), consistent with the much greater concentration of eosin Y than riboflavin at long times. The diffusion coefficient of eosin Y in the sclera is much less than that of riboflavin ($D_{s,EY}$ = 6.2 μm^2/s, $D_{s,R}$ = 27 μm^2/s), consistent with the much longer time required for eosin Y to reach its long-time asymptotic concentration than riboflavin.

Comparing eosin Y's behavior in the cornea and sclera shows its diffusivity is significantly greater in the cornea than in the sclera ($D_{c,EY}$ = 62, $D_{s,EY}$ = 6.2) and that it partitions into the cornea significantly less favorably than the sclera ($k_{c,EY}$ = 4.3, $k_{s,EY}$ = 13.0). In contrast to eosin Y, riboflavin's diffusion coefficient in the cornea is only three-times greater in sclera ($D_{c,R}$ = 79 μm^2/s, $D_{s,R}$ = 27 μm^2/s), and its partition coefficient is almost the same in the two tissues ($k_{c,R}$ = 1.7, $k_{s,R}$ = 1.5).

The extraction method and absorbance method for quantifying drug delivery were compared using three different delivery techniques: soak, drops, and 2% hyaluronic acid gel for 5 minutes (as described earlier). The two methods gave consistent results (Figure 4.8a), validating the absorption measurement as a tool to study drug delivery.

To facilitate controlled application of the drug formulation on the cornea, it is of interest to increase the viscosity of the solution. Here we compare four clinically relevant options: 2% hyaluronic acid (HA), 3% carboxymethylcellulose (CMC), 3% sodium alginate (SA), and 3% methylcellulose (MC). Three out of the four types of gel (hyaluronic acid, carboxymethylcellulose, sodium alginate) delivered approximately the same amount as

topical drops (Figure 4.8b). Although methylcellulose gel delivered less than half as much drug as the other formulations, this may simply be due to the difficulty of removing air bubbles from the resulting gel.

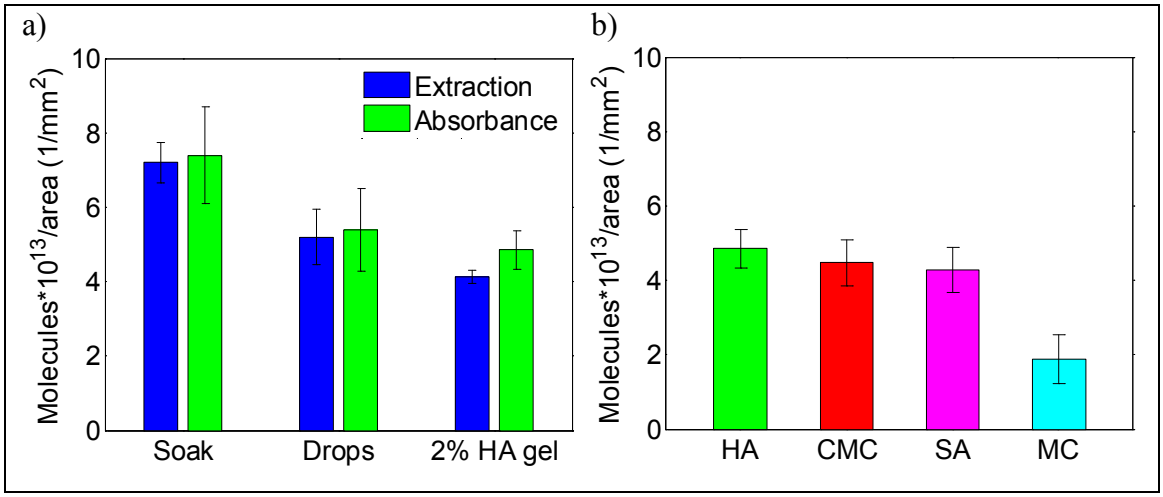

Figure 4.8. a) The extraction and the absorbance methods yield similar results for the number of molecules delivered to the cornea for three selected delivery techniques applied for 5 minutes. **b)** Comparison of different delivery vehicles using the absorbance measurement to determine the quantity of drug delivered in 5 minutes from gels using four different viscosity enhancing agents. (N = 4)

4.4 DISCUSSION

The values of the partition coefficient and diffusion coefficient enable prediction of the amount of drug transferred to the tissue and the distribution of drug in the tissue, which are very important to safety and efficacy in therapeutics. Corneal and scleral transport has been predominantly studied using an Ussing Chamber to measure the permeability of molecules through these two tissues. Permeability describes the rate of transport at steady state, which is not sufficient to predict the transient transport of drug from a topically

applied vehicle into the tissue. The permeability, P, is equal to the product of the partition coefficient and diffusion coefficient divide by the tissue thickness[36].

$$P = \frac{kD}{L} \qquad \text{Equation 9}$$

Permeability measurements through the corneal stroma have mostly been studied in rabbit corneas[42]. For molecules with similar sizes (4.0 to 5.1 Å), reported permeability through rabbit stroma for 15 compounds range from 0.30 to 0.58 μm/s[42]. Permeability is inversely proportional to thickness, and after taking into account porcine stromas are 2.5 times thicker than rabbit stromas[43, 44], the permeability values expected for the porcine cornea range from 0.13 to 0.25 μm/s, for molecules of comparable size to eosin Y and riboflavin. These values accord well with the values of permeability calculated using the diffusivity and partition coefficient for porcine cornea determined in this study, which are 0.16 and 0.31 μm/s for riboflavin and eosin Y, respectively.

Using the values of the partition coefficient and diffusivity for porcine sclera determined in this study, the calculated permeability is 0.050 μm/s for riboflavin and 0.099 μm/s for eosin Y. For molecules of similar sizes (3.3 to 4.9 Å), reported permeability through rabbit sclera is 0.25 to 0.71 μm/s for 4 compounds, human sclera is 0.15 to 0.44 μm/s for 6 compounds, and bovine sclera is 0.065 to 0.13 μm/s for 2 compounds[42]. When scaled for tissue thicknesses[45], the range of permeability values expected for porcine sclera is 0.050 to 0.14 μm/s (based on rabbit data), 0.060 to 0.18 μm/s (based on human data), 0.042 to 0.084 μm/s (based on bovine data). Thus, the literature values for scleral

permeability are consistent with the partition coefficient and diffusion values obtained in this study.

The observed values of the partition coefficients for the two drugs into the cornea and sclera provide interesting information on the interaction between the drugs and the constituents of the tissue. While a molecule's lipophilicity and charge are also expected to affect the partition coefficient[36], that cannot explain the significantly greater partition coefficients of eosin Y relative to riboflavin (Table 4.1): both compounds readily dissolve in water and both are negatively charged in solution at physiological pH[40, 46, 47]. The partition coefficient also depends on the binding interactions between the drug molecules and the tissue[38, 41].

A partition coefficient greater than one is indicative of an attractive interaction, between the drug and one or more constituents of the tissue. In the case of the corneal stroma and the sclera, the main constituents are collagen fibrils embedded in a matrix of proteoglycans and water. For hydrated corneal stromas (as in the present experiments), the estimated volume fraction of water is 89.7%, while that of collagen is 7.3% and the remaining 3% consists of proteoglycans, non-collagenous free proteins and salts[36]. The sclera has substantially greater collagen content and correspondingly lower water content: the estimated volume fraction of water is 77.7% and that of collagen is 18.4% (like the cornea, the remaining 3.9% v/v of the sclera consists of proteoglycans, non-collagenous free proteins and salts[36].

Riboflavin exhibits partition coefficients that are only mildly greater than one and are similar for the cornea ($k_{c,R}$ = 1.7 ± 0.2) and sclera ($k_{s,R}$ = 1.5 ± 0.6). These results indicate

that riboflavin does not have a strong affinity for collagen or proteoglycans. In contrast, eosin Y exhibits partition coefficients that are substantially greater than one and are substantially different in the cornea ($k_{c,EY}$ = 4.3 ± 0.7) and sclera ($k_{s,EY}$ = 13.0 ± 1.1). Eosin Y is known to bind to various proteins, including collagen[39, 40]. Eosin Y's partition coefficient in the sclera is 3 times that in the cornea, which correlates with the volume fraction of collagen present in these tissues (2.5 times greater in the sclera). Another molecule that is known to bind to collagen is sulforhodamine[48-50]. Its partition coefficient in the sclera is 13.6[38] similar to that of eosin Y.

Accurate values of the partition coefficient are important in understanding the transport of drug into the tissue. During transient introduction of a given drug to the tissue from a topically applied vehicle, the concentration profile as a function of depth into the tissue at a particular contact time is directly proportional to the partition coefficient (Equation 6). In prior literature on corneal collagen cross-linking with riboflavin, the concentration profile in the tissue has been estimated assuming a partition coefficient of 1[32], which under-estimates the riboflavin concentration. Based on the value determined in porcine tissue *in vitro* ($k_{s,R}$ = 1.7 ± 0.2), and the similarity between porcine and human cornea[51], we expect the actual concentration to be 70% greater than estimated using k = 1. This represents a significant error with respect to understanding the toxicity observed for riboflavin combined with UV irradiation.

While, the partition coefficient determines the concentration immediately inside the tissue relative to that in topically applied vehicle, the diffusion coefficient determines how rapidly molecules are transported into the tissue. Diffusion of drugs in the stroma

and sclera has been modeled by considering the tissue as a composite consisting of impermeable collagen fibrils embedded in a gel matrix of proteoglycan and water[36]. A molecule's diffusion rate through the stroma and sclera depends on its binding interaction with the tissue, the volume fraction of the impermeable collagen fibrils, and its molecular size[36].

The greater the affinity of the drug for the proteins or proteoglycans in the tissue, the lower the effective diffusion coefficient is. A one-dimensional diffusion model with binding interactions developed by Jiang *et al.*[38] accounts for the binding effect separately from the diffusion process. The effective diffusion coefficient, *D,* is modeled as the product of the "free" diffusivity (without binding), D_{ab}, and the fraction of molecules that are in the "free" state:

$$D = D_{ab}\frac{K_{eq}}{1 + K_{eq}} \qquad \text{Equation 10}$$

where K_{eq} is the ratio of free-to-bound molecules in the tissue at equilibrium,

$$K_{eq} = \frac{C_{free}}{C_{bound}} \qquad \text{Equation 11}$$

The model eliminates K_{eq} in favor of the partition coefficient, which can be viewed as

$$k = \frac{C_{tissue}}{C_{solution}} = \frac{C_{free} + C_{bound}}{C_{solution}} \qquad \text{Equation 12}$$

where $C_{solution}$ is the concentration of the compound in the bath solution in contact with the tissue, which is assumed to be equal to the concentration of "free" molecules in the tissue. This yields

$$k = 1 + \frac{1}{K_{eq}} \qquad \text{Equation 13}$$

Combining Equation 13 and 10, we can evaluate D_{ab} from our results for each pair of k and D

$$D_{ab} = kD \qquad \text{Equation 14}$$

Table 4.2. Deduced values for the "Free" diffusivity, D_{ab} from the observed effective diffusitivity, D and the partition coefficient, k, for eosin Y and riboflavin in the cornea and sclera.

		D (μm²/s)	k	D_{ab} (μm²/s)
Cornea	Eosin Y	62	4.3	267
	Riboflavin	79	1.7	134
Sclera	Eosin Y	6.2	13.0	81
	Riboflavin	27	1.5	41

In view of the model, the free diffusivity for riboflavin and eosin Y can be evaluated from each pair of k and D (Table 4.2). For each drug, its free diffusivity D_{ab} in the cornea is three times greater than in the sclera. Molecules diffusing through these tissues must diffuse around the impermeable collagen fibrils so the more collagen the tissue has, the more tortuous the diffusion path is expected to be.

For a given tissue, D_{ab} is proportional to permeability (Equation 9 and 12), which depends strongly on the molecular radius[42]. Therefore, it is interesting to note that the free diffusivity of riboflavin is half that of eosin Y. Riboflavin's hydrodynamic radius is 5.8 Å[52]. Although no reported value for eosin Y's hydrodynamic radius was found, it is expected to be similar to fluorescein's, which is 4.8 Å[42]. Based on the correlation between permeability of the corneal stroma and the hydrodynamic radius of the permeant[42], a decrease in hydrodynamic radius from 5.8 Å to 4.8 Å, is expected to increase stromal permeability by a factor of 1.7. Thus, the observed ratio of the free diffusivities of riboflavin and eosin Y can be understood in terms of their hydrodynamic radii.

The effective diffusion coefficient determines how rapidly molecules penetrate through a given tissue, which controls the transient distribution of drug inside the tissue following application of a drug formulation on its surface. In a safety study of corneal collagen cross-linking with riboflavin, the drug concentration profile was calculated using fluorescein's effective diffusion coefficient, $D = 65\ \mu m^2/s$[32]. This approximation is indeed close to riboflavin's diffusivity ($D = 79\ \mu m^2/s$); consequently the error resulting from the approximated diffusivity is small (~10%) relative to the error resulting from the approximation used previously for the partition coefficient (~70%) described above.

Selection of delivery vehicles for *in vivo* treatments of the cornea can be guided by quantitative comparison of the amount of drug transferred to the tissue. Soaking provides a benchmark (Figure 4.8a) that can be regarded as a best possible scenario (an infinite reservoir of drug in continuous contact with the tissue with some convective transport).

There are many options that provide results that approach that of soaking (i.e., reduced by 30-40% relative to soaking). Application of drops, approximately 3/4 as much drug transfer as soaking and is clinically feasible. Viscous gels provide approximately 2/3 as much drug transfer as soaking (Figure 4.8). The selected viscosity enhancers (hyaluronic acid[53, 54], carboxymethylcellulose[55, 56], sodium alginate[57], and methylcellulose[58] have been widely used in various ocular drug delivery systems. Among the different gels studied, carboxymethylcellulose (CMC) formulation was clear, smooth, free of air bubbles and the easiest to handle for spreading onto the cornea; therefore, CMC gel was selected as the delivery vehicle for *in vitro* and *in vivo* corneal treatment (Chapter 6).

4.5 CONCLUSION

Measurements of the amount of drug delivered to a target tissue (cornea or sclera) as a function of delivery time enable determination of the partition coefficient and diffusion coefficient of two drugs that are relevant to collagen cross-linking—riboflavin and eosin Y. The method can be extended to other drug molecules and to other tissues. The values of the diffusion coefficient and the partition coefficient provide essential information to predict the drug concentration profile in the tissue as a function of drug concentration, application time, and delay time between drug application and irradiation (Chapter 5). Knowledge regarding the drug concentration profile is critical to understanding the penetration of light into the tissue and, in turn, the spatial distribution of cross-link formation inside the tissue as a function of treatment conditions.

4.6 ACKNOWLEDGEMENTS

This work includes contributions from Viet Anh Nguyen Huu, Joyce Liu, and Dr. Matthew Mattson. Undergraduate Viet Anh Nguyen Huu contributed developing the extraction method and assisted in collecting data. Undergraduate Joyce Liu contributed to developing the absorbance method and collected data. Dr. Matthew Mattson assisted in collecting data and provided valuable advice for fitting data.

4.7 BIBLIOGRAPHY

1. Lee, V.H., Robinson, J.R., *Topical Ocular Drug Delivery: Recent Developments and Future Challenges.* Journal of Ocular Pharmacology and Therapeutics, 1986. **2**(1): p. 67.
2. Davies, N.M., *Biopharmaceutical Considerations in Topical Ocular Drug delivery.* Clinical and Experimental Pharmacology & Physiology, 2000. **27**(7): p. 558.
3. Urtti, A., *Challenges and Obstacles of Ocular Pharmacokinetics and Drug Delivery.* Advanced Drug Delivery Reviews, 2006. **58**(11): p. 1131.
4. Burstein, N.L., Anderson, J.A., *Corneal Penetration and Ocular Bioavailability of Drugs.* Journal of Ocular Pharmacology and Therapeutics, 1985. **1**(3): p. 309.
5. Wollensak, G., Iomdina, E., *Long-term Biomechanical Properties of Rabbit Sclera After Collagen Crosslinking Using Riboflavin and Ultraviolet A (UVA).* Acta Ophthalmologica, 2009. **87**(2): p. 193-198.
6. Wollensak, G., *Crosslinking Treatment of Progressive Keratoconus: New Hope.* Current Opinion in Ophthalmology, 2006. **17**(4): p. 356.
7. Raiskup-Wolf, F., Hoyer, A., Spoerl, E., Pillunat, L.E., *Collagen Crosslinking with Riboflavin and Ultraviolet-A light in Keratoconus: Long-term Results.* Journal of Cataract and Refractive Surgery, 2008. **34**(5): p. 796.
8. Kohlhaas, M., Spoerl, E., Speck, A., Schilde, T., Sandner, D. Pillunat, L.E., *A New Treatment of Keratectasia After LASIK by Using Collagen with Riboflavin/UVA Light Cross-linking.* Klinische Monatsblätter für Augenheilkunde, 2005. **222**(5): p. 430-6.

9. Kymionis, G. D., Diakonis, V.F., Kalyvianaki, M., Portaliou, D., Siganos, C., Kozobolis, V.P.*, et al.*, *One-Year Follow-up of Corneal Confocal Microscopy After Corneal Cross-Linking in Patients With Post Laser In Situ Keratosmileusis Ectasia and Keratoconus.* American Journal of Ophthalmology, 2009. **147**(5): p. 774.

10. Wollensak, G., Iomdina, E., Dittert, D., Salamatina, O., Stoltenburg G, *Crosslinking of Scleral Collagen in the Rabbit Using Riboflavin and UVA.* Acta Ophthalmologica Scandinavica, 2005. **83**(4): p. 477.

11. Rabinowitz, Y.S., *Keratoconus.* Survey of Ophthalmology, 1998. **42**(4): p. 297-319.

12. Bron, A.J., *Keratoconus.* Cornea, 1988. **7**(3): p. 163-9.

13. Krachmer, J.H., Feder, R.S., Belin, M.W., *Keratoconus and Related Noninflammatory Corneal Thinning Disorders.* Survey of Ophthalmology, 1984. **28**(4): p. 293-322.

14. Randleman, J.B., *Post-laser In-situ Keratomileusis Ectasia: Current Understanding and Future Directions.* Current Opinion in Ophthalmology, 2006. **17**(4): p. 406.

15. Binder, P., Lindstrom, R., Stulting, R.D., Donnenfeld, E., Wu, H., McDonnell, P.*, et al.*, *Keratoconus and Corneal Ectasia After LASIK.* Journal of Refractive Surgery, 2005. **21**(6): p. 749-752.

16. Binder, P.S., *Ectasia After Laser In Situ Keratomileusis.* Journal of Cataract & Refractive Surgery, 2003. **29**(12): p. 2419-29.

17. Klein, S.R., Epstein, R.J., Randleman, J.B., Stulting, R.D., *Corneal Ectasia After Laser In Situ Keratomileusis in Patients without Apparent Preoperative Risk Factors.* Cornea, 2006. **25**(4): p. 388.

18. McBrien, N.A., Gentle, A., *Role of the Sclera in the Development and Pathological Complications of Myopia.* Progress in Retinal and Eye Research, 2003. **22**(3): p. 307.

19. Rada, J.A., Shelton, S., Norton, T.T., *The Sclera and Myopia.* Experimental Eye Research, 2006. **82**(2): p. 185.

20. Curtin, B.J., *The Myopias: Basic Science and Clinical Management*. 1985: Harpercollins College Div.

21. Spoerl, E., Huhle, M., Seiler, T., *Induction of Cross-links in Corneal Tissue.* Experimental Eye Research, 1998. **66**(1): p. 97.

22. Wollensak, G., Spöerl, E., Reber, F., Pillunat, L., Funk, R., *Corneal Endothelial Cytotoxicity of Riboflavin/UVA Treatment In Vitro.* Ophthalmic Research, 2003. **35**(6): p. 324.

23. Wollensak, G., Iomdina, E., *Biomechanical and Histological Changes After Corneal Crosslinking with and without Epithelial Debridement.* Journal of Cataract & Refractive Surgery, 2009. **35**(3): p. 540-546.

24. Wollensak, G., Spoerl, E., *Collagen Crosslinking of Human and Porcine Sclera.* Journal of Cataract & Refractive Surgery, 2004. **30**(3): p. 689-695.

25. Alleyne, C.H., Cawley, C.M., Barrow, D.L., Poff, B.C., Powell, M.D., Sawhney, A.S.*, et al.*, *Efficacy and Biocompatibility of a Photopolymerized, Synthetic,*

Absorbable Hydrogel as a Dural Sealant in a Canine Craniotomy Model. Journal of Neurosurgery, 1998. **88**(2): p. 308.

26. Wollensak, G., Spoerl, E., Seiler, T., *Riboflavin/ultraviolet-a-induced Collagen Crosslinking for the Treatment of Keratoconus.* American Journal of Ophthalmology, 2003. **135**(5): p. 620-627.
27. SÃ¸ndergaard, A. P., Søndergaard, *Corneal Distribution of Riboflavin Prior to Collagen Cross-Linking.* Current eye research. **35**(2): p. 116.
28. Cui, L., Huxlin, K.R., Xu, L., MacRae, S., Knox, W.H., *High-resolution, Non-invasive Two-photon Fluorescence Measurement of Molecular Concentrations in Corneal Tissue.* Investigative Ophthalmology & Visual Science.
29. Maurice, D., *The Movement of Fluorescein and Water in the Cornea.* American Journal of Ophthalmology, 1960. **49**(5): p. 1011-1016.
30. Nagataki, S., Brubaker, R.F., Grotte, D.A., *The Diffusion of Fluorescein in the Stroma of Rabbit Cornea.* Experimental Eye Research, 1983. **36**(6): p. 765.
31. Shiraya, K., Nagataki, S., *Movement of Fluorescein Monoglucuronide in the Rabbit Cornea. Diffusion in the Stroma and Endothelial Permeability.* Investigative Ophthalmology & Visual Science, 1986. **27**(1): p. 24.
32. Spoerl, E., Mrochen, M., Sliney, D., Trokel, S., Seiler, T., *Safety of UVA-riboflavin Cross-linking of the Cornea.* Cornea, 2007. **26**(4): p. 385.
33. Maren, T.H., Jankowska, L., Sanyal, G., Edelhauser, H.F., *The Transcorneal Permeability of Sulfonamide Carbonic Anhydrase Inhibitors and Their Effect on Aqueous Humor Secretion.* Experimental Eye Research, 1983. **36**(4): p. 457.

34. Ahmed, I., Gokhale, R.D., Shah, M.V., Patton, T.F., *Physicochemical Determinants of Drug Diffusion Across the Conjunctiva, Sclera, and Cornea.* Journal of Pharmaceutical Sciences, 1987. **76**(8): p. 583.

35. Ambati, J., Canakis, C.S., Miller, J.W., Gragoudas, E.S., Edwards, A., Weissgold, D.J.*, et al.*, *Diffusion of High Molecular Weight Compounds through Sclera.* Investigative Ophthalmology & Visual Science, 2000. **41**(5): p. 1181.

36. Edwards, A., Prausnitz, M.R., *Fiber Matrix Model of Sclera and Corneal Stroma for Drug Delivery to the Eye.* AIChE journal, 2006. **44**(1): p. 214.

37. Boubriak, O.A., Urban, J.P., Akhtar, S., Meek, K.M., Bron, A.J., *The Effect of Hydration and Matrix Composition on Solute Diffusion in Rabbit Sclera.* Experimental Eye Research, 2000. **71**(5): p. 503.

38. Jiang, J., Geroski, D.H., Edelhauser, H.F., Prausnitz, M.R., *Measurement and Prediction of Lateral Diffusion within Human Sclera.* Investigative Ophthalmology & Visual Science, 2006. **47**(7): p. 3011.

39. Waheed, A.A., Rao, K.S., Gupta, P.D., *Mechanism of Dye Binding in the Protein Assay Using Eosin Dyes.* Analytical Biochemistry, 2000. **287**(1): p. 73.

40. Birkedal-Hansen, H., *Eosin Staining of Gelatine.* Histochemistry and Cell Biology, 1973. **36**(1): p. 73.

41. Prausnitz, M.R., Noonan, J.S., Rudnick, D.E., Edelhauser, H.F. , Geroski, D.H., *Measurement and Prediction of Transient Transport across Sclera for Drug Delivery to the Eye.* Industrial & Engineering Chemistry Research, 1998. **37**(8): p. 2903.

42. Prausnitz, M.R., Noonan, J.S., *Permeability of Cornea, Sclera, and Conjunctiva: A Literature Analysis for Drug Delivery to the Eye.* Journal of Pharmaceutical Sciences, 1998. **87**(12): p. 1479.

43. Chan, T., Payor, S., Holden, B.A., *Corneal Thickness Profiles in Rabbits Using an Ultrasonic Pachymeter.* Investigative Ophthalmology & Visual Science, 1983. **24**(10): p. 1408.

44. Bartholomew, L.R., Pang, D.X., Sam, D.A., Cavender, J.C., *Ultrasound Biomicroscopy of Globes from Young Adult Pigs.* American Journal of Veterinary Research, 1997. **58**(9): p. 942-8.

45. Cheruvu, N.P., Kompella, U.B., *Bovine and Porcine Transscleral Solute Transport: Influence of Lipophilicity and the Choroid–Bruch's Layer.* Investigative Ophthalmology & Visual Science, 2006. **47**(10): p. 4513.

46. Waheed, A. A., *Mechanism of dye binding in the protein assay using eosin dyes.* Analytical biochemistry, 2000. **287**(1): p. 73.

47. Anderson, R. F., *Energetics of the One-electron Reduction Steps of Riboflavin, FMN and FAD to Their Fully Reduced Forms.* Biochimica et Biophysica Acta - Bioenergetics, 1983. **722**(1): p. 158.

48. Ricard, C., JC., Vial, Douady, J., Van Der Sanden, B., *In Vivo Imaging of Elastic Fibers Using Sulforhodamine B.* Journal of Biomedical Optics, 2007. **12**(6): p. 064017.

49. Ricard, C., JC., Vial, Douady, J., Van Der Sanden, B. *Imaging Elastic and Collagen Fibers with Sulforhodamine B and Second-harmonic Generation*. in *Proceedings of SPIE*. 2008.

50. Chodosh, J., Dix, R.D., Howell, R.C., Stroop, W.G., Tseng, S.C., *Staining Characteristics and Antiviral Activity of Sulforhodamine B and Lissamine Green B.* Investigative Ophthalmology & Visual Science, 1994. **35**(3): p. 1046.

51. Kampmeier, J., Radt, B., Birngruber, R., Brinkmann, R., *Thermal and Biomechanical Parameters of Porcine Cornea.* Cornea, 2000. **19**(3): p. 355-63.

52. Shin, H. S., *Permeation of Solutes Through Interpenetrating Polymer Network Hydrogels Composed of Poly(vinyl alcohol) and Poly (acrylic acid).* Journal of Applied Polymer Science, 1998. **69**(3): p. 479.

53. Luo, Y., Kirkerb, K.R., Prestwich, G.D., *Cross-linked Hyaluronic Acid Hydrogel Films: New Biomaterials for Drug Delivery.* Journal of Controlled Release, 2000. **69**(1): p. 169.

54. Aragona, P., Papa, V., Micali, A., Santocono, M., Milazzo, G., *Long Term Treatment with Sodium Hyaluronate-containing Artificial Tears Reduces Ocular Surface Damage in Patients with Dry Eye.* British Journal of Ophthalmology, 2002. **86**(2): p. 181.

55. Christensen, M.T., Cohen, S., Rinehart, J., Akers, F., Pemberton, B., Bloomenstein, M.*, et al.*, *Clinical Evaluation of an HP-guar Gellable Lubricant Eye Drop for the Relief of Dryness of the Eye.* Current Eye Research, 2004. **28**(1): p. 55.

56. Korb, D.R., Scaffidi, R.C., Greiner, J.V., Kenyon, K.R., Herman, J.P., Blackie, C.A.*, et al.*, *The Effect of Two Novel Lubricant Eye Drops on Tear Film Lipid Layer Thickness in Subjects with Dry Eye Symptoms.* Optometry & Vision Science, 2005. **82**(7): p. 594-601.

57. Lin, H.R., Sung, K.C., Vong, W.J., *In Situ Gelling of Alginate/Pluronic Solutions for Ophthalmic Delivery of Pilocarpine.* Biomacromolecules, 2004. **5**(6): p. 2358.

58. Chrai, S.S., Robinson, J.R., *Ocular Evaluation of Methylcellulose Vehicle in Albino Rabbits.* Journal of Pharmaceutical Sciences, 1974. **63**(8): p. 1218.

Chapter 5

A Model for the Photodynamic Collagen Cross-linking Treatment

5.1 INTRODUCTION

Keratoconus is an ocular disease characterized by progressive corneal thinning, protrusion, and scarring, resulting in irregular astigmatism and myopia. It is a bilateral corneal ectasia with a prevalence of 1 out of 2,000, affecting people of all ethnicities and genders equally[1]. Cornea thinning appears to result from loss of material, but it is unclear how or what causes this to happen. Increases in collagenase and other protease activities have been cited as important in the development of corneal ulcerations and keratoconus[2-4]. The corneas of keratoconus eyes are found to have fewer collagen lamellae, fewer collagen fibrils per lamella, closer packing of collagen fibrils or various combinations of these factors resulting in a weakened structure.

Wollensak *et al.* has developed a treatment for halting the progression of keratoconus by inducing corneal collagen cross-linking[5, 6]. The treatment uses riboflavin activated by UVA to form cross-links inside the cornea. Cross-links serve two important roles in the treatment: to enhance the tissue strength and to increase resistance to collagen

degradation by enzymes[2, 7, 8]. Riboflavin/UVA has shown an ability to halt the progression of keratoconus in patients for studies lasting up to 6 years[5, 6]. However, there are drawbacks to the treatment, including cytotoxicity in the cornea which leads to corneal haze for weeks to months following surgery, and it uses a lengthy surgical procedure (60 minutes per eye). Because the treatment is toxic to both keratocytes and endothelial cells, the treatment was carefully designed to limit cytotoxicity to the anterior 350 μm[9-12]. A high drug concentration and long drug delivery time prior to cross-linking ensures that there is enough riboflavin in the tissue to block UV light from penetrating to the endothelium, and only patients with corneas thicker than 400 μm can be treated. Thus, there is a need for an improved cross-linking treatment to reduce toxicity and treatment time. Eosin Y/visible light can potentially provide such a treatment (Chapter 6).

Since treatment efficacy depends on both the quantity and distribution of cross-links formed along the tissue depth, studies have examined various properties of the treated tissue at different depths (i.e. change in biomechanical strength[7], maximum hydrothermal shrinkage temperature[13], collagen fiber diameter[14], and hydration[15]). These comparisons were made using bulk sections of the tissues, so they do not provide information regarding the extent of cross-linking as a function of tissue depth. Here, we create a model to quantify the extent of cross-linking as a function of depth for collagen cross-linking induced by photosensitizers. This model provides a more detailed map of the spatial distribution of cross-links for the riboflavin/UVA treatment. It can also be used as an optimization tool for selecting treatment parameters for the eosin Y/visible light treatment.

Photodynamic collagen cross-linking treatment has many treatment parameters including drug concentration, drug contact time, delay time between the end of contact time to the beginning of irradiation period, and irradiation intensity and duration (Figure 5.1). Each parameter affects the safety and efficacy of the treatment and all of the combined parameters yield a very large treatment parameter space. With such a large treatment parameter space, it would be very laborious and costly to optimize the treatment by carrying out experiments. A model can provide insights of how each parameter and combinations of parameters affect the outcome of the treatment.

5.2 METHODS

Design of experiments – The collagen gel photorheological technique discussed in Chapter 3 was used to gather collagen cross-linking rate data in order to model the extent and distribution of cross-link formation in the tissue. Collagen gel samples have uniform drug concentration profiles based on the preparation technique developed in Chapter 3. The protocols for collagen gel preparation and photorheological measurement are described in the Methods Section of Chapter 3. The pairs of drug concentrations and collagen gel thicknesses were selected such that the intensity profile is approximately uniform throughout the sample. Based on light intensity calculations, this is achieved when the ratio of light penetration depth over sample thickness is 1.2. The light intensity profile in the sample is given by:

$$I(z) = I_o e^{-(\mu + C\varepsilon)z} \qquad \text{Equation 1}$$

where I is the intensity, I_o is the incident intensity, z is the position inside the collagen gel sample, μ is the collagen gel's absorptivity, C is the drug concentration, and ε is the drug's molar absorptivity. Light enters the sample through a quartz window which is part of the lower plate geometry on the rheometer where the sample sits and travels through the sample to the upper tool made of aluminum. Some of the light hitting the upper tool gets reflected and some gets scattered. For simplicity, we approximate that all the light hitting the upper aluminum tool gets reflected and travels back down the sample and the profile of the reflected light is also given by Beer's law. Therefore, the total intensity the sample is exposed to at a given position is the sum of the incident light plus the reflected light.

$$I(z) = I_o e^{-(\mu+C\varepsilon)z} + I_o e^{-(\mu+C\varepsilon)L} e^{-(\mu+C\varepsilon)(L-z)} \qquad \text{Equation 2}$$

Based on this light intensity calculation approach, pairs of drug concentration and sample thickness were selected such that the light intensity profile is approximately uniform throughout the sample. For 450 μm thick riboflavin samples, the light intensity profile is approximately uniform throughout for concentrations less than or equal to 0.03%. For a 225 μm sample, the intensity profile is approximately uniform for concentrations less than or equal to 0.05%. The highest concentration was limited by the minimum thickness of collagen gel samples that could be loaded onto the rheometer. The thinnest collagen gel samples that could be prepared and handled to yield reproducible results were 225 μm thick which corresponds to a 0.05% riboflavin concentration. For 450 μm thick eosin Y samples, the light intensity profile is approximately uniform for concentrations less than

or equal to 0.01%. For 225 μm samples, the intensity profile is approximately uniform for concentrations less than or equal to 0.02%. Rate data at these thicknesses and concentrations were used to build a model for cross-linking inside the tissue with non-uniform drug concentration and light intensity profiles.

Design of the model – Photodynamic collagen cross-linking depends on both the local photosensitizer concentration and the light intensity which are functions of treatment parameters: drug concentration, contact time (duration the drug is in contact with the tissue), delay time (period between end of contact time and beginning of irradiation), and irradiation time (Figure 5.1). Since drug is applied topically to the cornea, the photosensitizer concentration varies along the tissue depth with time. The concentration profile can be calculated using Fick's diffusion equation. The light intensity also varies along the tissue as determined by Beer's law. The cross-linking profile is also expected to vary along the depth since the local cross-linking rate depends on the photosensitizer concentration and light intensity. In order to evaluate the instantaneous local cross-linking rate, the cornea is divided in thin sections along the visual axis so that each section has an approximately uniform concentration and intensity profile. Within each section, the instantaneous cross-linking rate is obtained from collagen gel photorhelogy data (rate of change in storage modulus) of collagen samples with uniform concentration profiles and approximately uniform light intensity profiles. The local change in storage modulus after a given irradiation time is the sum of the instantaneous changes in modulus at each time step.

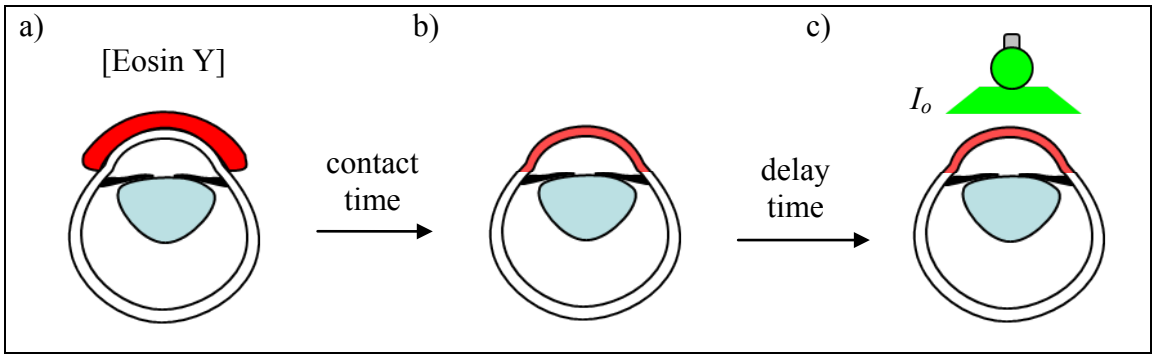

Figure 5.1. a) Topical application of the drug formulation onto the cornea. **b)** Remove drug from the cornea at the end of contact time. **c)** Irradiation after a delay time.

Using the partition coefficient and diffusion coefficient (Chapter 4) of the system we can calculate the concentration profile as a function of time for a selected topically applied drug concentration, contact time (duration the drug is in contact with the tissue), delay time (period between end of contact time and beginning of irradiation), and irradiation time.

The cornea is the targeted tissue and it has a thickness on the order of 1 mm. Since the tissue thickness is less than an order of magnitude compared to the diameter of the eye (~24 mm), it is modeled as a semi-infinite slab of uniform material in which molecules can diffuse. Fick's diffusion equation is given by

$$\frac{\partial C(z)}{\partial t} = D\frac{\partial^2 C(z)}{\partial z^2} \qquad \text{Equation 3}$$

where C is the drug concentration inside the tissue, t is time, z is the position inside the tissue, and D is the diffusion coefficient. An initial condition and two boundary

conditions are necessary to solve the equation. During the contact time, the appropriate conditions are

$$\text{Initial condition at } t = 0,\ C = 0 \text{ for all } z \geq 0 \qquad \text{Equation 4.1}$$

$$\text{Boundary condition at } z = 0,\ C = k \cdot C_{drug} \text{ for } t > 0 \qquad \text{Equation 4.2}$$

$$\text{Boundary condition at } z = \infty,\ C = 0 \text{ for all } t \text{ during the contact time} \qquad \text{Equation 4.3}$$

where k is the partition coefficient and C_{drug} is the bulk concentration of the drug solution applied. Initially before drug is applied to the tissue, the concentration is zero everywhere inside the tissue (Equation 4.1). After the drug is applied, the surface of the tissue where drug diffuses into is always in equilibrium with the drug solution (Equation 4.2). During the drug contact time, the concentration is zero far into the tissue (semi-infinite slab of material approximation, Equation 4.3). Applying the initial and boundary conditions to the diffusion equation, the concentration profile is given by

$$C(t,z) = k \cdot C_{drug} \cdot erfc\left(\frac{z}{\sqrt{4Dt}}\right) \qquad \text{Equation 5}$$

where *erfc* is the complementary error function. The concentration profile evolves after the drug solution is removed. The concentration profile after a delay time is also given by Fickian diffusion (Equation 1) but with a different set of initial and boundary conditions. The concentration profile at the end of the contact time (Equation 5) is the initial condition for computing the concentration profile during the delay time profile. We approximate the system with a no flux boundary condition at the anterior surface because

drops of balanced saline solution are applied just enough to prevent corneal dehydration during the delay time. Based on this procedure, a negligible quantity of drug would be removed through the anterior surface of the cornea.

$$\frac{dC}{dz}\Big|_{z=0} \approx 0 \quad \text{during the delay and irradiation time} \qquad \text{Equation 6}$$

The flux at the back of the cornea is given by

$$J|_{z=L} = h_m(C|_{z=L} - C_{ac}) \qquad \text{Equation 7.1}$$

where h_m is the mass transfer coefficient in the anterior chamber, C_{ac} is the concentration in the aqueous chamber. A calculation is done to determine how significant the flux through the back of the cornea into the aqueous chamber is relative to the amount of drug present in the tissue by comparing the flux leaving the cornea to enter the aqueous chamber, J_{out} to the average flux of drug entering the cornea, J_{in} during the contact time. As a conservative approximation, we use the greatest flux which is when C_{ac} is 0.

$$\frac{J_{out}}{J_{in}} = \frac{h_m C|_{z=L}}{C_{avg} L/t} \qquad \text{Equation 7.2}$$

where C_{avg} is the average drug concentration in the cornea after a given drug contact time. Reported values of h_m for fluorescein in the cornea range from 1.15 x 10^{-4} to 2.3 x 10^{-4} cm/min[16]. Using the largest reported value for h_m, for a 5 minute eosin Y contact time, J_{out}/J_{in} is 7.9 x 10^{-4}, and for a 30 minutes contact time J_{out}/J_{in} is 0.0655. The ratio

J_{out}/J_{in} is much less than 1 so the flux of drug leaving the cornea to enter the anterior chamber is not significant therefore the no flux boundary condition is also applied at the posterior surface of the cornea.

$$J|_{z=L} = -D\frac{dC}{dz}\Big|_{z=L} \approx 0 \qquad \text{Equation 7.3}$$

Apply the initial condition given by Equation 4.1 and the boundary conditions given by Equation 6 and 7.3 to Fick's diffusion equation to solve for the concentration profile with some delay time after the drug contact time. Since the boundary conditions are imposed on surfaces of constant coordinates ($z = 0$ and $z = L$), and the conditions are homogeneous, the equation can be solved using separation of variables

$$C(\tau, z) = \sum_{1}^{\infty} a_n \cos\left(n\pi\frac{z}{L}\right) exp\left(-\frac{n^2\pi^2 D}{L^2}\tau\right) \qquad \text{Equation 8.1}$$

where τ is the time since drug solution was removed from the corneal surface and a_n is

$$a_n = \frac{\int_0^L k \cdot C_{drug} \cdot erfc\left(\frac{z}{\sqrt{4Dt}}\right) \cos\left(n\pi\frac{z}{L}\right)}{\int_0^L \cos^2\left(n\pi\frac{z}{L}\right)} dz \qquad \text{Equation 8.2}$$

Equation 8.1 and 8.2 give the concentration profile after the drug contact time, and throughout the irradiation time. This model does not take into account the consumption of the photosensitizer as the reaction occurs. This is an acceptable approximation since

collagen gel cross-linking experiments show a constant rate for $\Delta G'$ throughout a 30-minute reaction period (Chapter 3). This implies the fraction of eosin Y consumption is negligible over this time period; therefore, as long as the irradiation period for the treatment is 30 minutes or less, this approximation is reasonable.

For each concentration profile, the corresponding light intensity profile is

$$I(z) = I_o * e^{-\int_0^z [\mu + C(z)\varepsilon] z \, dz} \qquad \text{Equation 9}$$

where I is the intensity, I_o is the incident intensity, μ is the tissue's absorptivity, and ε is the drug's molar absorptivity.

For a given drug concentration profile and the corresponding light intensity profile, the instantaneous local cross-linking rate is quantified by the rate of change in modulus, dG'/dt obtained from collagen gel photorheology. The total change in local modulus after a given irradiation time, t_{irr} is determined by summing over each instantaneous rate of increase in modulus.

$$\Delta G'(z,t) = \int_0^{t_{irr}} \left.\frac{dG'}{dt}\right|_{t,z} dt \qquad \text{Equation 10}$$

The average change in modulus of a sample, $\Delta G'_{avg}$, is determined by

$$\Delta G'_{avg} = \frac{1}{L}\int_0^L \Delta G'(z)\, dz \qquad \text{Equation 11}$$

to compare the extent of cross-linking for different treatment conditions.

5.3 RESULTS

Kinetics data – The rate of change in oscillatory storage modulus, *dG'/dt*, increased with increasing riboflavin concentration. Increasing the intensity at a given riboflavin concentration increased *dG'/dt* (Figure 5.2). The rate of change in modulus also increases with increasing eosin Y concentration. Increasing the intensity at a given eosin Y concentration increased *dG'/dt*. The highest riboflavin and eosin Y concentrations examined were limited by the minimum sample thickness that could be prepared and loaded onto the rheometer. Extrapolations using logarithmic fits provide estimated *dG'/dt* for concentrations above 0.05% riboflavin and 0.02% eosin Y.

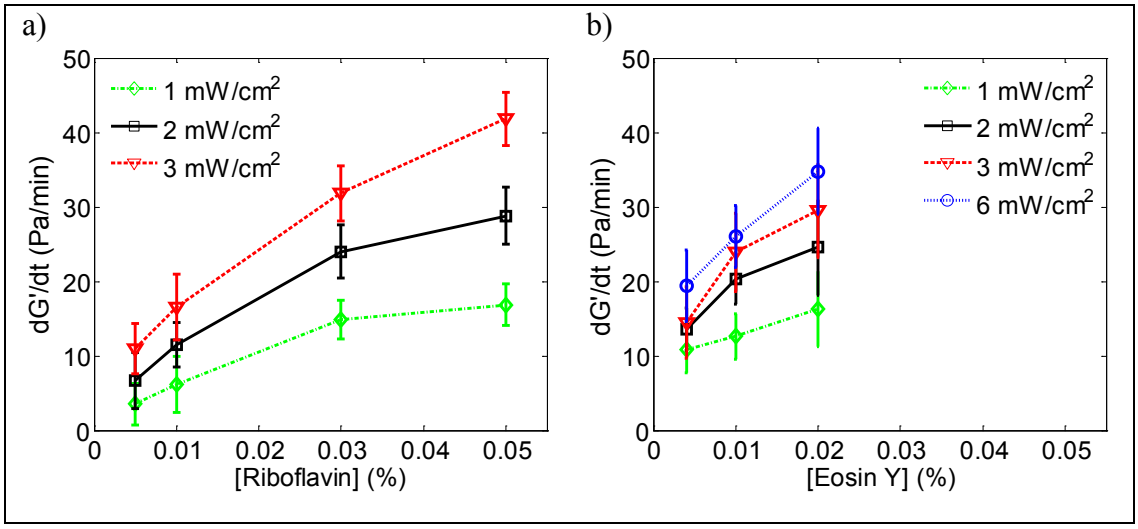

Figure 5.2. Rate of change in oscillatory storage modulus as a function of concentration for collagen gel samples with approximately uniform intensity profiles for **a)** riboflavin and **b)** eosin Y. (N = 4 to 12)

Model of riboflavin/UVA treatment – The riboflavin/UVA treatment currently going through clinical trials in the United States uses the procedure where riboflavin drops (0.1% riboflavin, 20% dextran) are applied every 2 minutes for 30 minutes followed UV irradiation (370 nm, 3 mW/cm^2) for 30 minutes while adding riboflavin drops every 5 minutes. For the clinical protocol treatment, the concentration profile is approximated for a drug contact time of 30 minutes (Figure 5.3a) which yields the corresponding intensity profile (Figure 5.3b) and cross-linking profile ($\Delta G'_{avg}$ is 503 Pa, Figure 5.3c).

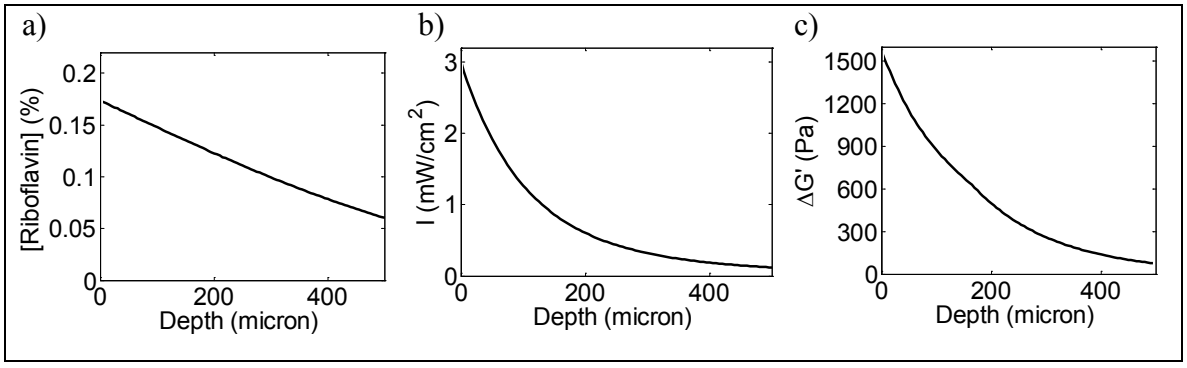

Figure 5.3. a) Concentration profile for 0.1% riboflavin with 30 minutes contact time. **b)** Light intensity profile for 3 mW/cm^2 irradiation. **c)** Profile of modulus increase for 30 minutes irradiation with $\Delta G'_{avg}$ increased by 503 Pa.

Model of eosin Y/visible light treatment – Drug concentration, contact time, and delay time determine the quantity and distribution of drug inside the tissue. For a given drug concentration profile, irradiation intensity and duration determine the extent of cross-linking inside the tissue. The effect each individual treatment parameter has on the cross-linking profile was examined (Table 5.1).

Table 5.1. Treatment parameters, their corresponding symbols, and figures showing their effects.

Treatment parameters	Symbols	Results
Drug concentration	*[Eosin Y]*	Figure 5.4
Drug contact time	t_c	Figure 5.5
Delay time	t_d	Figure 5.6
Irradiation intensity	I_o	Figure 5.7
Irradiation duration	t_{irr}	Figure 5.8

Effect of drug concentration – For a given contact time, increasing the drug concentration proportionately increases the concentration inside the tissue (Figure 5.4a). In turn, increasing the concentration causes the light intensity to decay more steeply (Figure 5.4b).

Increasing the concentration from 0.003% to 0.01% eosin Y, increases the extent of cross-linking everywhere in the tissue (average change in modulus, ($\Delta G'_{avg}$, increases from 80 Pa to 104 Pa, Figure 5.4c); however, further increasing the concentration from 0.01% to 0.03% decreases the light penetration depth from 146 μm to 38 μm (depth at which the intensity is *1/e* of the incident intensity), resulting in most of the tissue with very little light for activating the reaction in the posterior side of the tissue ($\Delta G'_{avg}$ decreased from 104 Pa to 55 Pa). At 0.03% concentration, 75% of the cross-links form in the anterior 135 μm, compared to 290 μm for 0.01% concentration.

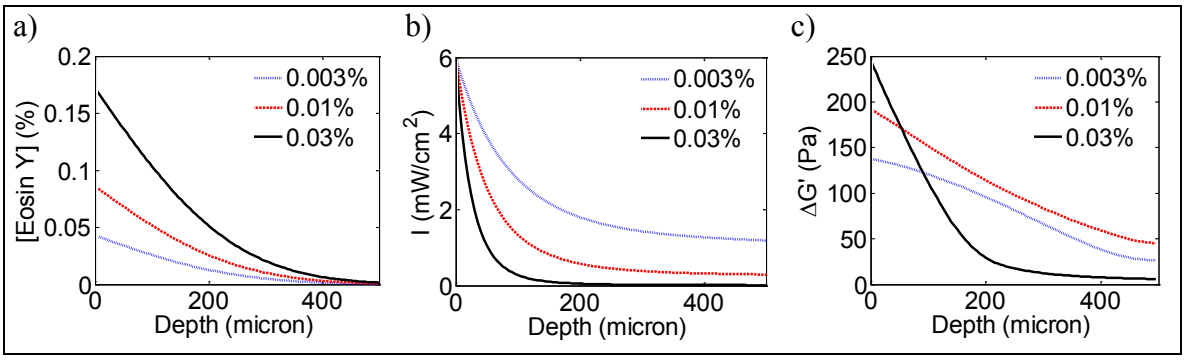

Figure 5.4. a) Eosin Y concentration profile inside the tissue for three different drug concentrations after 5 minutes contact time. **b)** Corresponding light intensity profiles for the three different drug concentrations. **c)** Profile of modulus increase for each drug concentration after 5 minutes irradiation at 6 mW/cm^2. The $\Delta G'_{avg}$ in the tissue is 80 Pa for 0.003%, 104 Pa for 0.01%, and 55 Pa for 0.03%.

Effect of drug contact time – For a given drug concentration, increasing the contact time increases the concentration everywhere in the tissue (provided the contact time is less than the characteristic time, which is the time it takes for drug molecules to penetrate the entire cornea, is given by $L^2/(4*D)$ ~ 15 minutes for eosin Y in the cornea). The increase in the amount of drug in the tissue (Figure 5.5a) causes the light intensity to decay more steeply with longer contact time (Figure 5.5b). Nevertheless, for 0.01% eosin Y, light penetrates the entire thickness even if the drug formulation is given 10 minutes contact time. Consequently increasing the contact time from 1 to 5 minutes, increases the extent of cross-linking everywhere in the tissue ($\Delta G'_{avg}$ increases from 76 to 104 Pa). Increasing the contact time from 5 to 10 minutes, results in a similar cross-linking profile (Figure 5.5c).

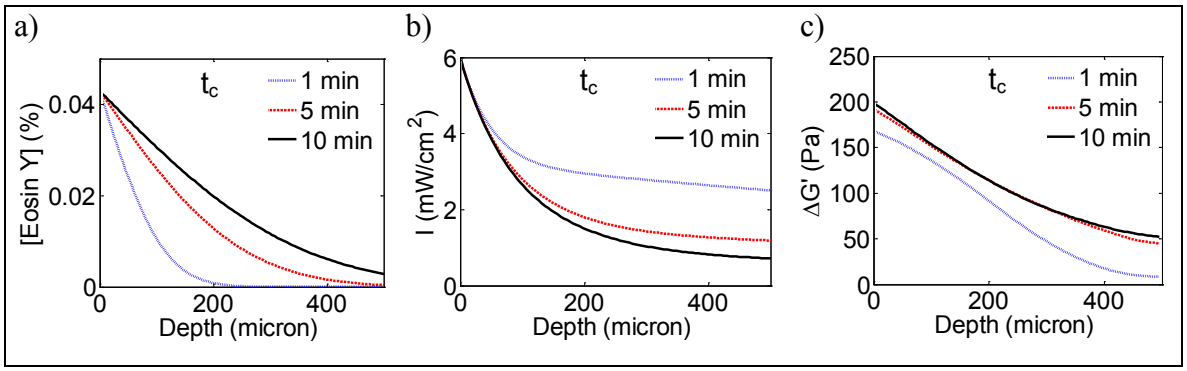

Figure 5.5. a) Eosin Y concentration profile inside the tissue for three different drug contact times using 0.01% eosin Y concentration. **b)** Corresponding intensity profiles for the three different drug contact times. **c)** Profile of modulus increase for each drug concentration after 5 minutes irradiation at 6 mW/cm^2. The $\Delta G'_{avg}$ in the tissue is 76 Pa for 1 minute, 104 Pa for 5 minutes, and 107 Pa for 10 minutes contact time.

Effect of delay time – For a short contact time (less than the characteristic diffusion time), increasing the delay time between removal of the drug formulation and the inception of irradiation results in a more uniform concentration profile (Figure 5.6a). For 5 minutes contact time using 0.01% eosin Y, increasing the delay time, allows the high concentration near the anterior surface to decrease. In turn, this allows light to penetrate more deeply (Figure 5.6b), producing a more uniform distribution of cross-links after 5 minutes of irradiation at 6 mW/cm^2 (Figure 5.6c). While increasing the contact time from 0 to 1 to 5 to 10 minutes yields increasingly uniform cross-linking profiles, it has little effect on $\Delta G'_{avg}$: 104 to 108 to 115 to 119 Pa, respectively.

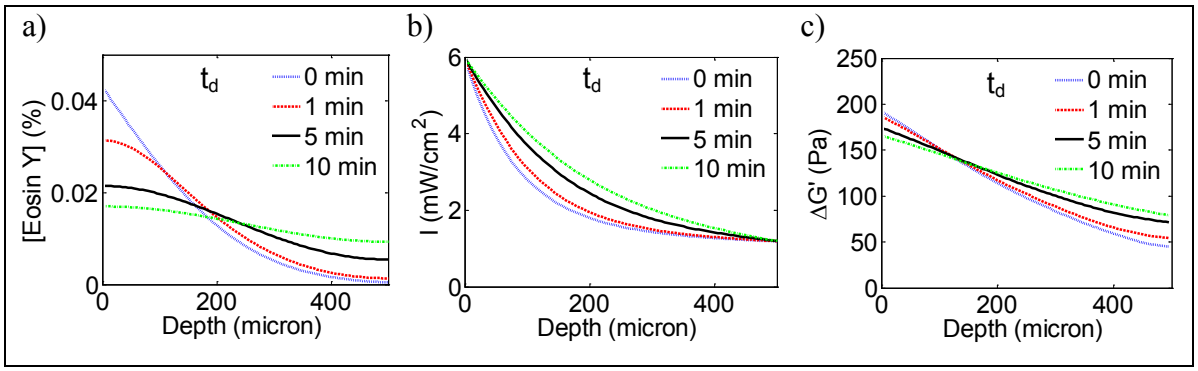

Figure 5.6. a) Eosin Y concentration profile inside the tissue for four different drug delay times using 0.01% eosin Y concentration with 5 minutes contact time. **b)** Corresponding intensity profiles for the four delay times. **c)** Profile of modulus increase for each drug concentration after 5 minutes irradiation at 6 mW/cm^2. The $\Delta G'_{avg}$ in the tissue is 104 Pa for 0 minute, 108 Pa for 1 minute, 115 Pa for 5 minutes, and 119 Pa for 10 minutes delay time.

Effect of irradiation intensity – For a given concentration profile (Figure 5.7a) and a selected light dose (1.8 J/cm^2), the combination of lower intensity and longer irradiation duration results in a greater $\Delta G'_{avg}$. This example uses the concentration profile predicted for topical application of a 0.01% eosin Y solution for 5 minutes contact time, removing the eosin Y from the surface and allowing 1 minute delay time, the corresponding light intensity profiles for three different irradiation intensities (Figure 5.7b), and the resulting cross-linking profiles for a light dose of 1.8 J/cm^2 (Figure 5.7c). The $\Delta G'_{avg}$ is 198 Pa for 15 minutes at 2 mW/cm^2, 139 Pa for 7.5 minutes at 4 mW/cm^2, and 108 Pa for 5 minutes at 6 mW/cm^2. The shape of the cross-linking profiles is similar for all irradiation intensities.

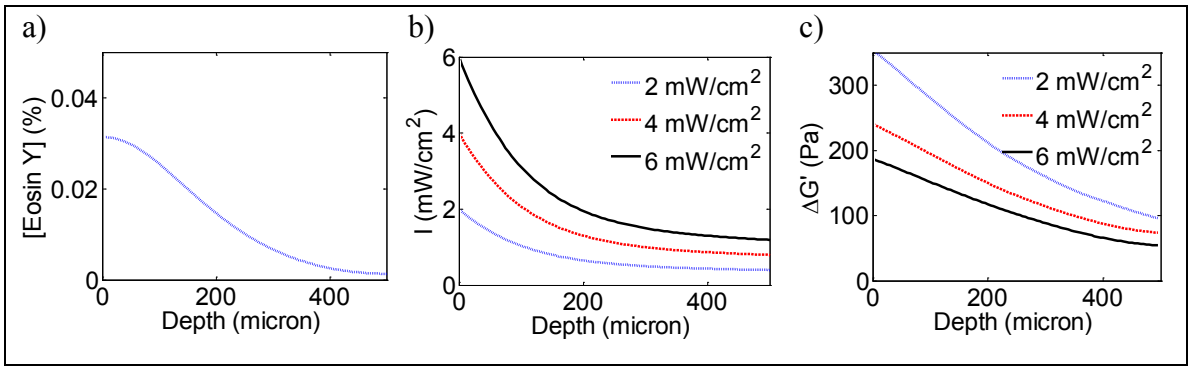

Figure 5.7. a) Concentration profile for 0.01% eosin Y concentration with 5 minutes contact time and 1 minute delay. **b)** Light intensity profiles for three different irradiation intensities. **c)** Profile of modulus increase for the same light dose of 1.8 J/cm^2 using three pairs of intensity and irradiation duration. The $\Delta G'_{avg}$ is 198 Pa for 15 minutes at 2 mW/cm^2, 139 Pa for 7.5 minutes at 4 mW/cm^2, and 108 Pa for 5 minutes at 6 mW/cm^2.

Effect of irradiation duration – For a given concentration profile (Figure 5.8a) and a selected irradiation intensity (6 mW/cm^2), $\Delta G'_{avg}$ increases proportionally with irradiation time. This example uses the concentration profile predicted for topical application of a 0.01% eosin Y solution for 5 minutes contact time, removing the eosin Y from the surface and allowing 1 minute delay time, the corresponding light intensity profile for 6 mW/cm^2 incident on the cornea (Figure 5.8b), and the resulting cross-linking profiles for three irradiation durations (Figure 5.8c). The $\Delta G'_{avg}$ is 108 Pa for 5 minutes, 223 Pa for 10 minutes, and 697 Pa for 30 minutes. The shape of the cross-linking profiles is similar for all irradiation intensities.

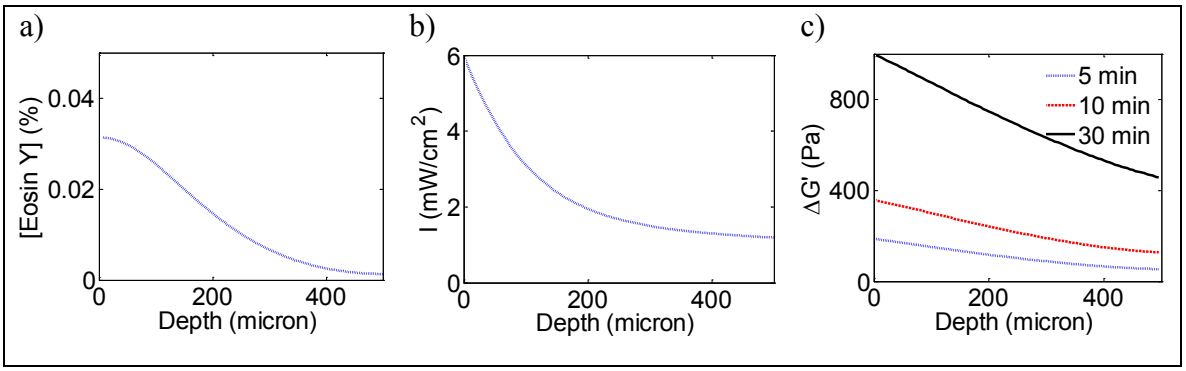

Figure 5.8. a) Concentration profile for 0.01% eosin Y concentration with 5 minutes contact time and 1 minute delay. **b)** Corresponding light intensity profile for 6 mW/cm^2 irradiation. **c)** Profile of modulus increase for three irradiation durations. The $\Delta G'_{avg}$ is 108 Pa for 5 minutes, 223 Pa for 10 minutes, and 697 Pa for 30 minutes.

5.4 DISCUSSION

Comparing riboflavin/UVA model to experimental data – Combining transport parameters and collagen cross-linking rates, we were able to build a model depicting the collagen cross-linking profile as a function of the depth in the tissue. Various studies have examined the extent of cross-linking in the anterior and posterior corneal stroma resulting from the riboflavin/UVA treatment by comparing changes in the resistance to enzymatic degradation[2], thermomechanical[13], collagen fibril diameter[14], hydration[15], and biomechanical behavior[7].

Enzymatic degradation studies suggested the anterior portion of the stroma was more resistant to degradation compared to the posterior portion since the degradation process started at the posterior and moved toward the anterior portion[2]. This result agrees with the model which predicts a monotonically decreasing cross-linking profile over a 500 μm thick cornea for the riboflavin/UVA treatment (Figure 5.4c).

In porcine corneas (800 μm), the anterior portion of treated samples showed significant increase in the maximal hydrothermal shrinkage temperature whereas the posterior portion exhibited a much smaller increase (70.3°C in control samples, 71.2°C in the posterior 400 μm, and 75.0°C in the anterior 400 μm)[13]. The model predicts a $\Delta G'_{avg}$ of 609 Pa in the anterior 400 μm compared to 72 Pa in the posterior 400 μm portion of the cornea. This is consistent with the observed behavior where there is a large increase in the shrinkage temperature in the anterior portion due to a greater extent of cross-linking compared to the posterior portion.

Collagen fiber diameter in treated rabbit corneas (400 μm) were found to increase by 12.2% (3.96 nm) in the anterior portion and by 4.6% (1.63 nm) in the posterior portion compared to untreated corneas[14]. The model predicts a $\Delta G'_{avg}$ of 916 Pa in the anterior 200 μm compared to 267 Pa in the posterior 200 μm. The change in collagen fiber diameter in the anterior cornea is much greater than that of the posterior cornea which is consistent with the modeling results.

Hydration studies in porcine corneas deduced an intensely cross-linked zone of 242 μm at the anterior surface, an intermediate cross-linked zone of 109 μm, and a non-cross-linked posterior zone of 501 μm[15]. The model predicts a $\Delta G'_{avg}$ of 833 Pa in the anterior 242 μm, 307 Pa in the next 109 μm, and 77 Pa in the 501 μm posterior portion.

In human corneas (500 μm), the anterior portion of treated samples showed greater increase in the biomechanical strength compared the posterior portion[7]. The anterior flap increased by 254 x 10^3 N/m^2 whereas the posterior flap increased by 36 x 10^3 N/m^2 relative to their corresponding controls. The model predicts a $\Delta G'_{avg}$ of 916 Pa in the

anterior 200 μm compared to 267 Pa in the posterior 200 μm. Comparison of the results from previous experimental observations with those from the model show very close agreement which suggests the model is a good predictor of the cross-linking profile resulting from the treatment.

Using the model, the predicted riboflavin concentration to maximize cross-linking with the clinical irradiation protocol (3 mW/cm^2 for 30 minutes) is 0.044%, which yields a $\Delta G'_{avg}$ of 618 Pa whereas the clinical concentration (0.1%) only yields a $\Delta G'_{avg}$ of 503 Pa (Figure 5.9). The clinical concentration yields a cross-linking rate that is only 81% of the optimal rate (collagen gel photorheology estimated 78% of the optimal rate, Chapter 3). In addition to providing a greater $\Delta G'_{avg}$, the optimal condition also produces a more uniform cross-linking profile. This is expected to be more advantageous since cross-links serve two purposes when halting the progression of keratoconus: to enhance biomechanical properties and to increase resistance to enzymatic degradation[2, 7, 8]. For an equivalent increase in tissue strength, a more uniform distribution of cross-links is expected to resist enzymatic degradation throughout the cornea better than a less uniform distribution.

Even though an optimal treatment condition exists, it cannot be used due to the cytoxicity nature of riboflavin combined with UVA. The treatment requires a 0.1% riboflavin concentration to prevent a toxic UVA light dose from reaching the endothelium[17]. Because the combination of riboflavin and UVA light is cytotoxic, the clinical protocol was optimized for safety rather than efficacy[9]. Given available data on the combination of drug doses and irradiation intensities that are toxic, the model can also be used to

predict depth of keratocytes apoptosis and endothelial toxicity for various combinations of treatment parameters.

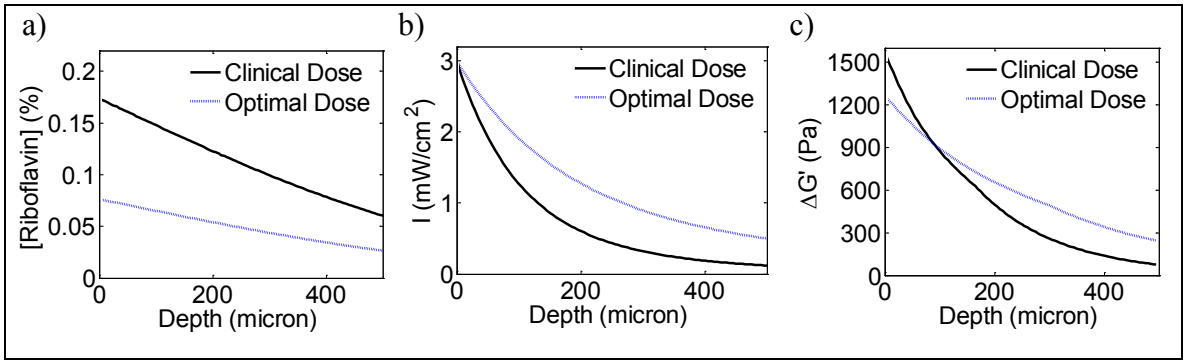

Figure 5.9. a) Riboflavin concentration profile after 30 minutes of topical drug application for clinical dose (0.1%) and optimal dose (0.044%). **b)** Light intensity profiles for 3 mW/cm^2 irradiance. **c)** Profile of modulus increase after 30 minutes of irradiation ($\Delta G'_{avg}$ is 503 Pa for clinical dose and 618 Pa for optimal dose).

Selecting parameters for eosin Y/visible light treatment – Unlike riboflavin/UVA treatment, eosin Y/visible light is much more biocompatible (Chapter 6). Therefore the treatment parameters can be selected based on performance for efficacy instead of safety constraints. The model can be used to examine the role of each treatment parameter and its effect on the overall treatment. In turn, this knowledge can guide selection of treatment conditions that are desirable for clinical use.

Selecting drug delivery protocol – The amount of drug transferred from the formulation into the cornea is determined by the drug concentration in the formulation and the contact time (time between topical application and removal of the formulation). The contact time, delay time, and irradiation duration determine how the drug is distributed inside the tissue at any given moment. Results from the model show that low eosin Y concentration (≤

0.003% applied for 5 minutes, Figure 5.4a) inside the tissue provides a low cross-linking rate yielding a relatively small $\Delta G'_{avg}$ for a given irradiation dose (Figure 5.4c). A high eosin Y concentration ($\geq$ 0.03% applied for 5 minutes, Figure 5.4a) extinguishes most of the light in the anterior portion of the tissue (Figure 5.4b) leaving the posterior section untreated, resulting in a very non-uniform treatment (Figure 5.4c) and a lower $\Delta G'_{avg}$ both of which are not favorable. Therefore, it is desirable to deliver a quantity of drug to the tissue that yields a fast reaction rate and a more uniform light intensity profile, producing a more uniform cross-linking profile. This desirable quantity is the amount such that the average concentration yields a light penetration depth similar to the tissue thickness. The optimal average drug concentration inside the tissue is 0.016%, and concentrations within the 0.016 ± 0.008% have cross-linking rates that are within 90% of the optimal concentration.

Various combinations of eosin Y concentration and contact time can be selected to achieve the optimal quantity of drug inside the tissue: 0.027% with 1 minute contact time, 0.012% for 5 minutes, or 0.0088% for 10 minutes. It is desirable for the treatment to have a short total treatment time and be reproducible. A longer treatment duration increases the risk of infection, increases patients' discomfort, and requires more of a surgeon's time which results in a higher cost. Applying a high drug concentration for a short contact time might have the disadvantage of high variability if the delivery time is not carefully monitored (Table 5.2). Increasing the contact time from 1 to 5 to 10 minutes decreases the variability in the quantity of drug delivered from 29% to 5% to 2%. A 5 minute drug contact time is recommended since it provides a relatively short contact time and low variability.

Table 5.2. Variability in drug quantity resulting from error in drug contact times by 30 seconds.

t_c (min)	t_c error (sec)	Error (%)
1	- 30	- 29%
	+ 30	+ 22%
5	- 30	- 5%
	+ 30	+ 4%
10	- 30	- 2%
	+ 30	+ 2%

Once the desired amount of drug is delivered, adding a delay time before irradiating produces a more uniform concentration profile provided the contact time is less than the characteristic time (15 minutes, Figure 5.6a). A more uniform drug concentration profile provides a more uniform cross-linking profile (Figure 5.6c). Given the characteristic time is ~15 minutes, a 10 minutes total of combined contact time and delay time is sufficient to produce a relatively uniform distribution of drug inside the tissue (Figure 5.6a). For a 5 minute contact time and 5 minute irradiation protocol, adding a delay time did not significantly alter the $\Delta G'_{avg}$ or the cross-linking distribution (Figure 5.6c). For longer irradiation durations, the delay time effect becomes even less significant since the concentration profile continues to evolve during the irradiation period.

Selecting irradiation protocol – Given a drug concentration profile, the irradiation intensity and duration determine the quantity of cross-linking but not the cross-linking distribution. Depending on how much cross-linking is necessary to halt the progression of keratoconus, the irradiation intensity and duration can be selected accordingly. In

selecting irradiation intensity and duration, factors that need to be considered are the safety limit of light permissible in the eye, maximum intensity level tolerable for patient comfort, and overall treatment duration. The light intensities and doses considered for corneal irradiation here are much lower than present in other applications such as bonding corneal incisions[18, 19], laser iridectomy and iridoplasty[20]. The light source (514 nm at 640 mW/cm^2 for 5 minutes or 192 J/cm^2) used in bonding corneal incision over a 1-cm diameter area did not result in tissue damage to the animals monitored over a 10-week period[18]. This amount of light is 2 orders of magnitude more than the light dose used in the examples above for a 5 minute irradiation period at 6 mW/cm^2. (Biocompatibility studies in Chapter 6 show a 3.6 J/cm^2 light dose combined with eosin Y is well tolerated by the cornea with no toxicity to the endothelium and very little damage to keratocytes compared to riboflavin/UVA treatment.)

Results show that for the same light dose, selecting a lower irradiation intensity with a longer duration results in more cross-linking than a higher intensity with a shorter duration. However, since the maximum exposure limit is very high, a higher intensity (6 mW/cm^2) and shorter irradiation period can be selected to minimize the overall treatment duration. The other factor to consider in selecting the intensity is the level of discomfort patients can tolerate.

5.5 CONCLUSION

The photo-activated collagen cross-linking treatment has multiple parameters that are interdependent and with a model we are able to predict the cross-linking profile resulting from adjusting individual or combinations of different parameters. The parameter space is

very large and carrying out experiments to find optimal values would be daunting. This is a powerful tool that can help narrow down the parameter space for selecting optimal values to be used in the clinic.

This model can be used to create customized treatments for individual patients depending on how severely the disease has progressed and how much cross-linking is necessary to treat the patient. Once the amount of cross-linking necessary to halt the progression of the disease in each patient is better understood, this model can also help customize treatments for individual patients so that they are effective, safe and as comfortable for the patients as possible.

5.6 BIBLIOGRAPHY

1. Rabinowitz, Y.S., *Keratoconus.* Survey of Ophthalmology, 1998. **42**(4): p. 297-319.
2. Spoerl, E., Wollensak, G., Seiler, T., *Increased Resistance of Crosslinked Cornea Against Enzymatic Digestion.* Current Eye Research, 2004. **29**(1): p. 35.
3. Berman, M.B., *Collagenase Inhibitors: Rationale for Their Use in Treating Corneal Ulceration.* International Ophthalmology Clinic, 1975. **15**(4): p. 49-66.
4. Rehany, U., Lahav, M., Shoshan, S., *Collagenolytic Activity in Keratoconus.* Annals of Ophthalmology, 1982. **14**(8): p. 751-754.
5. Wollensak, G., *Crosslinking Treatment of Progressive Keratoconus: New Hope.* Current Opinion in Ophthalmology, 2006. **17**(4): p. 356.
6. Raiskup-Wolf, F., Hoyer, A., Spoerl, E., Pillunat, L.E., *Collagen Crosslinking with Riboflavin and Ultraviolet-A light in Keratoconus: Long-term Results.* Journal of Cataract and Refractive Surgery, 2008. **34**(5): p. 796.
7. Kohlhaas, M., Spoerl, E., Schilde, T., Unger, G., Wittig, C. Pillunat, L.E., *Biomechanical Evidence of the Distribution of Cross-links in Corneas Treated with Riboflavin and Ultraviolet A Light.* Journal of Cataract & Refractive Surgery, 2006. **32**(2): p. 279.
8. Wollensak, G., Spoerl, E., Seiler, T., *Stress-strain Measurements of Human and Porcine Porneas After Riboflavin-ultraviolet-A-induced Cross-linking.* Journal of Cataract & Refractive Surgery, 2003. **29**(9): p. 1780-1785.
9. Kolli, S., Aslanides, I.M., *Safety and Efficacy of Collagen Crosslinking for the Treatment of Keratoconus.* Expert Opinion on Drug Safety. **9**(6): p. 949.

10. Wollensak, G., Spoerl, E., Wilsch, M., Seiler, T., *Endothelial Cell Damage After Riboflavin-ultraviolet-A Treatment in the Rabbit.* Journal of Cataract & Refractive Surgery, 2003. **29**(9): p. 1786-90.

11. Wollensak, G., Iomdina, E., *Biomechanical and Histological Changes After Corneal Crosslinking with and without Epithelial Debridement.* Journal of Cataract & Refractive Surgery, 2009. **35**(3): p. 540-546.

12. Wollensak, G., Spoerl, E., Wilsch, M., Seiler, T., *Keratocyte Apoptosis After Corneal Collagen Cross-linking Using Riboflavin/UVA Treatment.* Cornea, 2004. **23**(1): p. 43-49.

13. Spoerl, E., Wollensak, G., Dittert, .D.D., T., Seiler, *Thermomechanical Behavior of Collagen-cross-linked Porcine Cornea.* Ophthalmologica, 2004. **218**(2): p. 136.

14. Wollensak, G., Wilsch, M., Spoerl, E., Seiler, T., *Collagen Fiber Diameter in the Rabbit Cornea After Collagen Crosslinking by Riboflavin/UVA.* Cornea, 2004. **23**(5): p. 503-507.

15. Wollensak, G., Aurich, H., Pham, D.T., Wirbelauer, C., *Hydration Behavior of Porcine Cornea Crosslinked with Riboflavin and Ultraviolet A.* Journal of Cataract & Refractive Surgery, 2007. **33**(3): p. 516-521.

16. Coakes, R.L., Brubaker, R.F., *Method of Measuring Aqueous Humor Flow and Corneal Endothelial Permeability Using a Fluorophotometry Nomogram.* Investigative Ophthalmology & Visual Science, 1979. **18**(3): p. 288.

17. Spoerl, E., Mrochen, M., Sliney, D., Trokel, S., Seiler, T., *Safety of UVA-riboflavin Cross-linking of the Cornea.* Cornea, 2007. **26**(4): p. 385.

18. Proaño, C.E., Mulroy, L., Jones, E., Azar, D.T., Redmond, RW. Kochevar, I.E., *Photochemical Keratodesmos for Bonding Corneal Incisions.* Investigative Ophthalmology & Visual Science, 2004. **45**(7): p. 2177.

19. Mulroy, L., Kim, J., Wu, I., Scharper, P., Melki, S.A., Azar, D.T.*, et al.*, *Photochemical Keratodesmos for Repair of Lamellar Corneal Incisions.* Investigative Ophthalmology & Visual Science, 2000. **41**(11): p. 3335.

20. Ritch, R., Liebmann, J.M., *Argon Laser Peripheral Iridoplasty.* Ophthalmic Surgery and Lasers, 1996. **27**(4): p. 289-300.

Chapter 6

Cross-linking the Cornea with Minimal Toxicity

6.1 INTRODUCTION

Keratoconus is a bilateral corneal disorder with a prevalence of 1 out of 2,000 without racial or gender bias[1, 2]. This eye disease is characterized by progressive corneal thinning, protrusion, and scarring, resulting in irregular astigmatism and myopia. Corneal thinning appears to result from loss of material, partly due to the increased collagen degradation rate[3, 4]. The cornea of keratoconic eyes are found to have fewer collagen lamellae, fewer collagen fibrils per lamella, closer packing of collagen fibrils or various combinations of these factors resulting in a weakened structure[1].

Corneal thinning results in visual impairment that can be corrected by spectacles in the early stages of the disease. As corneal irregularities increase, eyeglasses are not sufficient to provide clear vision, so contact lenses are used. Patients who do not tolerate contact lenses, may undergo surgical procedures, such as thermokeratoplasty[5], epikertaophakia[6], and intracorneal ring segments[7] to reduce refractive errors induced by irregular corneal thinning associated with the disease; however, these treatments do not halt the progression of the keratoconus. When the disease progresses to the stage

where contact lenses no longer suffice, a corneal transplant (keratoplasty) is required. About 20% of patients with keratoconus ultimately require keratoplasty[1].

Pioneering research of Wollensak, Seiler, and Spoerl demonstrated that photodynamic corneal collagen cross-linking using riboflavin and UVA could halt the progression of keratoconus[8-10]. Five major human clinical trials in different countries ranging from 3 months to 6 years have demonstrated riboflavin/UVA treatment is effective in treating keratoconus[11]. The current protocol requires topical application of drug solution (0.1% riboflavin with 20% dextran) to the cornea every 2 minutes for 30 minutes before irradiating, and every 5 minutes during 30 minutes of irradiation with 3mW/cm^2 UVA light.

The combination of riboflavin and UVA is toxic to both keratocytes and endothelial cells. Since endothelial cells cannot regenerate in human eyes, the treatment was carefully designed to restrict toxicity to the anterior 350 μm of the corneal stroma[12]. This is achieved by selecting a high drug concentration and applying it for an extended duration to limit the amount of UVA light reaching the endothelium. The treatment cannot be used on patients with corneas under 400 μm since it causes “significant necrosis and apoptosis of endothelial cells” in rabbit corneas[13]. Keratocyte apoptosis causes corneal haze until they completely regenerate after 6 months, and in some cases, it takes up to 12 months to recover completely[3, 14, 15]. Even though there is toxicity, patients are willing to risk damaging their eyes to receive this treatment (currently being used in Europe and is going through FDA clinical trials in the U.S.) over the alternative treatment (corneal transplant).

Because riboflavin/UVA treatment has many safety concerns, it has been suggested that selecting a photosensitizer in the visible spectrum might reduce harmful effects[11]. Eosin Y is a photosensitizer with an absorption peak in the visible range (514 nm) which has shown the ability to cross-link collagen[16, 17] and stabilize sclera tissue[18]. It has also been approved for use in the body by the FDA[19].

6.2 METHODS

In Vitro Treatment – Eyes from New Zealand White Rabbit ranging from 2 to 3 kg were provided by collaborator Dr. Keith Duncan at the University of California at San Francisco. Eyes were shipped and stored in balanced saline on ice until use within 48 hours of enucleation. The epithelial cell layer was removed by scraping with a scalpel until epithelial material could be seen on the scalpel and the surface of the cornea changed from a smooth texture to a matte texture. The eyes were then placed into Dulbecco's phosphate buffer saline (DPBS) until treatment (within 30 minutes). Orbital tissues (muscle, fat, conjunctiva) covering the sclera and corneoscleral limbus were left in place for treatment to simulate the *in vivo* condition with respect to drug reaching the sclera.

Eosin Y/visible light treatment (EY/vis) – Eosin Y gel (0.04% w/w eosin Y and 3% w/w carboxymethylcellulose in DPBS) was prepared and then transferred into a 10 mL syringe. Using the syringe, ~0.5 mL of gel was applied onto the cornea. After 5 minutes contact time, the gel was removed from the corneal surface by squirting DPBS onto the cornea. The eye was then placed onto a holder with the cornea facing up to receive

irradiation from an array of green light emitting diodes (seven 5-mm LEDs at 525 ± 16 nm, 6 mW/cm^2 in the plane of the cornea). Irradiation was applied for 10 minutes.

The concentration and contact time were selected based on the results in Chapter 5 showing a cornea immersed in 0.016 ± 0.008% eosin Y solution for 5 minutes delivers the optimal amount of drug. To err on the side of having more drug in the cornea, a concentration of 0.02% was selected. In order to deliver an equivalent amount of drug in a gel form, twice the concentration is necessary in a gel formulation (0.04% eosin Y, 3% carboxymethylcellulose in DPBS) based on measurements using the light absorption technique discussed in Chapter 2. Results from the model in Chapter 5 show that adding a delay time before irradiation does not significantly affect the cross-linking profile. Therefore, the corneas in these experiments were irradiated immediately after removal of the drug formulation from the corneal surface.

Riboflavin/UVA treatment (R/UVA) – Following the R/UVA protocol used in clinical trials in the United States, the eye was placed onto a holder with the cornea facing up to receive drops of riboflavin (0.1% w/w riboflavin-5'-monophosphate and 20% w/w T-500 dextran in DPBS) and irradiation. Riboflavin drops were applied onto the cornea every 2 minutes for 30 minutes. The eye was then irradiated using a similar light set up described above but with UV LEDs (370 ± 12 nm, 3 mW/cm^2). Irradiation was applied for 30 minutes while adding riboflavin drops every 5 minutes.

Control treatment – Nothing was done to the eye other than removal of the epithelium.

After treatment, all eyes were placed into DPBS (Table 6.1). Orbital tissues were removed with scissors to expose the sclera and ensure accurate analysis of the eye shape.

Table 6.1. *In vitro* treatment summary

Treatment	Drug	Light (min)	# of Eyes
EY/vis	Eosin Y gel, 5 min	10	8
R/UVA	Riboflavin drops, 30 min	30	8
Control	None	None	12

Intact Globe Expansion – Intact globe expansion was performed following the procedure described by Mattson, *et al.*[20]. Eyes were mounted onto acrylic cylinders inside of a transparent plexi-glass observation cell filled with DPBS (Figure 6.1). To minimize bacteria growth during the experiment, several drops of antibiotic eye drops (Bausch & Lomb neomycin, polymyxin B sulfate and gramicidin ophthalmic solution USP) were added to the DPBS solution in the observation cell. The eyes were aligned with the major axis of the equator parallel to the imaging plane. There are two holes sealed with rubber septa used for inserting 30 gauge hypodermic needles to control the intraocular pressure (IOP). The needles were inserted into the eyes through the posterior sclera. The needles were connected to a DPBS reservoir set at a height h above the eyes to impose a desired IOP governed by hydrostatic pressure (IOP = ρgh; ρ = density, g = gravitational acceleration). To minimize activation of any residual photosensitizer present in the tissue, the experiment was performed in the dark except for 15 seconds of illumination from a fluorescent lamp every15 minutes to provide light for the photographs. For the first hour, the IOP was held at 15 mmHg to restore the shape of the eye (since shipping and

handling results in a variable shape). Then IOP was switched to 300 mmHg until the experiment completed (when rupture was observed or the level of fluid in the reservoir began to drop due to leaks in the tissue).

Photographs of the eyes were taken every 15 minutes throughout the experiment then analyzed for changes in ocular dimensions (corneal perimeter – CP, corneal length – CL, and corneal diameter – CD) using a custom MATLAB program. The rate of change for each of the three corneal dimensions was characterized using the difference between their initial value (using the image acquired 15 min after the pressure was changed from 15 to 300 mmHg) and their final value (described below) divided by the elapsed time between the initial and final images. The initial image is selected to be 15 minutes after switching on high pressure to avoid the variability in the transient response during the first few minutes after the large IOP change. For example, the rate of change of the corneal perimeter, $d(\Delta CP)/dt$, is calculated using

$$\frac{d(\Delta CP)}{dt} = \frac{CP_f - CP_i}{CP_i} \times \frac{1}{t_c} \qquad \text{Equation 1}$$

where CP_i is the initial corneal perimeter, CP_f is the corneal perimeter measured at end of the creep period. The end of the creep period is selected to be 2 hours before the first eye undergo tissue failure occurred so that calculated rates are due to creep and not tissue defects leading to failure (20 hours for *in vitro* experiments and 30 hours for *in vivo* experiments). CL and CD were computed using the same equation replacing CP with the either CL or CD.

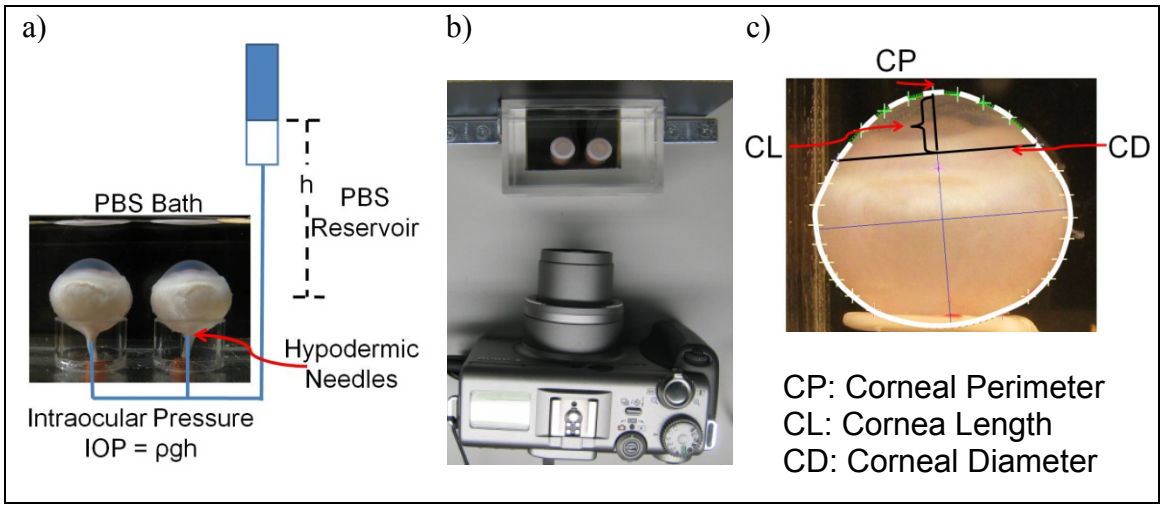

Figure 6.1. a) Intact globe expansion apparatus. Ocular dimensions **b)** are recorded with photographs and **c)** measured with custom MATLAB software.

In Vivo Treatment – New Zealand White Rabbits ranging from 2 to 3 kg were treated at UCSF in collaboration with Dr. Keith Duncan. Each rabbit was given general anesthesia with 1-5% inhaled isofluorane administered by mask. A speculum was inserted into the rabbit eyelid to keep the eye open for treatment. Drops of 0.5% proparacaine were applied onto the eye followed by sterilization with 5% povidone-iodine (betadyne). The eye was then rinsed with ocular balanced saline solution (BSS). The epithelium was removed by dipping a Weckcell sponge into 40% ethanol solution then rubbing it against the corneal surface until the epithelium came off.

Eosin Y/visible light treatment – Approximately 0.5 mL (between 0.4 to 0.6 mL) eosin Y gel was applied to the cornea using a syringe. After 5 minutes contact time, the gel was removed by rinsing the cornea with BSS. Within 1 minute, the cornea was irradiated with with 525 ± 16 nm light at 6 mW/cm^2 for 10 minutes. The fellow eye served as a control: BSS drops were applied to the cornea for 1 minute then followed by 10 minutes of irradiation as above.

Riboflavin/UVA treatment – Riboflavin drops were applied onto the cornea every 2 minutes for 30 minutes. The eye was then irradiated with 370 ± 12 nm light at 3 mW/cm^2. Irradiation was applied for 30 minutes while adding riboflavin drops every 5 minutes. The fellow eye served as a control, receiving BSS drops for 1 minute followed by 30 minutes UV irradiation while adding BSS drops every 5 minutes.

Table 6.2. *In vivo* treatment summary for efficacy study

Treatment	Drug	Light (min)	# of Eyes
EY/vis Treated	Eosin Y gel, 5 min	10	8
EY/vis Control	BSS, 1 min	10	8
R/UVA Treated	Riboflavin drops, 30 min	30	4
R/UVA Control	BSS, 1 min	30	3*

*One R/UVA Control eye was damaged during enucleation.

After irradiation, the eye was rinsed with BSS followed by application of antibiotic eye drops. The treatment was completed and the speculum was removed (Table 6.2). Animals were sacrificed 24 hours after treatment. The eyes were enucleated, stored in BSS on ice, and shipped to Caltech overnight. All eyes were tested within 12 hours of arrival (within 36 hours of enucleation) using the intact globe expansion apparatus described above.

Biocompatibility – Treatments were performed *in vivo* at UCSF in collaboration with Dr. Keith Duncan according to the procedures described above. After treatment, eyes were observed for inflammation, corneal haze, and epithelial regrowth over a period of 7 days.

Another set of *in vivo* studies was performed for histology. The treatments used the same *in vivo* procedure described above. Animals were sacrificed 24 hours after treatment.

Eyes were enucleated and fixed in 10% formalin, embedded in paraffin, and sections were cut and stained with eosin and hematoxylin.

Table 6.3. *In vivo* treatment summary for biocompatibility study

Animal	Eye	Drug	Light (min)
1	OD	Eosin Y gel, 5 min	0
	OS	None	0
2	OD	Eosin Y gel, 5 min	10
	OS	None	10
3	OD	Riboflavin drops, 30 min	30
	OS	BSS, 1 min	30

6.3 RESULTS

Results for *in vitro* treated eyes showed that treated eyes resisted expansion relative controls as measured by all three corneal dimensions (Table 6.4, * indicates $p < 0.05$). The rate of change of CP, $d(\Delta CP)/dt$, is most closely related to the (approximately biaxial) strain rate during exposure to IOP = 300 mmHg. Due to the strength of the sclera, the corneal diameter generally expands less than the corneal perimeter (i.e., $d(\Delta CD)/dt < d(\Delta CP)/dt$) and, consequently, CL increases more than CP (i.e., $d(\Delta CL)/dt > d(\Delta CP)/dt$).

Table 6.4. 10^4 * Rate of change in corneal dimensions. (CP = corneal perimeter, CL = corneal length, CD = corneal diameter)

		d*(Δ*CP*)/*dt	***d*(Δ*CL*)/*dt***	***d*(Δ*CD*)/*dt***
In vitro	Control (N = 12)	23 ± 7	59 ± 19	16 ± 8
	EY/vis (N = 8)	*3 ± 5	*2 ± 9	*5 ± 4
	R/UVA (N = 8)	*13 ± 10	*15 ± 18	*13 ± 7
In vivo	Control (N = 11)	12 ± 6	18 ± 11	10 ± 4
	EY/vis (N = 8)	*6 ± 5	10 ± 8	*5 ± 5
	R/UVA (N = 4)	*2 ± 3	8 ± 3	*0 ± 3

*Indicates statistically significant difference ($p < 0.05$) from control group for each treatment type (*in vitro* and *in vivo*).

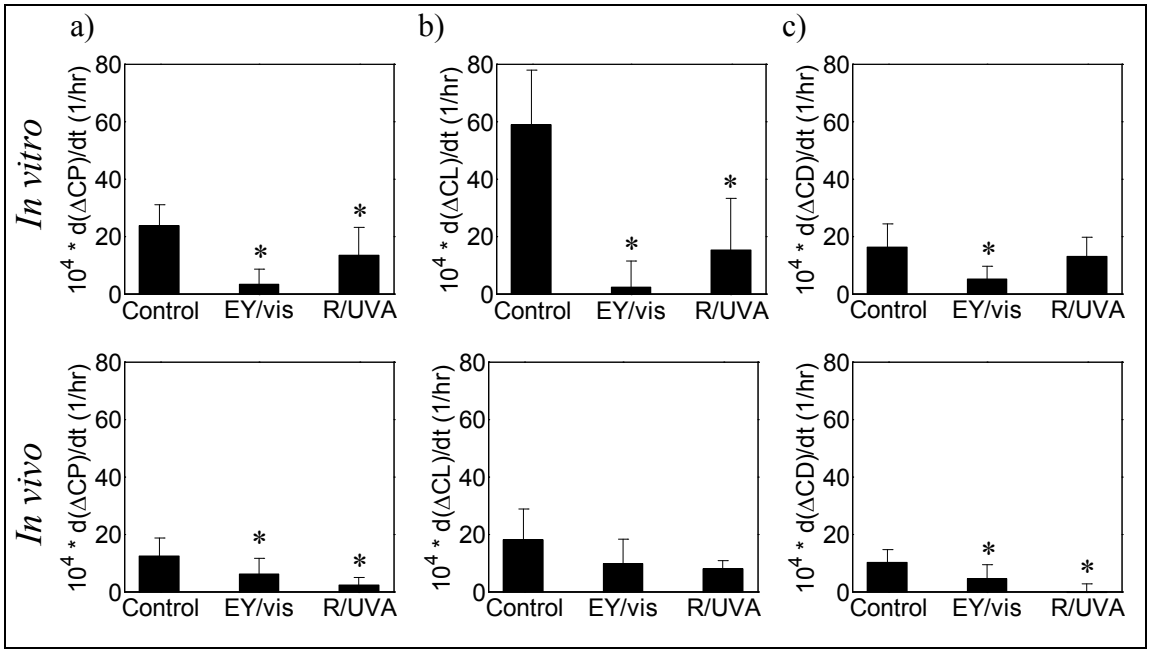

Figure 6.2. Rate of change in **a)** corneal perimeter (CP) **b)** corneal length (CL) and **c)** corneal diameter (CD) for different treatment groups. The asterisk indicates a statistically significant difference compared to the control group ($p < 0.05$). (For *in vitro* experiments, Control: N = 12; EY/vis: N = 8; R/UVA: N = 8. For *in vivo* experiments, Control = 11; EY/vis: N = 8; R/UVA: N = 4)

By any of these measures, the deformation of the treated corneas is 1/2 or less that observed for controls (Figure 6.2). The EY/vis treatment is comparable to the riboflavin/UVA treatment; there is no statistically significant difference between these two groups.

Results for *in vivo* treated eyes show fellow controls respond identically in the EY/vis and R/UVA groups: respectively, the rates of increase of CP were 0.19 ± 0.12 %/hr and 0.14 ± 0.07 %/hr; of CL were 0.27 ± 0.20 %/hr and 0.28 ± 0.09 %/hr; and of CD were 0.15 ± 0.08 %/hr and 0.08 ± 0.06 %/hr. Therefore, the results for the controls are treated in aggregate. Control eyes from the *in vivo* study resist deformation relative to controls in the *in vitro* study (cf., top row to bottom row of Figure 6.2). The exact origin of this difference is not yet known.

Results for *in vivo* treated eyes showed that treated eyes resisted expansion relative to controls (Table 6.1, * indicates $p < 0.05$). The creep rates of the *in vivo* treated groups are less than or approximately ½ those of the controls for all three corneal dimensions (Figure 6.2). The EY/vis treatment is comparable to the riboflavin/UVA treatment; there is no statistically significant difference between these two groups.

Two types of biocompatibility studies compare riboflavin/UVA and eosin Y/vis: examination of corneal recovery during the first week after treatment; and histological examination of acute toxicity during the first 24 hours. In the first, animals were examined on Day 2 and Day 7 after treatment, recording observations of inflammation, corneal haze, and epithelial regrowth (Table 6.5). The EY/vis treatment was indistinguishable from balanced salt solution (BSS) control in all animals by all

measures, with the exception of a delay in re-epithelialization in one animal. R/UVA treated eyes showed moderate inflammation and severe corneal haze on Day 2, which was absent in BSS controls and EY/vis treated eyes. The inflammation resolved and the corneal haze became mild after 7 days. Epithelial regrowth only occurred in patchy areas covering approximately 1/3 of the debrided area after 7 days, in stark contrast to BSS controls or EY/vis treated eyes.

Table 6.5. Eosin Y/ visible light treatment biocompatibility

		Day 2		Day 7		
Animal	**Eye**	**Inflam-mation**	**Corneal Haze**	**Inflam-mation**	**Cornea l Haze**	**Epithelial Regrowth**
1	EY/vis	None	None	None	None	100%
	BSS/vis	None	None	None	None	100%
2	EY/vis	None	None	None	None	100%
	BSS/vis	None	None	None	None	100%
3	EY/vis	None	None	None	None	~50%
	BSS/vis	None	None	None	None	100%
4	EY/vis	Mild	Mild	None	None	~50%
	BSS/vis	Mild	Mild	None	None	~50%

Table 6.6. Riboflavin/UVA treatment biocompatibility

		Day 2		Day 7		
Animal	**Eye**	**Inflam-mation**	**Corneal Haze**	**Inflam-mation**	**Cornea l Haze**	**Epithelial Regrowth**
1	R/UVA	Moderate	Severe	None	Mild	~33%
	BSS/UVA	Mild	Mild	None	None	100%
2	R/UVA	Moderate	Severe	None	Mild	~33%
	BSS/UVA	Mild	Mild	None	None	100%

Histology performed on corneal cross-sections of animals sacrificed 24 hours after treatment shows that BSS controls are insensitive to irradiation with either visible or UVA light (second row, Figure 6.3). Apoptosis of keratocytes and the presence of some inflammatory cells are observed in the anterior 1/3 of the stroma in all of the BSS controls, in accord with that associated with the response to de-epithelialization[21]. The posterior half of the stroma and the endothelium in all three BSS controls show the usual number and morphology of keratocytes, as well as an intact endothelium. Apoptosis of keratocytes and the presence of some inflammatory cells in the anterior 1/3 of the stroma are also evident in the corneas that received EY (no light) and EY/vis (top, Figure 6.3a-b). The number and morphology of keratocytes in the posterior half of the stroma and the intact endothelium observed in both EY (no light) and EY/vis are similar to the BSS controls (compare top to bottom, Figure 6.3a-b). The corneas treated with EY (no light) and EY/vis are indistinguishable, indicating that phototoxicity is negligible in the case of EY/vis. The R/UVA treated eye was completely devoid of keratocytes in the stroma and no endothelial cells remained (Figure 6.4c top), in accord with prior literature on the phototoxicity of R/UVA[13]. The fellow eye treated with BSS/UVA has an intact endothelial cell layer, a normal distribution of keratocytes in most of the cornea with a few inflammatory cells in the anterior section of the stroma (Figure 6.4c bottom), in accord with prior studies that showed the phototoxicity of riboflavin is not elicited by the UVA irradiation alone[22].

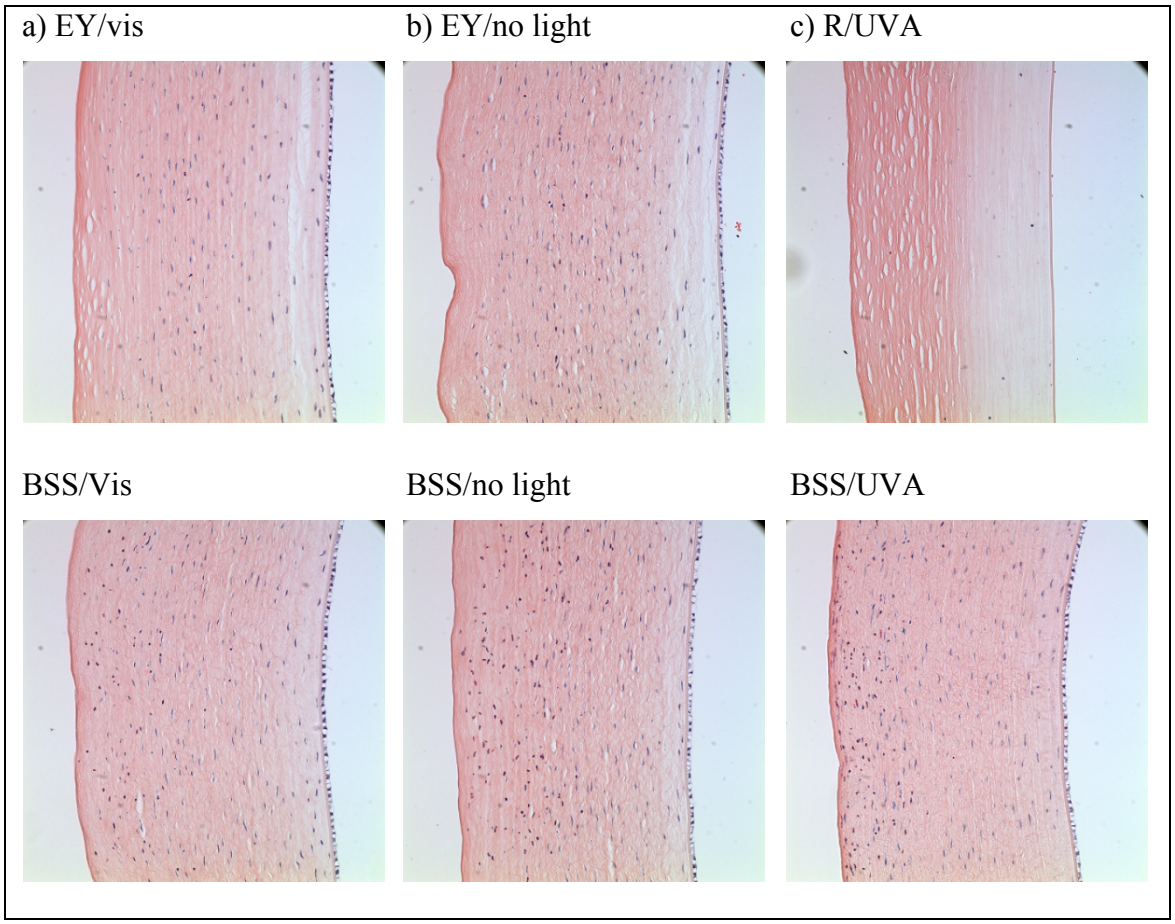

Figure 6.3. Representative corneal cross-sections 24 hours after treatment. The left side of each image is the anterior side and the right side is the posterior side of the cornea. The epithelium is absent because it was removed in the treatment procedure. Cornea treated with **a)** eosin Y and 525 nm light (top), BSS and 525 nm light (bottom) **b)** eosin Y and no light (top), BSS and no light (bottom) and **c)** riboflavin and 370 nm light, BSS and 370 nm light.

6.4 DISCUSSION

Eosin Y/vis treatment and R/UVA treatment produce similar stabilization of rabbit cornea as indicated by resistance to creep when challenged by elevated intra-ocular pressure. Similar efficacy is observed both when the treatment is applied *in vitro* and when treatment is performed *in vivo* in a rabbit model. The R/UVA treatment is found to be effective in studies lasting up to 6 years due to the stable nature of the cross-links

formed. Cross-links induced by EY/vis are expected to be equivalent to the ones formed by R/UVA (Chapter 2). So they should resist hydrolysis and enzymatic degradation in a similar manner. Therefore, it is worth investigating the expectation that EY/vis would also provide the long term efficacy.

While the efficacy of the two treatments are comparable, the toxicity of R/UVA is much more severe than that of EY/vis as measured by the degree of inflammation, epithelial regrowth, corneal haze (Table 6.4 and 6.5), and cytotoxicity (Figure 6.3). In addition, the total treatment time for the R/UVA protocol (60 minutes) is four times longer than that for the EY/vis treatment (15 min) (Figure 6.2).

Consistent with previous studies, corneal haze was observed after R/UVA treatment[3, 14, 15], which has been attributed to keratocytes apoptosis. Keratocyte apoptosis causes edema formation leading to stromal haze. In accordance, keratocyte apoptosis was observed throughout the rabbit corneas treated with R/UVA (Figure 6.3). Numerous studies have documented keratocyte apoptosis resulting from R/UVA treatment down to a depth of 300-350 μm, which leads to corneal haze in patients post-operatively ranging from weeks to months until keratocytes repopulate the cornea[9, 23-25]. Typically, repopulation of keratocytes begins 2-3 months after treatment and reaches a normal density after 6 months[25, 26]. Corneal haze of various degrees in patients has been reported to last for up to 12 months before resolving completely[10]. In 7.6% of the cases, corneal haze becomes permanent[27] resulting in impaired vision.

EY/vis treatment induced little or no corneal haze, which is consistent with histology results showing a normal distribution of keratocytes in most of the stroma (Table 6.4 and

Figure 6.3a). Keratocyte apoptosis in the anterior section of the cornea was also observed in the control groups due to removal of the corneal epithelium[21]. Based on these observations in a rabbit model, it is worth investigating the expectation that EY/vis would cause very mild keratocyte toxicity, little corneal haze and faster recovery in patients. If this were borne out in clinical studies, the implication would be that patients could receive corneal cross-linking without the inconvenience of months of corneal haze currently experienced by patients receiving R/UVA treatment.

In addition to keratocyte toxicity, R/UVA treatment also induced endothelial cytotoxicity (Figure 6.3c, bottom), which has also been observed in previous studies[13, 28]. Endothelial cytotoxicity in rabbit corneas resulting from the treatment has been attributed to their thin corneas (400 μm or less). In such thin corneas, the light intensity reaching the endothelium is high enough to cause damage. Therefore, it has been established that the treatment cannot be performed on patients with corneas thinner than 400 μm[9, 12, 13]. EY/vis treatment was very well tolerated by the endothelial cell layer in rabbit corneas; treated eyes have indistinguishable endothelial cell layers compared to fellow control eyes (Figure 6.3a). Based on these observations in a rabbit model, it is worth investigating the expectation that EY/vis treatment would be safe for treatment of advanced keratoconus patients with corneas thinner than 400 μm. If this were borne out in clinical studies, the EY/vis treatment might also be safe for post-LASIK ectasia patients, who tend to have thin corneas due to removal of corneal tissue during LASIK[29].

6.5 CONCLUSION

Corneal collagen cross-linking by production of singlet oxygen upon irradiation of a photosensitizer occurs with both riboflavin (irradiated with UVA) and eosin Y (irradiated with green light). Cross-links formed by riboflavin are found to be stable in studies lasting up to 6 years and those formed by eosin Y are expected to be equivalent (Chapter 2), so it should produce long-term stability as well. The two approaches are shown to confer similar stabilization of rabbit cornea. Stark differences between the two treatments are seen in corneal toxicity, with little phototoxicity observed for the EY/vis treatment. Of particular interest, no endothelial toxicity was observed with EY/vis in a rabbit model, even though the cornea is less than 400 μm thick. Therefore, future clinical studies are recommended to determine if EY/vis treatment is safe for patients with corneas thinner than 400 μm. Relative to the usual R/UVA clinical protocol, the EY/vis protocol requires 1/4 the treatment time (15 minutes). If clinical studies confirm the results seen in a rabbit model, the EY/vis treatment might reduce patient discomfort and treatment cost relative to R/UVA. Clinical studies are highly recommended to further investigate safety and efficacy of EY/vis treatment, which has the ability to retain the benefits of corneal cross-linking demonstrated by R/UVA while significantly reducing toxicity and treatment duration.

6.6 ACKNOWLEDGEMENTS

This work includes contributions from Viet Anh Nguyen Huu, Dr. Matthew Mattson, and Dr. Keith Duncan. Undergraduate Viet Anh Nguyen Huu assisted in treating eyes *in vitro.* Dr. Matthew Mattson built the *in vitro* and *in vivo* light sources, the intact globe

expansion apparatus, and the MATLAB data analysis software. Dr. Keith Duncan provided eyes for in vitro treatment and performed *in viv*o treatments, biocompatibility and histology studies.

6.7 BIBLIOGRAPHY

1. Rabinowitz, Y.S., *Keratoconus.* Survey of Ophthalmology, 1998. **42**(4): p. 297-319.
2. Bron, A.J., *Keratoconus.* Cornea, 1988. **7**(3): p. 163-9.
3. Kolli, S., Aslanides, I.M., *Safety and Efficacy of Collagen Crosslinking for the Treatment of Keratoconus.* Expert Opinion on Drug Safety. **9**(6): p. 949.
4. Sawaguchi, S., Yue, B.Y., Sugar, J., Gilboy, J.E., *Lysosomal Enzyme Abnormalities in Keratoconus.* Archives of Ophthalmology, 1989. **107**(10): p. 1507-1510.
5. Gasset, A.R., Kaufman, H.E., *Thermokeratoplasty in Treatment of Keratoconus.* American Journal of Ophthalmology, 1975. **79**(2): p. 226-232.
6. Spitznas, M., Eckert, J., Frising, M., Eter, N., *Long-term Functional and Topographic Results Seven Years After Epikeratophakia for Keratoconus.* Graefe's Archive for Clinical and Experimental Ophthalmology, 2002. **240**(8): p. 639.
7. Colin, J., Cochener, B., Savary, G., Malet, F., *Correcting Keratoconus with Intracorneal Rings.* Journal of Cataract & Refractive Surgery, 2000. **26**(8): p. 1117-1122.
8. Wollensak, G., Sprl, E., Seiler, T., *Treatment of Keratoconus by Collagen Cross Linking.* Der Ophthalmologe, 2003. **100**(1): p. 44-49.
9. Wollensak, G., *Crosslinking Treatment of Progressive Keratoconus: New Hope.* Current Opinion in Ophthalmology, 2006. **17**(4): p. 356.

10. Raiskup-Wolf, F., Hoyer, A., Spoerl, E., Pillunat, L.E., *Collagen Crosslinking with Riboflavin and Ultraviolet-A light in Keratoconus: Long-term Results.* Journal of Cataract and Refractive Surgery, 2008. **34**(5): p. 796.

11. Ashwin, P.T., McDonnell, P.J., *Collagen Cross-linkage: A Comprehensive Review and Directions for Future Research.* British Journal of Ophthalmology, 2010. **94**(8): p. 965.

12. Spoerl, E., Mrochen, M., Sliney, D., Trokel, S., Seiler, T., *Safety of UVA-riboflavin Cross-linking of the Cornea.* Cornea, 2007. **26**(4): p. 385.

13. Wollensak, G., Spoerl, E., Wilsch, M., Seiler, T., *Endothelial Cell Damage After Riboflavin-ultraviolet-A Treatment in the Rabbit.* Journal of Cataract & Refractive Surgery, 2003. **29**(9): p. 1786-90.

14. Wollensak, G., Hammer, T., Herrmann, C.I., *Haze or Calcific Band Keratopathy After Crosslinking Treatment?* Der Ophthalmologe, 2008. **105**(9): p. 864-865.

15. Mazzotta, C., Balestrazzi, A., Baiocchi, S., Traversi, C., Caporossi, A., *Stromal Haze After Combined Riboflavin/UVA Corneal Collagen Cross-linking in Keratoconus: In Vivo Confocal Microscopic Evaluation.* Clinical & Experimental Ophthalmology, 2007. **35**(6): p. 580.

16. Brinkman, W. T., *Photo-cross-linking of Type I Collagen Gels in the Presence of Smooth Muscle Cells: Mechanical Properties, Cell Viability, and Function.* Biomacromolecules, 2003. **4**(4): p. 890.

17. Nakayama, Y., Kameoa, T., Ohtakaa, A., Hiranob, Y., *Enhancement of Visible Light-induced Gelation of Photocurable Gelatin by Addition of Polymeric Amine.*

Journal of Photochemistry and Photobiology A - Chemistry, 2006. **177**(2-3): p. 205.

18. Mattson, M., *Understanding and Treating Eye Diseases: Mechanical Characterization and Photochemical Modification of the Cornea and Sclera.* Dissertation (Ph.D), California Institute of Technology, 2008.
19. Alleyne, C.H., Cawley, C.M., Barrow, D.L., Poff, B.C., Powell, M.D., Sawhney, A.S.*, et al.*, *Efficacy and Biocompatibility of a Photopolymerized, Synthetic, Absorbable Hydrogel as a Dural Sealant in a Canine Craniotomy Model.* Journal of Neurosurgery, 1998. **88**(2): p. 308.
20. Mattson, M.S., Huynh, J., Wiseman, M., Coassin, M., Kornfield, J.A. Schwartz, D.M., *An In Vitro Intact Globe Expansion Method for Evaluation of Cross-linking Treatments.* Investigative Ophthalmology & Visual Science, 2010. **51**(6): p. 3120-3128.
21. Wilson, S. E., Chaurasia, S. S., Medeiros, F. W., *Apoptosis in the Initiation, Modulation and Termination of the Corneal Wound Healing Response.* Experimental Eye Research, 2007. **85**(3): p. 305-311.
22. Wollensak, G., Spoerl, E., Reber, F., Seiler, T., *Keratocyte Cytotoxicity of Riboflavin/UVA-treatment In Vitro.* Eye, 2004. **18**(7): p. 718.
23. Mazzotta, C., Traversi, C., Baiocchi, S., Caporossi, O., Bovone, C., Sparano, M.C.*, et al.*, *Corneal Healing After Riboflavin Ultraviolet-A Collagen Cross-linking Determined by Confocal Laser Scanning Microscopy In Vivo: Early and Late Modifications.* American Journal of Ophthalmology, 2008. **146**(4): p. 527.

24. Wollensak, G., Spoerl, E., Wilsch, M., Seiler, T., *Keratocyte Apoptosis After Corneal Collagen Cross-linking Using Riboflavin/UVA Treatment.* Cornea, 2004. **23**(1): p. 43-49.

25. Mazzotta, C., Balestrazzi, A., Traversi, C., Baiocchi, S., Caporossi, T., Tommasi, C*., et al.*, *Treatment of Progressive Keratoconus by Riboflavin-UVA-induced Cross-linking of Corneal Collagen: Ultrastructural Analysis by Heidelberg Retinal Tomograph II In Vivo Confocal Microscopy in Humans.* Cornea, 2007. **26**(4): p. 390.

26. Kymionis, G. D., Diakonis, V.F., Kalyvianaki, M., Portaliou, D., Siganos, C., Kozobolis, V.P*., et al.*, *One-Year Follow-up of Corneal Confocal Microscopy After Corneal Cross-Linking in Patients With Post Laser In Situ Keratosmileusis Ectasia and Keratoconus.* American Journal of Ophthalmology, 2009. **147**(5): p. 774.

27. Letko, E., Majmudar, P.A., Forstot, S.L., Epstein, R.J., Rubinfeld, R.S., *UVA-light and Riboflavin-mediated Corneal Collagen Cross-linking.* International Ophthalmology Clinics, 2011. **51**(2): p. 63.

28. Wollensak, G., Spöerl, E., Reber, F., Pillunat, L., Funk, R., *Corneal Endothelial Cytotoxicity of Riboflavin/UVA Treatment In Vitro.* Ophthalmic Research, 2003. **35**(6): p. 324.

29. Hjortdal, JØ., Møller-Pedersen, T., Ivarsen, A., Ehlers, N., *Corneal Power, Thickness, and Stiffness: Results of a Prospective Randomized Controlled Trial of PRK and LASIK for Myopia.* Journal of Cataract & Refractive Surgery, 2005. **31**(1): p. 21.